Dissertation zur Erlangung des Doktorgrades

der Fakultät für Chemie und Pharmazie

der Ludwig-Maximilians-Universität München

Synthesis and application of spermine-based poly(β-amino ester)s and PEI-based copolymers for siRNA delivery

Yao Jin

aus

Xingtai, Hebei, China

2022

Erklärung
Diese Dissertation wurde im Sinne von § 7 der Promotionsordnung vom 28. November 2011 von Frau Prof. Dr. Olivia M. Merkel betreut.

Eidesstattliche Versicherung

Diese Dissertation wurde eigenständig und ohne unerlaubte Hilfe erarbeitet.

München, 22.09.2022

Yao Jin

Dissertation eingereicht am: 22.09.2022

1. Gutachterin: Prof. Dr. Olivia. M. Merkel

2. Gutachter: Prof. Dr. Ernst Wagner

Mündliche Prüfung am: 24.10.2022

Table of content

Table of content **3**

List of abbreviations **6**

Abstract **8**

General Introduction **10**

1. RNA interference 10

2. Advantages of siRNA over other RNAi therapeutics 11

3. Barriers to siRNA delivery 11

3.1 Extracellular barriers 12

3.2 Cellular barriers 13

4. Cellular uptake pathway 17

5. Biomaterials in siRNA delivery 19

5.1 Lipids and lipid analogues 20

5.2 Polycations and polymers 21

5.3 Others 27

6. Aims of the projects 28

Chapter I **29**

1. Introduction 30

2. Materials & Methods 32

2.1 Materials 32

2.2 Synthesis and characterization of spermine-based poly(β-amino ester)s 32

2.3 Preparation and characterization of polyplexes 34

2.4 siRNA encapsulation efficiency by SYBR gold assay 35

2.5 In vitro compatibility assessment 35

2.6 Quantification of cellular uptake 35

2.7 In vitro eGFP knockdown 36

2.8 Endosome entrapment 36

2.9 Cellular uptake pathway 37

2.10 Migration assay 37

2.11 Western blot analysis of KRAS gene silencing 38

3. Results & Discussion 39

3.1 Synthesis and characterization of spermine-based poly(β-amino ester)s 39

3.2 siRNA encapsulation efficiency 42

3.3 Characterization of the polyplexes 43

3.4 In vitro compatibility 45

3.5 Cellular uptake 45

3.6 In vitro eGFP knockdown 46

3.7 Endosome Entrapment 48

3.8 Cellular uptake pathway 50

3.9 Migration assay 51

3.10 Western blot analysis 53

4. Conclusion 54

Chapter II **57**

1. Introduction 57
2. Materials and Methods 59
2.1 Materials 59
2.2 Synthesis and characterization of amphiphilic poly(β-amino ester)s 60
2.3 Preparation and characterization of P(SpDBAE) polyplexes 61
2.4 SYBR gold assay of P(SpDBAE) polyplexes 62
2.4 In vitro cell compatibility of P(SpDBAE) and P(SpDBAE) polyplexes 62
2.5 Cellular uptake of P(SpDBAE) polyplexes 63
2.6 GFP knockdown of P(SpDBAE) polyplexes 63
3. Results and Discussion 64
3.1 Polymer synthesis 64
3.3 SYBR Gold assay of P(SpDBAE) 67
3.4 In vitro compatibility of P(SpDBAE) and P(SpDBAE) polyplexes 68
3.5 Cellular uptake of P(SpDBAE) polyplexes 69
3.6 GFP knockdown of P(SpDBAE) polylexes 70
4. Conclusion 73

Chapter III 75

1. Introduction 76
2. Materials and methods 78
2.1 Materials 78
2.2 Synthesis and characterization of the polymers 79
2.3 Preparation and characterization of polyplexes 81
2.4 siRNA encapsulation efficiency 81
2.5 Cellular uptake 82
2.6 GFP knockdown 82
2.7 GAPDH gene knockdown 82
2.8 Cell viability 83
2.9 Endosomal entrapment 84
3. Results and discussion 84
3.1 Synthesis and characterization of P(SpOABAE) 84
3.2 siRNA encapsulation efficiency 87
3.3 Size and zeta potential of the polyplexes 88
3.4 Cellular uptake 90
3.5 GFP knockdown 91
3.6 Cell viability 93
3.7 GAPDH knockdown 94
3.8 Endosomal entrapment 96
4. Conclusion 97

Chapter IV 103

1. Introduction 104
2. Results & Discussion 106
2.1 Size and zeta potential of NPs-siRNA complexes 106
2.2 SYBR gold assay of PEI-PCL/PEG-PCL nanoparticles 108
2.3 Cellular uptake of PEI-PCL/PEG-PCL nanoparticles 109
2.4 Heparin competition assay of PEI-PCL/PEG-PCL nanoparticles 110
2.5 Synthesis of PEI5K-PCL5K-PEI5K 111

2.6 Characterization of PEI-PCL-PEI/PEG-PCL nanoparticles 112
2.7 siRNA encapsulation efficiency of the PEI-PCL-PEI/PEG-PCL nanoparticles 115
2.8 Dye quenching assay 115
2.9 Cellular uptake of PEI-PCL-PEI/PEG-PCL nanoparticles 116
2.10 GFP knockdown of PEI-PCL-PEI/PEG-PCL nanoparticles 117
3. Conclusion 119
4. Experimental Section/Methods 119

Summary and outlook 129

References 133

List of publications and conference contributions 152

Acknowledgments 153

List of abbreviations

AF488	Alexa fluor 488
AF647	Alexa fluor 647
AFM	Atomic force microscopy
CLSM	Confocal laser scanning microscopy
CHO	Chinese hamster ovary
CPP	Cell-penetrating peptides
DAPI	6-diamidino-2-phenylindole dihydrochloride
DCM	Dichloromethane
DLS	Dynamic light scattering
DSP	Dithiobis(succinimidylpropionate)
DMF	N, N-dimethylformamide
DMSO	Dimethyl sulfoxide
DTBP	Dimethyl•3,3'-dithiobispropionimidate•2HCl
EDTA	Ethylenediaminetetraacetic acid
ESI-MS	Electrospray ionization mass spectrometry
FBS	Fetal bovine serum
FDA	Food and Drug Administration
G418	Geneticin
GAPDH	Glyceraldehyde-3-phosphate dehydrogenase
GFP	Green fluorescence protein
GPC	Gel permeation chromatography
HEPES	(4-(2-hydroxylethyl)-1-piperazineethanesulfonic acid)
^{1}H NMR	^{1}H-nuclear magnetic resonance
LDA	Laser doppler anemometry
MFI	Median fluorescence intensity
MTT	Thiazolyl blue tetrazolium bromide
P(BSpBAE)	Poly(tri-boc-spermine-based β-amino ester)s
P(BSpDBAE)	Poly(tri-boc-spermine and decylamine-based β-amino ester)s

P(BSpOABAE)	Poly(tri-boc-spermine and oleylamine-based β-amino ester)s
P(SpBAE)	Poly(spermine-based β-amino ester)s
P(SpDBAE)	Poly(Spermine and decylamine-based β-amino ester)s
P(SpOABAE)	Poly(spermine and oleylamine-based β-amino ester)s
PBAE	Poly(β-amino ester)s
PBS	Dulbecco's phosphate buffered saline
PCL	Polycaprolactone
PCR	Polymerase chain reaction
PEG	Polyethylene glycol
PEI	Polyethylenimine
RISC	RNA-induced silencing complex
RNAi	RNA interference
SDS-PAGE	Sodium dodecyl-sulfate polyacrylamide gel electrophoresis
siRNA	Small interfering RNA
siG12S	siRNA against KRAS G12S mutations
siGFP	siRNA against GFP
siNC	Scrambled siRNA
TBST	Tris-buffered saline pH 8.0 + 1% Tween 20
TFA	Trifluoroacetic acid
THF	Tetrahydrofuran
TNBS	2,4,6-trinitrobenzene sulfonic acid
TRBP	Transactivating response RNA-binding protein

Abstract

After RNA interference (RNAi) was first discovered by Fire and Melo over 20 years ago,[1] siRNA-based therapeutics are finally becoming reality. With the approval of siRNA-based drugs such as Onpattro®, Givlaari®, and Oxlumo® by the U.S. FDA, a new interest in siRNA delivery was fostered in industrial and academic research groups. However, siRNA is a hydrophilic, and negatively charged macromolecule, thus limiting its passive cellular uptake; besides, naked siRNA is rapidly degraded by RNase and cleared fast by the kidneys.[2] To overcome the barriers to siRNA delivery, various siRNA delivery systems have been developed including viral and non-viral vectors. Cationic polymers are important non-viral vectors for siRNA delivery. In this dissertation, we focused on the synthesis of novel cationic polymers including the spermine-based poly(β-amino ester)s and low molecular weight PEI-based copolymers.

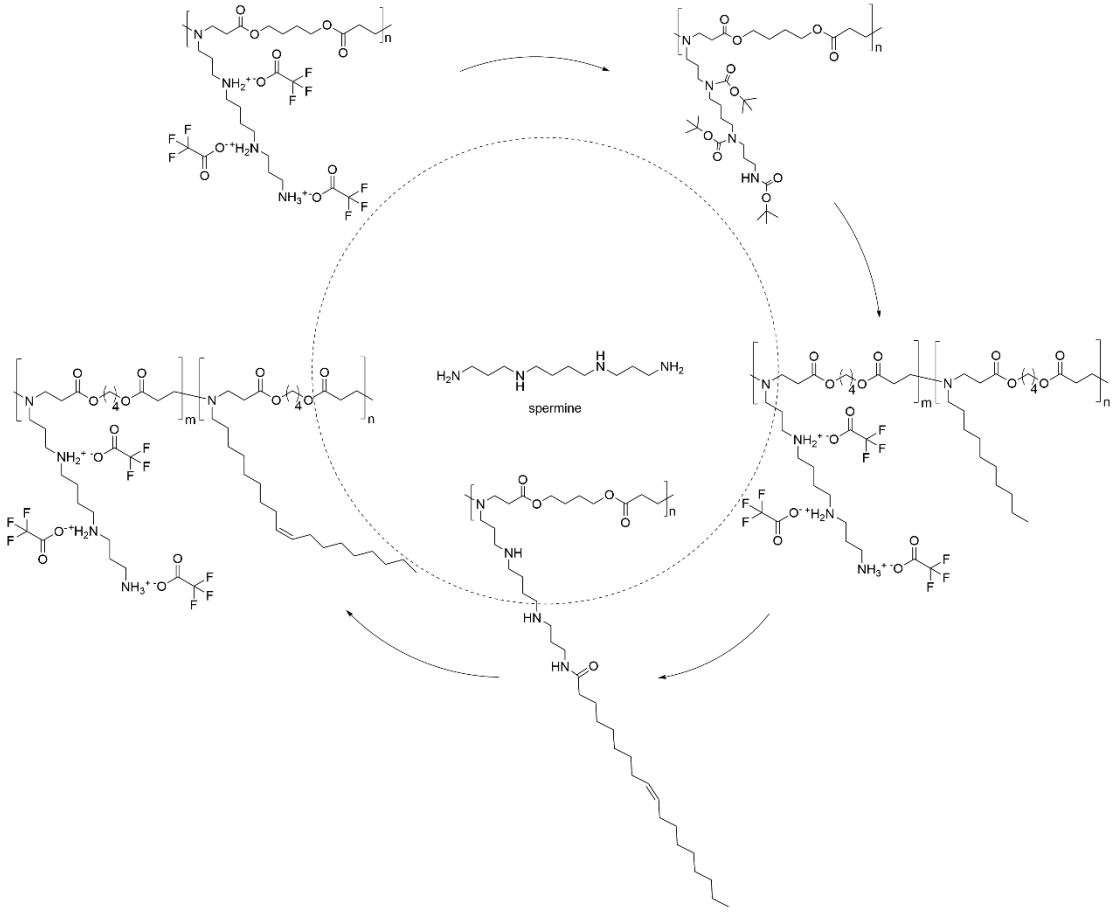

Scheme 1. The chemical structures of spermine-based poly(β-amino ester)s.

The chemical structures of the spermine-based poly(β-amino ester)s investigated

in this thesis are shown in Scheme 1. All the polymers were confirmed by ^{1}H NMR, and the siRNA encapsulation efficiency of the polymers was determined by SYBR gold assays. The size and zeta potential of the polyplexes were characterized by dynamic lights scattering and laser Doppler anemometry using a Zeta-sizer Nano ZS (Malvern Instruments Inc., Malvern, UK). The cellular uptake of the polyplexes was determined using fluorophore-labeled siRNA and determined by flow cytometry. The gene silencing efficiency of the polyplexes was evaluated using enhanced green fluorescence protein-expressing cells (H1299/eGFP cells). The polyplexes were also evaluated for therapeutically relevant gene silencing.

In experiments using low molecular weight PEI-based copolymers, the commercially available PEI-PCL (800 Da – 40 kDa) was blended with PEG-PCL (5 kDa – 4 kDa) to prepare nanoparticles using nanoprecipitation (solvent displacement). Three formulation methods were developed and the siRNA encapsulation efficiency was determined by SYBR gold assay, the size and zeta potential of the nanoparticles were characterized by Zeta-sizer Nano ZS (Malvern Instruments Inc., Malvern, UK). Due to the low cellular uptake of the NPs-siRNA complexes, PEI-PCL-PEI (5 kDa-5 kDa - 5 kDa) was synthesized and evaluated. The nanoparticles composed of PEI-PCL-PEI/PEG-PCL finally achieved efficient gene silencing.

General Introduction

1. RNA interference

RNA interference, abbreviated as RNAi, was first discovered in mammalian cells in 1998.[1]Only 3 years later, Morgan's and Tuschl's groups reported that 21 to 25 nucleotide (nt)-long double-stranded RNAs can silence specific genes in mammalian cells without causing nonspecific interferon response. Such duplexes are now widely known as small interfering RNAs (siRNAs).[3, 4] The RNAi mechanism was first discovered in *Caenorhabditis elegans* and can be generally described with the following steps: 1) Endogenous dsRNA is identified by a ribonuclease protein called dicer which cleaves the dsRNA into small double-stranded fragments (siRNAs). 2) The siRNAs consisting of a passenger strand and a guide strand were then reported to assemble with Argonaute 2 (Ago2), the catalytic core of the RNA-induced silencing complex (RISC).[5, 6] 3) Once assembled into RISC, the passenger strand of the siRNA duplex is cleaved and released, leaving the guide strand to direct the activated RISC to its complementary RNA sequence in the target mRNA. This finally leads to the cleavage of the target mRNA and post-transcriptional gene silencing.[7] This silencing efficiency can ensure a therapeutic effect for 3 – 7 days in cells with a high mitotic index and several weeks in non-dividing cells.[8]

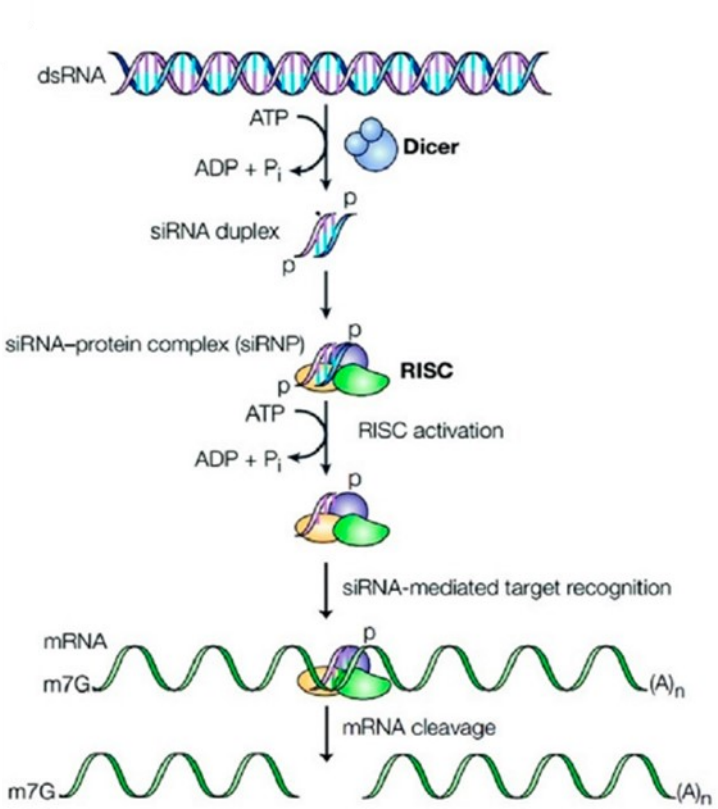

Figure 1. RNA interference induced by siRNA[9] (Reproduced with permission. Copyright the Royal Society of Chemistry, 2003).

2. Advantages of siRNA over other RNAi therapeutics

Besides siRNA, microRNA (miRNA), and short hairpin (shRNA) can also induce RNAi. miRNA is characterized by a single-strand (~22 nucleotides) and stem-loop structure. However, miRNA cannot bind to mRNA perfectly, thus degrading many untargeted mRNAs causing toxicity. [2, 10] shRNA has a tight hairpin structure. To act appropriately, the shRNA needs to be delivered to the nucleus and express the promoter successfully, which complicates its applications.[11] Compared with miRNA and shRNA, siRNA has fewer obstacles, rendering it highly attractive for RNAi therapeutics.

3. Barriers to siRNA delivery

Although siRNA has fewer obstacles than miRNA and shRNA, its delivery still has remained a challenge for many years and there are several barriers to successful siRNA delivery. The barriers depend on the target organ and desired

route of administration: localized administration, or systemic administration. Localized siRNA delivery has fewer barriers than systemic siRNA delivery, avoiding the first pass effect in the liver and in many cases interaction with serum nucleases.

3.1 Extracellular barriers

When systemically administrated, naked siRNA is readily degraded by serum exo- and endonucleases in the bloodstream. Both naked siRNA and its metabolites are eliminated by renal filtration. These obstacles decrease the plasma half-life of siRNA to less than 10 min. [8, 12-14]The approaches to overcome siRNA degradation and elimination include chemical modifications of the RNA and the use of nanocarriers. Modifying the sugars, backbone, or bases of oligoribonucleotides can enhance the stability of siRNA to overcome intravascular degradation.[15] The most common RNA modifications are illustrated in Table 1.

Table 1. Chemical modifications of siRNA[2]

Modification	Modification method	Outcome	Reference
Base	Internal uridine to rf (2,4-difluorotoluyl ribonucleoside) substitution	Enhanced resistance to serum nucleases	[16]
Sugar	2'-Deoxy-2'-fluoro-β-D-arabino,	Increase the half-life in serum	[17]
	2'-O-MOE modification,		
	2'-O-Me modification		
	Locked nucleic acids	Increased half-life reduces immune activation	[18]
	4'-Thio modified the ring oxygen		
		Enhanced resistance towards nucleases	[19]
Backbone	Phosphorothioate (PS) modifications	The longer half-life of duplex	[20]
	Morpholino oligomers	More potent	

Since modification of siRNA alone may not be enough to achieve target delivery and therapeutic activity, physical encapsulation with nanocarriers is needed in many cases. However, the the size of nanocarriers can cause recognition of the siRNA delivery system by the reticuloendothelial systems (RES). [8] The RES/mononuclear phagocytic system includes the liver, spleen, lung, and bone marrow. It

contains fenestrated capillaries and is saturated with phagocytic cells, such as macrophages, and monocytes.[21] Nanoparticles with sizes over 100 nm are often reported to be trapped by the RES in the liver, bone marrow, spleen, and lung, leading to degradation by activated monocytes and macrophages.[21] However, the RES filtration process sometimes is helpful when the nanoparticles are supposed to target an RES-rich organ.[22] The surface charge and size of the nanoparticles may affect RES uptake and biodistribution. Thus efficiently modulating the surface chemistry, charge, and size of the nanoparticles can avoid RES clearance.[23] For example, nanocarriers can be grafted with PEG (polyethylene glycol) and other surfactant copolymers such as poloxamers that allow the nanoparticles to exhibit a long circulation time in blood.[24, 25] However, excessive PEGylation can shield the positive charge of the nanoparticle surface and decrease cellular uptake. For instance, with the increase from 1-2 to 5 mol% PEGylation of siRNA-lipopolyplexes, the siRNA-mediated gene silencing of PTEN protein in vitro was eradicated.[26] In addition, PEG can induce complement activation which is involved in the clearance of siRNA delivery systems.[27] An “accelerated blood clearance (ABC) phenomenon” with loss of long-circulation characteristic was evidenced after repeated injections of PEGylated liposomes of approximately 100 nm due to involvement of anti-PEG IgM and substantial complement activation.[28] Ju et al. investigated the levels of anti-PEG antibodies in 130 adults after the injection of COVID-19 vaccine BNT162b2 produced by Pfizer-BioNTech and mRNA-1273 produced by Moderna.[29] The anti-PEG IgG increased 13.1-fold on average (mRNA-1273) and 1.78-fold after vaccination with BNT162b2. Additionally, anti-PEG IgM levels increased 68.5-fold (mRNA-1273) and 2.64-fold (BNT162b2).[29] To overcome the PEG immunogenicity in the future, it is meaningful to find alternatives to PEG.

3.2 Cellular barriers

Once extravasated into the interstitium, siRNA formulations need to cross the cell membrane and reach the cytoplasm. However, the cell membrane is a formidable barrier, especially for naked siRNAs. As negatively charged and hydrophilic macromolecules cannot cross cell membranes passively, their cellular uptake is limited. Therefore, the encapsulation of siRNA with viral or non-viral vectors represents effective siRNA delivery approaches.

Following cellular internalization, the endosomal entrapment and lysosomal degradation of siRNA-nanocarrier is a major impediment for non-viral carriers and often contributes to low transfection efficiency. Thus, a carrier that allows for the escape from endosomes is essential for gene silencing by siRNA. The nanocarriers can escape from the endosome via different mechanisms, although a complete understanding is not achieved yet:

3.2.1 Osmotic rupture

Osmotic rupture is also known as the “proton sponge effect”, which was the first theory to explain the high transfection efficiency of PEI.[30] Once cationic PEI polyplexes are entrapped within endo-lysosomes, the remaining non-protonated amino groups of the polyplexes can be protonated due to the proton influx mediated by the membrane-bound V-ATPase, thus buffering and delaying the acidification within the vesicles. Counter-ion pathways such as chloride channels and transporters mediate the influx of anions (Cl^-) or efflux of cations (H^+) and compensate for the accumulation of protons and thus lead to an osmotic imbalance.[31, 32] Moreover, it is hypothesized that the volume of the PEI polyplexes will be enlarged due to the stronger repulsion of the intramolecular positively charged amino groups, which is the so-called “umbrella effect”.[33, 34] The evolving osmotic imbalance is counteracted by the entrance of water. The continuous swelling of the endosome and the expansion of the polymer finally results in the bursting of the endo-lysosomal compartment and the entrapped cargo was subsequently released within the cytoplasm.[35]

Besides PEI, several other cationic polymers were found to act as “proton sponges”; for instance, poly(amidoamine) (PAMAM) and poly[2-(Dimethylamino)ethyl methacrylate] PDMAEMA. The excellent behavior of PAMAM (pK_a 3 to 6) and PDMAEMA (pK_a ~ 7.5) were also related to the high buffer capacities of tertiary amino groups within the polymer structures.[36] Poly-$_L$-Lysine (PLL) has poor transfection ability, which is probably caused by the primary amino groups being fully protonated and its resulting poor buffering capacity below pH 8.[37, 38] However, the “proton sponge” hypothesis is still controversially discussed in the scientific community due to the inconsistency of experimental evidence.[35]

3.2.2 Nanocarrier swelling

Some stimuli-responsive polymers swell in response to pH or ionic concentration or simply by absorbing water, and this strategy is practically used side by side with osmotic swelling of the endosome caused by the proton sponge or the pH buffering effect.[39] For example, Lee et al. synthesized a virus-mimetic nanogel consisting of a hydrophobic polymer core and two layers of a hydrophilic shell. The core was made of poly(L-histidine-co-phenylalanine), PEG (M_n 2000 Da) as the inner shell, and bovine serum albumin (BSA) as a capsid-like outer shell. The size of the nanoparticles at pH 7.4 was 55 nm, but at pH 6.4 the nanoparticles swelled to 355 nm. The authors suggested that the nanogels could have escaped from the endosomes by swelling and the buffering effect due to the histidine residue.[40]

3.2.3 Membrane destabilization

The membrane destabilization effect can be mediated by polyplexes or free polymers. Different from the “proton sponge” effect, a key characteristic of membrane destabilization is that the endo-lysosomal compartment is intact during and after the escape. Once the cationic polyplexes are entrapped within an endo-lysosomal compartment, the polyplexes can be protonated due to the acidic environment caused by the activity of the membrane-bound ATPases. The protonated polyplexes directly interact with the anionic lipids of the inner membrane leaflet, which destabilizes the membrane locally to form nanoscale holes from which the polyplexes finally escape.[41-43] It was hypothesized that a dynamic equilibrium between dissociated polymer chains and polyplexes supports the polymer-mediated membrane destabilization. The free polymer is assumed to intercalate into the cell plasma membrane before endocytosis and the polymer cannot be cleared. The free polymers interact with the membrane in terms of a “carpet structure” or polymer-supported membrane holes, as a result, the lipid layer is imparied, and the nanoparticles are released. [41, 44] This free-polymer mediated membrane destabilization model may also explain the cytotoxic effects of cationic polymers.[45]

3.2.4 Membrane fusion

This model of endosomal escape is achieved by the fusion of lipids, peptides, or proteins with the endosomal membrane. This phenomenon is a typical characteristic of viruses. The membrane peptide of viruses changes its conformation when exposed to pH change and allows the virus to fuse with the lipid bilayer membrane of the endosomes.[39, 46] For example, the haemagglutinin protein from the influenza virus undergoes a conformational change upon exposure to low pH inside the endosome and fuses with its membrane to allow content leakage into the cytosol.[47] Some peptides such as the HIV-1 fusion peptide gp41 can fuse with plasma and endosomal membranes at neutral pH.[48] Coupling the fusogenic proteins to cationic polymers has been proven a useful strategy for nucleic acid delivery. For example, when Kwon et al. modified PEI with a lytic peptide from the endodomain of HIV gp41 (HGP), the GAPDH expression in Hela cells was significantly inhibited compared with unmodified polyplexes and the endosomal escape was observed by confocal microscopy.[49] Oliveria et al. added the influenza-derived fusogenic peptide diINF-7 to a commercially available transfection reagent Lipofectamine™. The endosomal escape of siRNA was strongly promoted and the inhibition of EGFR expression in human epidermoid carcinoma A431 cells was increased more than 2-fold.[50] The incorporation of so-called fusogenic lipids such as dioleoylphosphatidylethanolamine (DOPE) into a lipoplex can increase the interaction of nanoparticles with the membranes of endosomes, thus promoting endosomal release.[51, 52] Unsaturated cationic lipids can enhance siRNA delivery and gene knockdown efficacy compared with those containing saturated cationic lipids.[51]

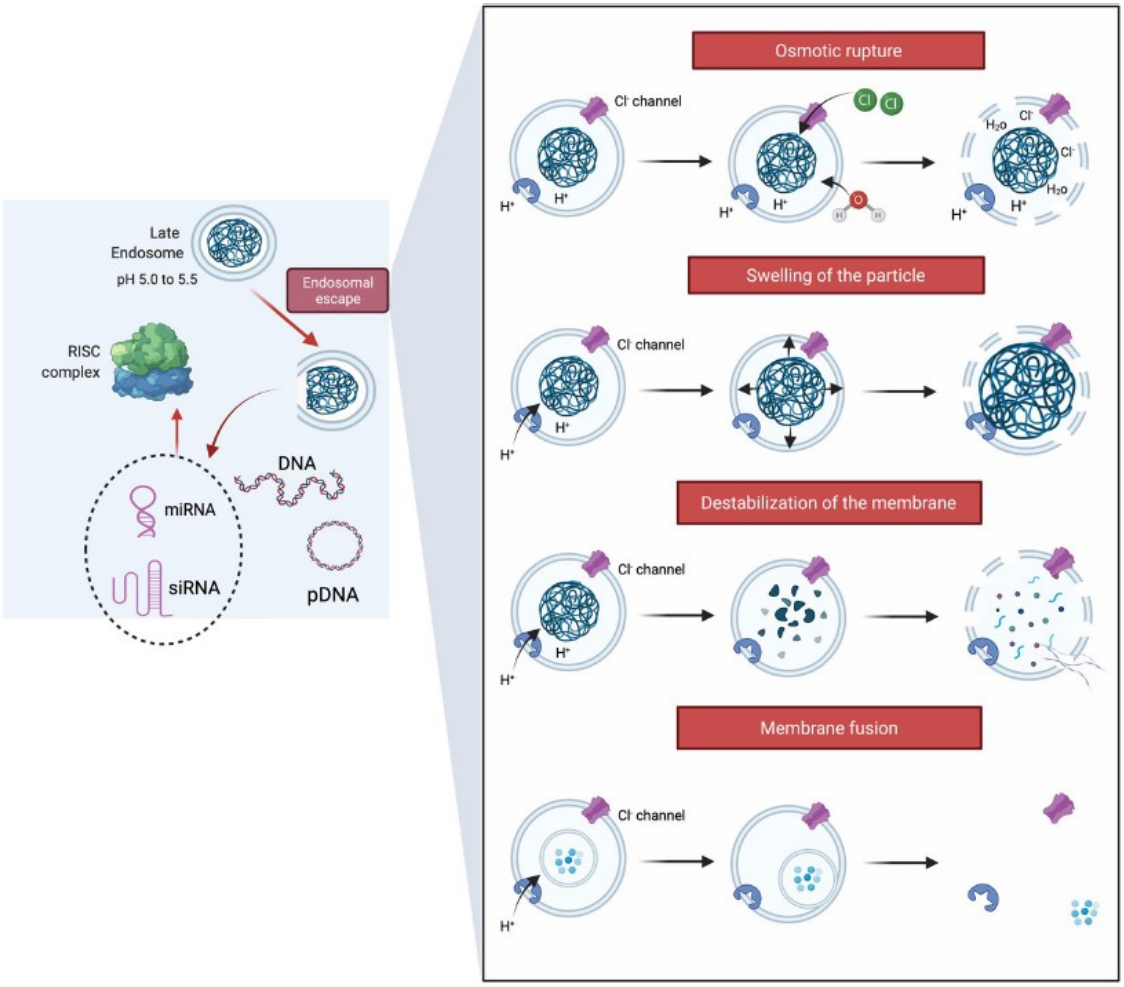

Figure 2. Proposed mechanism of endosomal escape 1) Osmotic rupture, proton sponge effect, 2) swelling of nanocarriers, 3) membrane destabilization, 4) membrane fusion (Reproduced with permission. Copyright Springer Nature, 2022)[39]

4. Cellular uptake pathway

The affinity of cationic polyplexes to the cell membrane is mostly facilitated by surface glycoproteins or receptors.[53, 54] The uptake of cationic polyplexes, in principle, is described by the process of endocytosis, whereby the exact endocytosis pathway strongly affects the intracellular trafficking of the cargo as well as the transfection efficiency.[35] The endocytosis pathway depends on the size of the polyplexes, the polymer type, and the cell type.[55-57] Clathrin-dependent and independent endocytosis, caveolae-dependent endocytosis, and macropinocytosis are commonly involved in the cellular internalization of cationic polyplexes.[58, 59] Both clathrin-dependent and clathrin-independent endocytosis results in the lo-

calization of polyplexes within early endosomes. The activity of membrane-incorporated vacuolar-type ATPases (V-ATPase, proton pump) drops the pH of these compartments from neutral to a lower pH of 6.5 to 6. From early endosomes, which are directed to sorting endosomes, the content is recycled back by exocytosis or other intracellular recycling circuits involving the trans-Golgi network. In addition, the cargo in early endosomes can mature into late endosomes with lower pH of around 5.5 to 5.0 and finally fuse with lysosomes, which has a lower pH 5.0 to 4.5 and degrading enzymes (lysosomal hydrolases).[35] Autophagy is another lysosomal-mediated degradation pathway, where maturated autophagosomes fuse with lysosomes to become an autolysosome responsible for the degradation processes, which plays a critical role in the clearance of misfolded proteins, invaded pathogens,[60] damaged organelles or nanomaterials.[61] Since autophagy can be induced by endosomal membrane damage, when the polyplexes escape from damaged endosomes, released polyplexes could still be cleared by autophagy, thus posing a further challenge for the successful gene delivery.[61]

In contrast to clathrin-dependent endocytosis, the polyplexes internalized by caveolae-mediated endocytosis are surrounded by a neutral pH value and less hostile environment within the caveosomes. The caveosomes and their cargo move on to the Golgi apparatus and the endoplasmic reticulum (ER) employing microtubules.[57, 62] Nevertheless, caveolae are able to interact with early endosomes, thus not entirely avoiding the acidification processes.[63]

Macropinocytosis was initially defined as the actin-driven non-specific bulk uptake of extracellular fluid, the hallmark of which is actin-driven membrane ruffling, leading to the formation of enclosed vesicles with a size greater than 200 nm.[64] More molecular regulators were found governing this process. For instance, Ras, phosphoinositide 3'-kinase (PI3 K), SGEF, ARF6 at the plasma membrane, and PIKfyve, Rabankyrin-5, SWAP-70, SNX1, SNX9, and SNX18 are associated with macropinosomes.[65] Once polyplexes are internalized into macropinosomes, they may enter the classical endosomal/lysosomal pathway or be recycled back to the plasma membrane.[65, 66]

The fate of the polyplexes and the related transfection efficiency strongly depends on the cellular uptake pathway. To avoid intracellular expulsion or enzymatic degradation of the nucleic acids, polyplexes should escape from endocytic vesicles

at an early stage of endocytosis.[35] Currently, most nanocarriers enter cells via several endocytosis pathways by default rather than design. With the rapidly growing fundamental knowledge of these endocytosis processes, there are opportunities to design the polyplexes or other nanocarriers to target specific pathways or cells and achieve more efficient siRNA delivery and gene silencing.

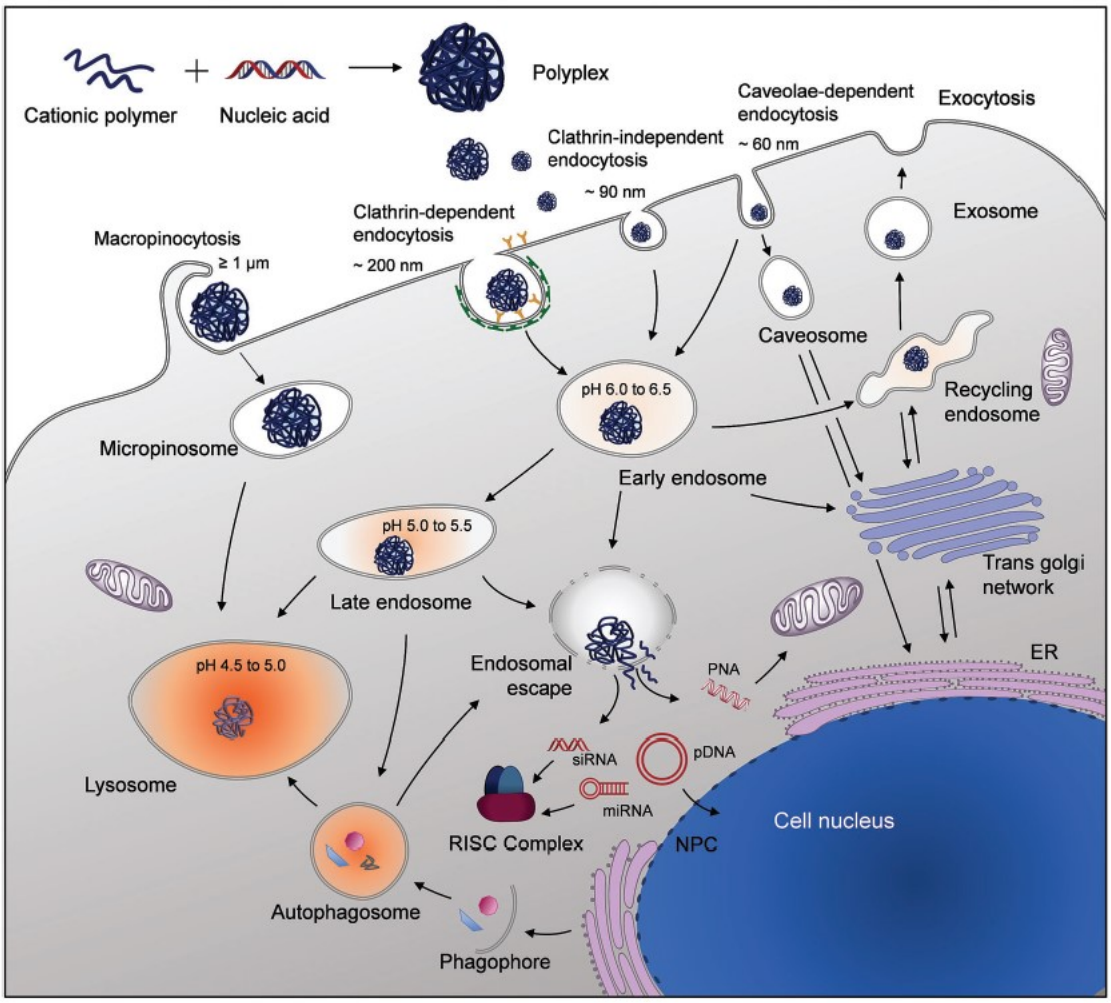

Figure 3. The formation of polyplexes and its endocytosis pathways[35] (Reproduced with permission. Copyright the Royal Society of Chemistry).

5. Biomaterials in siRNA delivery

Various carriers have been developed for siRNA delivery during the past years. The nanocarriers for siRNA delivery can be generally divided into two categories, viral vectors, and non-viral vectors. Viral vectors were first studied for siRNA delivery. However, viral vectors can activate immune responses and cause unacceptable toxicity.[22, 67] Therefore, non-viral vectors such as synthetic lipids and polymers have been developed to offer alternatives to viral vectors for nucleic

acid delivery, and are carefully designed and formulated to avoid immune responses.[68] Below, several categories of non-viral vectors are highlighted related to this thesis and examples of their construction and use are provided.

5.1 Lipids and lipid analogues

Phospholipids are natural components of cell membranes that form lipid bilayers.[69] Liposomes have been developed as drug delivery carriers and are widely used to encapsulate small molecule drugs.[69] Lipids with single or multiple cationic centers which can form lipid-based nanoparticles (LNPs) are highly effective carriers for siRNA delivery.[70] For example, Zimmermann et al. utilized liposomes to deliver siRNA systemically to target the apolipoprotein B (ApoB) in non-human primates, where they found that intravenous injection of an LNP formulation mediated RNAi-mediated gene silencing in cynomolgus monkeys. After a single siRNA injection for 48 h, the APOB messenger RNA expression in the liver showed a dose-dependent reduction, with maximal silencing efficiency of more than 90%.[71] The formulation is composed of an ionizable lipid, 1,2-dilinoleyloxy-N, N-dimethyl-3-aminopropane (DLin-DMA), which is an ether analog of 1,2-dioleoyl-3-(N, N-dimethylamino)propane (DODAP). These studies were important groundwork for the formulation and approval of Onpattro® but also for the hast approval of mRNA vaccines during the COVID-19 pandemic[72]. The representative cationic lipids were summarized in **Figure 4**.

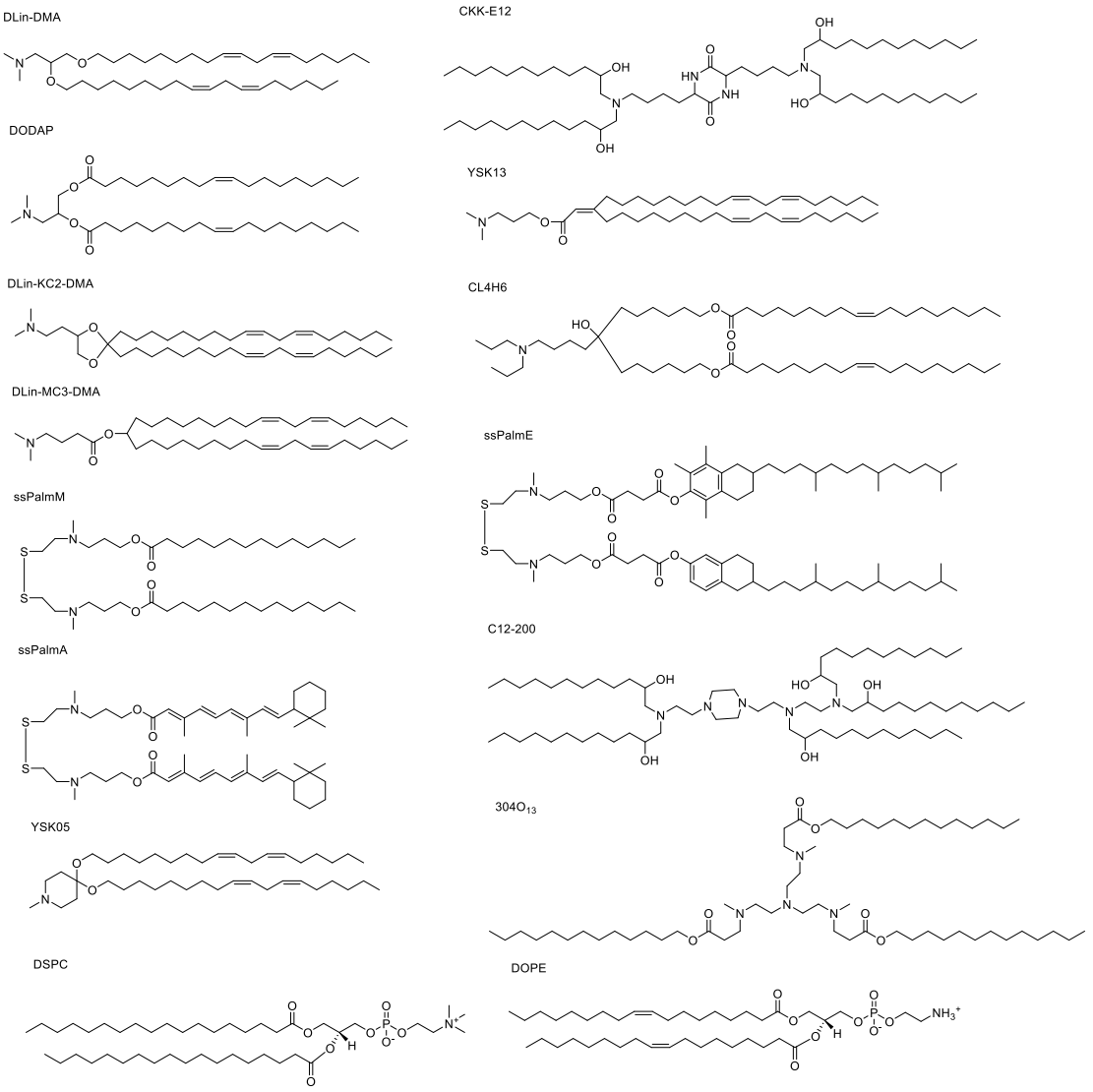

Figure 4. The chemical structure of several representative cationic lipids.

LNPs possess excellent biocompatibility, biodegradability, low toxicity and immunogenicity, structural flexibility, and ease of large-scale preparation.[73] Cationic liposomes have been developed for the treatment of diseases and have shown promising pharmacological effects in animal models, but their instability in blood and toxicities are often the major concerns for clinical application.[74]

5.2 Polycations and polymers

The use of polycations and polymers as intracellular delivery systems for nucleic acid delivery, including plasmid DNA (pDNA), and siRNA has been studied for several decades.[75, 76] The physiochemical properties of polymers can be rationally designed and adjusted through bottom-up chemical synthesis.[77] The eventual structure of the resulting polymer covers linear, branched, hyperbranched, and

star-shaped molecules which can be fabricated into micelles, polyplexes, polymer-siRNA conjugates, any many more. Some representative polycations and polymers are summarized in **Figure 5**, and several of them will be introduced in detail.

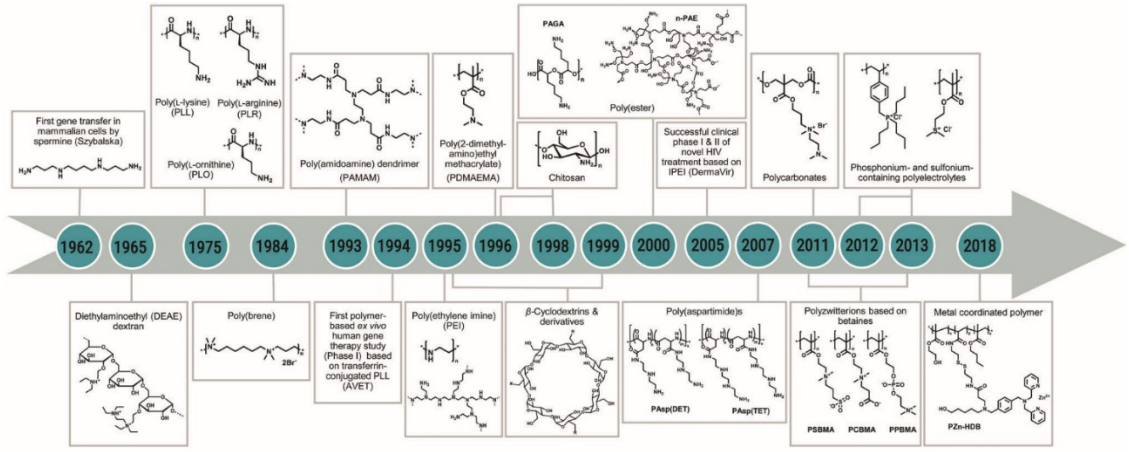

Figure 5. Polycations and polymers used for nucleic acid delivery in the past 50 years[35] (Reproduced with permission. Copyright Royal society of chemistry, 2018)

5.2.1 Spermine and its derivatives

Spermine is a naturally occurring linear tetraamine with two primary amines and two secondary amines which was first reported as a component of seminal plasma by Leeuwenhoek in 1678.[78] Spermines aid in packaging cellular DNA into a compact state in eukaryotic cells which is essential in cell growth processes.[79, 80] Spermine was first reported to deliver genes into mammalian cells in the early 1960s.[81] However, exogenous spermine poorly condenses and transfects nucleic acids into cells, which could be a result of its low molecular weight (~ 200 Da).[82, 83] Polymerization of spermine to increase its molecular weight has been proven to increase its siRNA delivery. Kolhatkar et al. synthesized star-shaped tetraspermine (SSTS) for delivery of an oligonucleotide termed “T-oligo”. SSTS exhibited lower cytotoxicity than spermine and BPEI, and it also facilitated cellular uptake and nuclear accumulation of T-oligo.[84] Lote et al. synthesized bisspermine and tetraspermines with linear, cyclic, dendritic, and quatrefoil architecture. Dendritic tetraspermine exhibited the highest binding affinity of siRNA.[85] Similarly, Elsayed et al. synthesized linear bisspermine, linear tetraspermine, and dendritic tetraspermine for siRNA delivery.[79] They found that the transfection efficiency

can be enhanced by increasing the degree of polymerization and the charge density with minimal cytotoxicity. Surprisingly, linear tetraspermine/siRNA polyplexes showed higher cellular uptake although the polyplexes were almost neutral compared with the dendritic tetraspermine.[79] This observation was interpreted as each molecule of the linear tetraspermine being capable of interacting with more siRNA molecules than the dendritic tetraspermine, resulting in a better charge neutralization but better encapsulation and higher cellular uptake of siRNA. The linear tetraspermine also showed the best gene-silencing efficiency at both mRNA and protein expression levels.[79]

In a different approach, grafting spermine to other polymers was an alternative and successful strategy for nucleic acid delivery. Chitosan is a family of linear binary polysaccharides comprised of beta (1-4) linked 2-amino-2-deoxy-beta-D-glucose (GlcN; D-unit). Chitosan is biocompatible, biodegradable, and low-toxic with high cationic potential, however, its transfection efficiency is low.[86, 87] Liang et al. conjugated spermine to chitosan to synthesize Chitosan-graft-spermine (CHI-g-SPE).[88] CHI-g-SPE copolymer showed high DNA binding capacity and high protection of DNA from enzymatic degradation. The CHI-g-SPE/DNA polyplexes also showed higher GFP expression compared with chitosan/GFP complexes.

5.2.2 Polyethylenimine and its derivatives

Polyethylenimine (PEI) was first synthesized in 1995 and is a commonly used cationic polymer for nucleic acids delivery, including DNA, siRNA, and oligonucleotides. Two morphologies of PEI, linear PEI (LPEI) and branched (BPEI), are commercially available with a broad molar mass range from 200 g/mol to 750 000 g/mol. PEI can encapsulate nucleic acids and form polyplexes with sizes of less than 100 nm, which can transfect cells efficiently both in vitro and in vivo.[89] The 25 000 g/mol PEI is the most utilized polymer in gene transfer.[90-92] Independent of the structure of PEI, 50% to 55% of the amino groups of PEI can be protonated as revealed by potentiometric titrations and computational approaches.[93, 94] The close vicinity (7 Å distance between two charges) of the amino groups can cause electrostatic repulsion which can explain this partial protonation behavior.[37, 95, 96] The highest buffer capacities of PEI lie between pH 8 and 10 based on the pK_a value. Nevertheless, PEI has a broad buffer capacity from the basic to the acidic

milieu with pH 4 to 7 (pK_a ~ 4.5). These properties enable PEI to achieve efficient endosomal escape ability via the “proton sponge effect”. PEI offers more efficient protection against nuclease degradation than other polycations, for example, poly(L-lysine), possibly due to its high charge density and more efficient complexation. However, the excessive amount of positive charges result in high toxicity of PEI, which is currently the main obstacle of its application in the clinic. [89] Many strategies have been proposed to overcome this obstacle. For instance, the cross-linking of low molecular weight PEI,[97], coupling PEI with hydrophilic or hydrophobic molecules,[98] shielding the positive charge by the decoration of polyplexes’ surfaces, and the conjugation of PEI with ligands.[99]

Low molecular weight PEI displays low toxicity, yet transfection efficiency is also low. Inspired by the effective transfection behavior of high molecular weight PEI, Gosselin et al. cross-linked PEI (M_w 800 Da) with DSP (Dithiobis(succinimidylpropionate)) and DTBP (Dimethyl•3,3’-dithiobispropionimidate•2HCl) and evaluated the transfection efficiency in CHO cells using a luciferase reporter gene. The results showed that the cross-linking reagent, the extent of conjugation, and the N/P ratio affect the transfection efficiency of the cross-linked PEI.[97] Similarly, Ge et al. conjugated PEI (M_w 800 Da) with 1,4-butanediol bis(chloroformate), and the polymer condensed siRNA at an N/P ratio of 38.35 or above. The nanoparticles achieved around 46.46% gene silencing efficiency in the SMMC-7721 cell line which stably expresses the GL3 luciferase gene. The nanoparticles at N/P 115.05 were injected into the SMMC-7721 tumor-bearing mice and inhibited 63.71% of luciferase expression. Dahlman and Barnes et al.[100] modified low molecular weight PEI (~ Mw 600 Da) with C15 epoxide-terminated lipids at a molar ratio of 1:14 and formulated with C_{14}PEI2000 to produce nanoparticles termed 7C1. 7C1 reduced endothelial gene expression over by 90% at a dose of 0.10 mg/kg and by 50% at a dose of 0.02 mg/kg. Different from traditional lipid-based nanoparticles, this formulation can deliver siRNA to lung endothelial cells at low doses without off-target effects in other cells, and organs.[100]

Multifunctional ABC type block copolymers consisting of polyethylene glycol (PEG), a polyester block like poly-ε-caprolactone (PCL), and polyethylenimine (PEI) are alternative carriers for nucleic acids delivery.[101, 102] PEG is hydrophilic and its chain is flexible, electrically neutral, and absent of functional groups. Serum protein cannot bind to PEG-modified surfaces, thus the blood circulation time of PEGylated nanoparticles can be extended.[103] PCL is biodegradable in aqueous media and arranges as a hydrophobic core and can thus be a reservoir for

water-insoluble drugs.[104] Endres et al. studied PEG-PCL-lPEI triblock copolymers in detail and utilized low molecular weight PEI (Mw 2500 Da) with various molecular weights of PEG and PCL segments. The polymers with more hydrophilic segments assembled into micelle-like structures and diameters of several tens of nanometers, while the more hydrophobic polymers precipitated into larger particles with more than 100 nm in. More PEG also led to increased stability and decreased cytotoxicity.[101] Endres and his colleagues also used PEG500-PCL10000-PEI2500 for siRNA and quantum dot delivery. The nanoparticles showed a rapid cellular uptake within 2 h and 61 ± 5% knockdown in vitro and 55 ±18% knockdown in vivo.[105]

Coupling PEI with ligands is another representative strategy for siRNA delivery. Modifying PEI with targeting ligands can selectively deliver siRNA to specific cells or organs, thus decreasing the toxicity of the polyplexes and reaching the site of action. For example, our group developed a conjugate consisting of transferrin (Tf) and PEI, namely Tf-PEI. The polyplexes prepared from Tf-PEI demonstrated optimal physiochemical properties such as size, zeta potential, and siRNA encapsulation efficiency. The cellular uptake and gene knockdown efficiency in human primary ATCs were enhanced. Moreover, Tf-PEI polyplexes selectively delivered siRNA to activated T cells in the lung confirmed in a murine asthmatic model.[106] Kandil et al. conjugated the membrane lytic melittin to PEI (Mel-PEI) to enhance the endosomal escape of the polyplexes. In combination with Tf-PEI (Tf-Mel-PEI), the polyplexes delivered plasmid DNA to Jurkat cells successfully and demonstrated higher transfection efficiencies than Lipofectamine™ 2000. Tf-Mel-PEI also achieved significant GFP knockdown in H1299-eGFP cells, around 70% of GAPDH knockdown in Jurkat cells, and 76% GAPDH knockdown in activated human primary $CD4^+$ T cells.[107] Liu et al. synthesized polyethylenimine-graft-polycaprolactone-block-poly(ethylene glycol)-folate (PEI-PCL-PEG-Fol) to deliver siRNA to cancer cells. The PEI-PCL-PEG-Fol/siRNA polyplexes showed enhanced cellular uptake and gene knockdown in SKOV-3 cells which overexpress the alpha folate receptor.[108] The polyplexes also showed excellent stability in vivo during the analysis of 2 h and a longer circulation half-life than hyPEI25kDa/siRNA polyplexes. Due to the effective folate targeting and the prolonged circulation, 17% deposition of the i.v. injected siRNA per gram was observed in the tumor after 24 h.[108]

5.2.3 Poly(β-amino ester)s

Poly(β-amino ester)s abbreviated as PBAE or PAE refer to a group of polymers synthesized from acrylates and amines by a one-pot, atom-economic Michael addition without the production of any side products.[109] In 1983, PBAEs were first synthesized by Chiellini et al. based on poly(amidoamines) developed by Ferruti in 1970.[110, 111] The research interest for PBAEs was raised significantly after its use as a transfection reagent for DNA delivery by Langer's group in 2000.[112] PBAEs with several intrinsic features make them particularly attractive for gene delivery: PBAEs contain positive charges due to the presence of amino groups to complex genetic material; the hydrolysis of ester bonds in the polymer backbones increases its biodegradability and biocompatibility; the possibility to tailor the properties (e.g. buffering capacity, pK_a value) by combination of different monomers.[112, 113] PBAEs are significantly less toxic than other cationic polymers, such as PEI,[114] poly(L-Lysine) (PLL),[115] poly[2-(dimethylamino)ethyl methacryalte] (PDMAEMA).[116] Nevertheless, increasing the number of carbons in the backbone or side chain leads to increased cytotoxicity.[117] The degradation of PBAEs under physiological conditions yields small molecular weight and biologically inert derivatives (β-amino acids) which were determined to be noncytotoxic compared with PEI.[112, 114, 118]

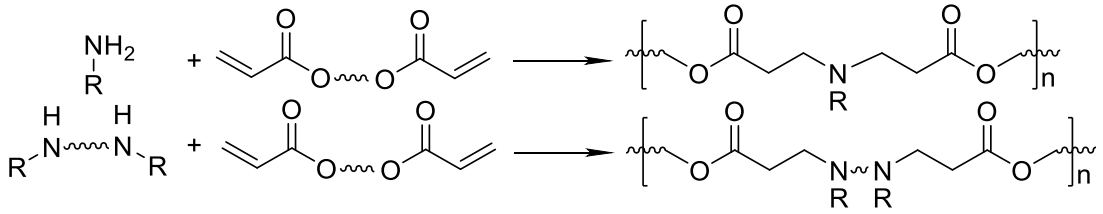

Figure 6. Synthesis route of poly(β-amino ester)s by addition of primary or bis(secondary amine) to diacrylates.

According to the architectures of PBAEs, they can be classified as linear PBAEs, branched/hyperbranched PBAEs, star-shaped PBAEs, etc. The first generation of PBAEs refers to a linear architecture, and they are widely used for gene delivery. Langer's group heavily investigated the structure-property relationship of PBAEs. For example, Lynn and coauthors synthesized 140 different PBAEs from 7 diacrylates and 20 amines with molar masses ranging from 2000 to 50 000 Da.[114] Two of them were synthesized from 1,4-butanediol diacrylate with 3-(1H-

imidazol-1-yl)propan-1-amine, and polymers based on 1,4-cyclohexanediylbis(methylene) diacrylate synthesis with 4-amino-1-butanol mediated the highest gene delivery efficacy and revealed transfection levels 4-8 times higher than PEI.[114] This work was further complemented by Akinc and his colleagues in 2003 and Anderson et al. in 2005.[119, 120] Several best-performed PBAEs are shown in **Figure 7.**

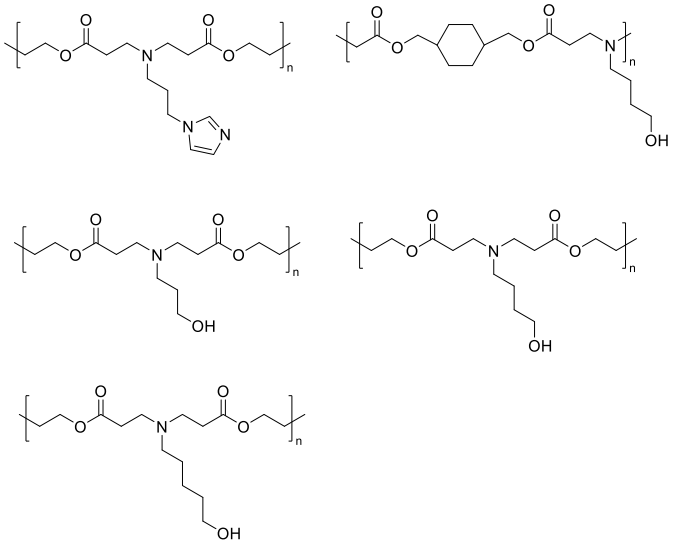

Figure 7. Several representative PBAEs performed best for gene delivery according to literature.

5.3 Others

Besides the lipids and polymers introduced above, many other vectors for siRNA delivery have been described, for instance, inorganic nanoparticle-based delivery systems (e.g. nanoparticles composed of gold,[121] iron oxide,[122] mesoporous silica,[123] calcium phosphate[124] and carbon[125], etc.). Compared to lipid and polymer-based nanoparticles, inorganic nanoparticles feature smaller dimensions and narrower size distributions.[126] siRNA conjugates are another promising siRNA delivery platform. siRNA molecules can be directly conjugated to a polymer[127] or targeting ligand.[128] One example consists of clinically used trivalent GalNAc-siRNA conjugates targeting high capacity ASGPR (asialoglycoprotein receptor) on the cell surface[129] leading to the development of well-defined, single-component systems that optimize the minimal use of delivery material and extend the duration of activity.[130]

6. Aims of the projects

The main aim and task for this Ph.D. thesis was the synthesis of novel polymers for siRNA delivery. As introduced above, the delivery of siRNA remains challenged by a lot of barriers. Therefore, developing safe and efficient polymers for siRNA delivery is an important contribution to this field. To achieve our aims, we utilized two strategies in general: One is to develop spermine-based poly(β-amino ester)s for siRNA delivery, and the other one is to synthesize low molecular weight PEI-based copolymers for siRNA delivery. The aims for each chapter were summarized as follows:

Chapter 1. This chapter is the starting point of spermine-based poly(β-amino ester)s. The aims are 1) to synthesize the Boc-anhydride protected spermine (tri-Boc-spermine), which is an essential monomer for the synthesis of spermine-based PBAEs; 2) to develop the method of synthesizing PBAEs including optimization of solvents, temperature, reaction time, etc.; 3) to prepare polyplexes with the PBAEs and characterize them; 4) to evaluate the polyplexes in vitro to determine the gene silencing efficiency of PBAEs; 5) to asses therapeutically relevant gene silencing by PBAE polyplexes.

Chapter 2. This chapter is based on the results of Chapter 1, mainly to investigate if the hydrophobic modification of PBAEs can influence the siRNA delivery and gene silencing efficiency of PBAEs.

Chapter 3. This chapter is a logical extension of the first two chapters and aimed at assessing the role of hydrophobic modifications in siRNA delivery to obtain a deeper understanding of the structure/property relationship of the PBAEs. The use of the hydrophobic segment oleylamine was inspired by the current use of unsaturated lipids for siRNA delivery.

Chapter 4. This chapter investigated low molecular weight PEI (LMW-PEI) based copolymers for siRNA delivery. The aims include 1) developing the nanoparticle preparation method; 2) synthesis of LMW-PEI-based block copolymers; 3) characterization of nanoparticles; 4) and evaluation of the nanoparticles in vitro to understand the impact of polymer composition and preparation technique.

Chapter I

Synthesis and application of spermine-based poly(β-amino ester)s for siRNA delivery

Yao Jin, Friederike Adams, Lorenz Isert, Domizia Baldassi, and Olivia M. Merkel*

Contributions: I performed all the experiments with support of the coauthors and wrote the manuscript.

Abstract: Polyethylenimine (PEI) is a highly efficient cationic polymer for nucleic acid delivery, and although it is commonly used in preclinical studies, its clinical application is limited due to concerns regarding its cytotoxicity. Poly(β-amino ester)s are a new group of biodegradable and biocompatible cationic polymers which can be used for siRNA delivery. In this study, we synthesized Boc-protected and deprotected poly(β-amino ester)s, P(BSpBAE) and P(SpBAE) respectively, based on spermine and 1,4-butanediol diacrylate to deliver siRNA. The polymers were synthesized by Michael addition in a step-growth polymerization and characterized via ^{1}H-NMR spectroscopy and size-exclusion chromatography (SEC). The polymers can encapsulate siRNA as determined by SYBR gold assays. Both polymers and polyplexes were biocompatible in vitro. Furthermore, cellular uptake of P(BSpBAE) and P(SpBAE)-polyplexes was higher than for branched PEI (25 kDa) polyplexes at same N/P ratios. P(BSpBAE) polyplexes achieved 60% eGFP knockdown in vitro, which indicates that the Boc-protection can improve siRNA delivery and gene silencing efficiency of PBAEs. P(BSpBAE) polyplexes and P(SpBAE) polyplexes showed different cellular uptake mechanisms, and P(BSpBAE) polyplexes showed lower endosomal entrapment, which could explain why P(BSpBAE) polyplexes more efficient mediated gene silencing than P(SpBAE) polyplexes. Furthermore, transfection of an siRNA against mutated KRAS in KRAS-mutated lung cancer cells led to around 35% P(BSpBAE) to 45% P(SpBAE) inhibition of KRAS expression and around 33% P(SpBAE) to 55% P(BSpBAE) decreased motility in a migration assay. These results suggest that the newly developed spermine-based poly(β-amino ester)s are promising materials for therapeutic siRNA delivery.

Keywords: poly(β-amino ester)s; spermine; siRNA delivery; PBAE; lung cancer; KRAS

1. Introduction

RNA interference (RNAi) is a promising strategy to silence gene expression by microRNA or small interfering RNA (siRNA)[131]. After the first discovery of RNAi by Fire and Mello in 1998, RNAi-based therapeutics are now progressing rapidly. siRNA is a double-stranded RNA of 21-25 nucleotides per strand, which can be used to mediate RNAi and downregulate overexpressed or pathologically expressed genes.[132] During the COVID-19 pandemic caused by the SARS-CoV-2 virus, potential siRNA sequences against the SARS-CoV-2 genome or accessory proteins or targeting host factors have been suggested provide alternative ways in the fight against SARS-CoV-2.[133] However, the delivery of siRNA has remained a challenge. Due to its hydrophilicity, negative charges and high molecular weight (~13300 g/mol), siRNA duplexed cannot cross cell membrane passively, and thus their cellular uptake is limited. In addition, siRNA is rapidly degraded in blood and renally cleared.[134]

Numerous siRNA vectors have been developed in the past years, which can be mainly divided into viral vectors and non-viral vectors. Viral vectors can achieve high transduction but are associated with many safety problems such as immune responses and carcinogenesis.[135] Non-viral vectors, such as polycationic polymers including polyethylenimine (PEI), have emerged as favorable candidates due to their good efficiency at a low commercial cost.[136] However, low-molecular-weight PEI cannot deliver siRNA effectively, while high-molecular-weight (HMW) PEI is cytotoxic as a highly charged non-degradable macromolecule. HMW-PEI has been shown to induce cell necrosis and apoptosis in a variety of cell lines.[137]

Poly(β-amino ester)s abbreviated as PBAEs or PAEs refer to a polymer class synthesized from acrylatic compounds and amine-based monomers by Michael addition. The first representative of this class was synthesized based on linear poly(amido amines) by Ferruti et al. in the 1970s and named poly(β-amino ester) in 2000.[112] Prof. Langer's group first used this polymer for DNA delivery, and since then, the interest in poly(β-amino ester) grew significantly.[138] PBAEs are biocompatible, biodegradable and stimuli-responsive, which makes them very

promising for siRNA delivery.[139] PBAEs are biodegradable due to their hydrolysable ester bonds, which also decrease their cytotoxicity.[140] The charge-reversible amine groups can be protonated at specific pH-values and interact with negatively charged cargos electrostatically to deliver them.[141] In addition, PBAEs are compatible with various other polymers: for example, PEG, PCL, PLA, and other blocks can be conjugated to PBAEs to form block copolymers.[109]

Spermine is a naturally occurring tetraamine aiding in packaging cellular DNA into a compact state in eukaryotic cells[142]. However, spermine poorly condenses siRNA and shows a limited siRNA transfection efficiency because of its low molecular weight. Besides, the endosomal escape of spermine is also limited.[79] Polymerization of spermine to increase its molecular weight has been shown to be beneficial for siRNA delivery.[79, 85]

In lung cancer, KRAS (Kirsten rat sarcoma viral oncogene homolog) is the most frequently mutated gene, and KRAS mutations are found in approximately 27% of all lung adenocarcinomas.[143] The activating mutations in KRAS cause constitutive activation of the GTPase protein in the absence of growth factor signaling and result in a sustained proliferation signal within the cell which is related to the migration and invasion of cancer cells.[144] The inhibition of mutant KRAS has been proven to be critical for the successful treatment of lung tumors.[145, 146]

In this study, we designed spermine-based poly(β-amino ester)s to deliver siRNA against mutated KRAS. We tested the encapsulation efficiency of the polymers, characterized the polyplexes, and evaluated the polyplexes in vitro using H1299 cells and eGFP expressing H1299/eGFP cells. The endosomal entrapment and cellular uptake pathway of the polyplexes were also investigated. To achieve a therapeutic relevant gene silencing, siRNA against mutated KRAS (siG12S) was delivered to KRAS mutated A549 lung adenocarcinoma cells using P(BSpBAE) and P(SpBAE) polyplexes, and therapeutic efficacy was evaluated by migration assays and western blot analysis.

2. Materials & Methods

2.1 Materials

Spermine (Fisher Scientific, Acros, USA), ethyl trifluoroacetate (Sigma Aldrich, Taufkirchen, Germany), 1,4-butanediol diacrylate (TCI, Japan), di-tert-butyl dicarbonate (Sigma Aldrich, Taufkirchen, Germany), chloroform D (Eurisotop, Germany), Deuterium oxide (Sigma Aldrich, Taufkirchen, Germany) were purchased from the suppliers indicated. Methanol, n-hexane, dichloromethane, isopropanol, dimethyl sulfoxide (DMSO), and dry ice are provided by Ludwig-Maximilians-University Munich.

Branched PEI (25 kDa), HEPES (4-(2-hydroxyethyl)-1-piperazineethanesulfonic acid), thiazolyl blue tetrazolium bromide (MTT), chloroquine diphosphate, paraformaldehyde solution, 4', 6-diamidino-2-phenylindole dihydrochloride (DAPI), FluorSave Reagent, RPMI-1640 medium, fetal bovine serum (FBS), Penicillin-Streptomycin solution, Dulbecco's Phosphate Buffered Saline (PBS), trypsin-EDTA solution (0.05%), and Geneticin (G418) disulfate solution were purchased from Sigma-Aldrich (Taufkirchen, Germany). SYBR Gold Dye, Lipofectamine™ 2000, and Alexa Fluor 488 (AF488) were purchased from Life Technologies (Darmstadt, Germany).

Amine-modified eGFP siRNA (5´-pACCCUGAAGUUCAUCUGCACCACcg, 3´-ACUGGGACUUCAAGUAGACGGGUGGC) and scrambled siRNA (5´-pCGUUAAUCGCGUAUAAUACGCGUat, 3´-CAGCAAUUAGCGCAUAUUAUGCGCAUAp) were purchased from Integrated DNA Technologies (Leuven, Belgium). "p" denotes a phosphate residue, lower case letters are 2'-deoxyribonucleotides, capital letters are ribonucleotides, and underlined capital letters are 2'-O-methyl-ribonucleotides. siRNA against KRAS G12S (siG12S) was purchased from Eurofins Genomics (Ebersberg, Germany).

2.2 Synthesis and characterization of spermine-based poly(β-amino ester)s

2.2.1 Synthesis of tri-tert-Butyl Carbonyl Spermine (tri-Boc-spermine)

Tri-Boc-spermine was synthesized according to the literature with slight modifications.[147, 148] Spermine (1 eq.) was dissolved in methanol and stirred at -78 ℃ , ethyl trifluoroacetate (1 eq.) was then added into the solution of spermine drop-

wise, kept stirring at -78 ℃ for an hour and at 0 ℃ for an hour to afford predominantly the mono-trifluoroacetate (2, **Scheme 1**). Without isolation, di-tert-butyl dicarbonate (4 eq.) in methanol was added dropwise into the solution and stirred at room temperature for 2 days to protect all other amines to afford the tri-Boc-protected mono-trifluoroacetate (3, **Scheme 1**). Finally, the pH of the solution was adjusted to be above 11 by 25% ammonia and stirred overnight to cleave the trifluoroacetamide protecting group.

The reaction mixture was concentrated in vacuum and the residue was diluted with dichloromethane (DCM) and then washed with water and saturated NaCl aqueous solution, before it was dried by $MgSO_4$, filtered, and DCM was evaporated. After purification by column chromatography (CH_2Cl_2\MeOH\NH_3, aq. 7:1:0.1, SiO_2, $KMnO_4$; R_f = 0.413), the desired product tri-Boc-spermine (4, **Scheme 1**) was isolated as a colorless oil. Yield: 37%.

^{1}H NMR, 400 MHz, $CDCl_3$: 1.43–1.48 [m, 31H, 6-CH_2, 7-CH_2, O–C–(CH_3)3×3, overlapping]; 1.65 (m, 6H, 2-CH_2, 11-CH_2, NH_2); 2.68 (t, 2H, 12-CH_2); 3.08–3.23 (m, 10H, 1-CH_2, 3-CH_2, 5-CH_2, 8-CH_2, 10-CH_2). ESI-MS: m/z = 503.37963 ($C_{25}H_{50}N_4O_6$ + H)$^+$.

2.2.2 Synthesis of spermine and 1,4-butanediol diacrylate-based poly(β-amino ester)s

Tri-Boc-spermine (4, **Scheme 1**) (1 eq.) was mixed with 1,4-butanediol diacrylate (1 eq.), and stirred at 120 ℃ overnight. The product was dissolved with DCM, precipitated in n-hexane, and dried in vacuum to afford polymeric tri-Boc-spermine- and 1,4-butanediol diacrylate-based poly(β-amino ester) abbreviated as P(BSpBAE) (5, **Scheme 1**), which was then characterized by ^{1}H NMR spectroscopy and SEC (measurement relative to polystyrene and in chloroform at 30°C, 4 mg/mL). Yield: 83%.

^{1}H NMR (400 MHz, $CDCl_3$) δ 4.20 – 4.01 (m, 4H, 2CH_2), 3.19 (d, 12H, 6CH_2), 2.77 (s, 4H, 2CH_2), 2.43 (d, 4H, 2CH_2), 1.66 (d, 8H, 4CH_2), 1.55 – 1.34 (m, 33H, 9CH_3+4CH_2).

P(BSpBAE) (5, **Scheme 1**) was then dissolved in a mixture of trifluoroacetic acid (TFA) and DCM (TFA: DCM 1:20 v/v) and stirred for 2 h at room temperature to deprotect amino functional groups. DCM and TFA were evaporated in vacuo, and the residue was dissolved in distilled water and lyophilized to obtain the final

product: Spermine- and 1,4-butanediol diacrylate-based poly(β-amino ester) (6, **Scheme 1**), which will be termed as P(SpBAE) in short. Yield: 63%.

^{1}H NMR (400 MHz, D_2O) δ 4.19 (s, 4H, $2CH_2$), 3.55 (t, 4H, $2CH_2$), 3.36 (dd, 2H, CH_2), 3.13 (dt, 10H, $5CH_2$), 2.96 (d, 4H, $2CH_2$), 2.23 (s, 2H, CH_2), 2.09 (p, 2H, CH_2), 1.77 (d, 8H, $4CH_2$).

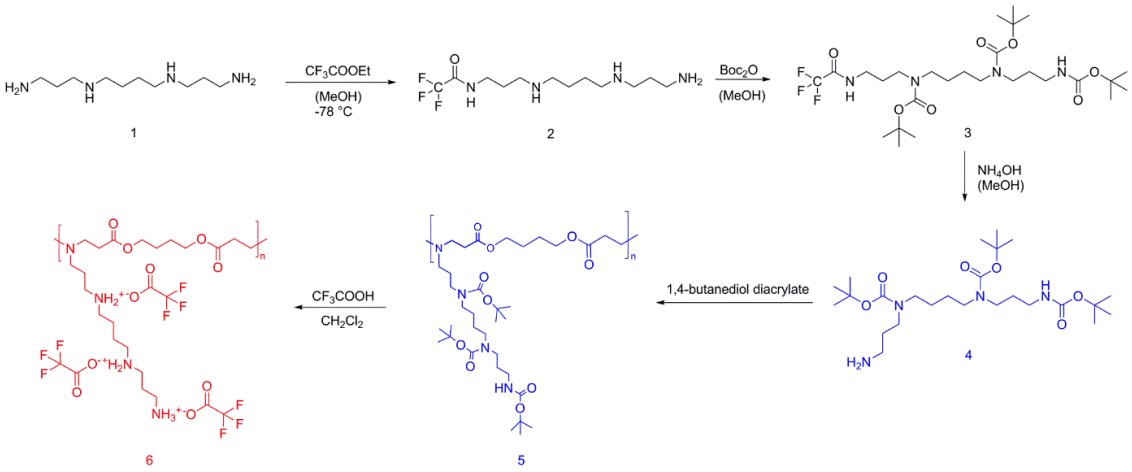

Scheme 1. Synthesis route of spermine and 1,4-butanediol diacrylate based poly(β-amino ester)s

2.3 Preparation and characterization of polyplexes

The polymer P(SpBAE) was dissolved in distilled water at a concentration of 1 mg/mL, and the polymer P(BSpBAE) was dissolved in acetone due to its limited solubility in water at a concentration of 10 mg/mL as stock solutions. To prepare polyplexes (the complexes of siRNA and polymer), various amounts of polymers calculated according to the respective N/P ratios were first diluted in 50 µL 10 mM HEPES buffer (pH 5.3). Subsequently, siRNA in 50 µL 10 mM HEPES buffer was mixed with polymer solution via pipetting. After incubation at room temperature for 30 min, the size and zeta potential of the polyplexes in 10 mM HEPES buffer were tested using a Zetasizer Nano ZS (Malvern Instruments, Malvern, UK).

The amount of polymer was calculated according to the following equation:

m (polymer in pg) = *n* siRNA (pmol) × 52 × N/P × Protonable unit (g/mol),

where 52 is the number of nucleotides of the 25/27mer siRNA; N/P ratio is the molar ratio of the protonable polymer amino groups (N) and the siRNA phosphate groups (P); The protonable unit was calculated by dividing the molar mass of the

repeating unit by the number of the protonable chemical groups in each repeating unit.

2.4 siRNA encapsulation efficiency by SYBR gold assay

To evaluate the siRNA encapsulation capacity of P(BSpBAE) and P(SpBAE), SYBR Gold assays were carried out.[149] SYBR Gold is a proprietary unsymmetrical cyanine dye which can bind with free RNA or DNA molecules and emits thousand-fold fluorescence upon excitation.[150] In brief, polyplexes were prepared as described above at N/P ratios 0, 1, 3, 7, 10, 15, and 20. Subsequently, 100 µL of each polyplex solution was added to a black FluoroNunc 96-well pate (FisherScientific, Darmstadt, Germany). 4X SYBR Gold aqueous solution (30 µL per well) was added to each well and incubated for 10 min in the dark. The fluorescence intensity was determined using a fluorescence plate reader (Spark, TECAN, Männedorf, Switzerland, excitation: 485/20 nm, emission: 535/20 nm.). The fluorescence intensity of free siRNA (N/P = 0) was used as a control and set as 100% fluorescence.

2.5 In vitro compatibility assessment

The cytotoxicity of P(BSpBAE) and P(SpBAE) polymers and polyplexes was evaluated via MTT assays.[151] In brief, H1299 cells were seeded in 96-well plates (5000 cells/well). After incubation in a CO_2 incubator for 24 h, dilutions of P(BSpBAE) and P(SpBAE) in RMPI-1640 complete medium were added and incubated to reach a final concentration ranging from 1 to 100 µg/mL, and cells were grown in the CO_2 incubator for another 24 h. Subsequently, the PBAEs solution was removed and MTT (3-(4,5-Dimethylthiazol-2-yl)-2,5-diphenyltetrazolium Bromide) in serum-free RPMI-1640 medium was added and incubated at 37 °C for 4 h. Afterwards, the MTT solution was replaced with DMSO and incubated at room temperature for 30 min. The optical density was finally determined at 570 nm and corrected with background measured at 680 nm using a microplate reader (TECAN, Männedorf, Switzerland). The cytotoxicity of polyplexes at N/P 10 was determined accordingly.

2.6 Quantification of cellular uptake

The cellular uptake of P(BSpBAE) and P(SpBAE) polyplexes was quantified by flow cytometry. The polyplexes were prepared as described above using Alexa

Fluor 488-labeled siRNA (AF488-siRNA). PEI and Lipofectamine ™ 2000 were used as controls. H1299 cells were seeded in a 24-well plates (50 000 cells/well). After incubation in the CO_2 incubator (37 ℃, 5% CO_2) for 24 h, polyplexes containing 50 pmol AF488-siRNA at N/P 10 in RPMI-1640 complete medium were added and incubated in the incubator for 24 h. Subsequently, the polyplexes solution was discarded, and the cells were rinsed with PBS and detached with 0.05% Trypsin-EDTA. The detached cells were then washed with PBS another 2 times and analyzed via flow cytometry (Attune NxT Acoustic Focusing Cytometer, Thermo Fisher Scientific, Darmstadt, Germany) with or without quenching by Trypan blue.

2.7 In vitro eGFP knockdown

To determine if the polyplexes can silence genes on the protein levels, silencing of the enhanced green fluorescent protein reporter gene (eGFP) was quantified by flow cytometry. H1299/eGFP cells were seeded in 24-well plates (25 000 cells in 500 µL medium/well). After growth in the CO_2 incubator (37 ℃, 5% CO_2) for 24 h, the cells were transfected with P(BSpBAE) polyplexes and P(SpBAE) polyplexes composed of scrambled siRNA (siNC, 50 pmol/well) or siRNA against GFP (siGFP, 50 pmol/well) with or without chloroquine (100 µM). Lipofectamine™ 2000 formulated with siNC and siGFP were used as respective control treatment. After 48h in the incubator, the cells were detached and washed with PBS for flow cytometry measurements (Attune NxT Acoustic Focusing Cytometer, Thermo Fisher Scientific, Darmstadt, Germany).

2.8 Endosome entrapment

To visualize the endosomal entrapment behavior of the polyplexes, cells were imaged by confocal laser scanning microscopy (CLSM) after transfection with fluorescent siRNA. In brief, H1299 cells were seeded on 13-mm microscope cover glasses (VWR, Allison Park, PA, USA) in each well of a 24-well plate (50 000 cells/well). After growth for 24 h, the cells were further incubated with polyplexes formulated with 50 pmol of Alexa Fluor 488-labeled siRNA (AF488-siRNA) for 24 h. Subsequently, the polyplex containing medium was discarded and 75 nM Lysotracker Red™ DND 99 (Thermo Fisher Scientific, Darmstadt, Germany) solutions in full medium were added and incubated at 37 ℃ for 1 h in the CO_2 incu-

bator. The cells were then washed with PBS twice and fixed with 4% paraformaldehyde (PFA) at room temperature for 15 min. After washing with PBS twice more, the cells were stained with DAPI (1 µg/mL) for 20 min. Finally, the cells were washed with PBS twice and mounted with FluorSave reagent (Sigma-Aldrich, Darmstadt, Germany). The fluorescence images were acquired using a laser scanning microscope (Leica SP8 inverted, software: LAS X, Leica microsystems GmbH, Wetzlar, Germany). A diode laser (405 nm), and argon laser (488 nm and 552 nm) were used for excitation. Emission in the blue channel for DAPI (627 nm – 750 nm), green channel for AF488 (750 nm – 755 nm), and red channel (755 nm – 760 nm) for lysotracker, were recorded respectively.

2.9 Cellular uptake pathway

To further understand the mechanism behind the different behavior of P(SpBAE) polyplexes and P(BSpBAE) polyplexes, we investigated the cellular uptake pathway of both types of polyplexes. KRAS mutated A549 cells were seeded in 24-well plates 24 h before use (50 000 cells/well). Various inhibitors of specific pathways, namely nystatin (10 µg/mL), wortmannin (12 ng/mL), chlorpromazine (10 µg/mL) and methyl-β-cyclodextrin (3 mg/mL) were added, and cells were incubated in the CO_2 incubator at 37 ℃ for 1 h. Polyplexes were subsequently added (50 pmol AF488-siRNA/well, N/P 10) and incubated for 24 h. After incubation, the polyplex-containing medium was discarded, and the cells were rinsed with PBS and detached with 0.05% Trypsin-EDTA. The detached cells were then washed with PBS, quenched with Trypan blue, and analyzed via flow cytometry (Attune NxT Acoustic Focusing Cytometer, Thermo Fisher Scientific, Darmstadt, Germany).

2.10 Migration assay

To determine therapeutically relevant gene silencing efficiency of the PBAEs, a migration assay was carried out to evaluate the potential of the polyplexes to treat lung cancer.[145, 152] For this assay, Boyden chambers (VWR, 8 µm pore size) placed in 24 well plates were used. In brief, cells were seeded and transfected as described in section 2.7. Subsequently, 20 000 transfected A549 cells in 300 µL serum-free RPMI-1640 medium were added to the upper chambers, and 500 µL of complete RPMI-1640 medium was added to the lower compartment. The plates were incubated at 37 ℃ and 5% CO_2 in the incubator for 16 h, after which

the cells were washed with PBS and fixed with 4% paraformaldehyde for 30 min at room temperature. Cells on the upper surfaces of the membrane were removed with a cotton tip, and the membranes were washed 2 times with PBS. Subsequently, cells on the bottom surfaces of the membrane were stained with 0.1% crystal violet prepared in 20% ethanol for 30 min and washed with PBS 5 times to remove unbound crystal violet. The cells were then dried at 37 ℃ and observed under the microscope (Keyence Biozero, Neu-Isenburg, Germany). Per sample, 3 fields were counted per chamber.

2.11 Western blot analysis of KRAS gene silencing

To quantify the ability of PBAE polyplexes to silence mutated KRAS, A549 cells were seeded in 6-well plates 24 h before use at a density of 2×10^5 cells/well. P(SpBAE) polyplexes and P(BSpBAE) polyplexes loaded with siNC and siG12S at a concentration of 50 nM were incubated with the cells at 37 ℃ and 5% CO_2 in a humidified incubator for 72 h. Cells were then washed with ice-cold PBS and then lysed in lysis buffer (800 µL RIPA buffer, 100 µL Phosphatase inhibitor, and 100 µL Protease inhibitor). The extracted protein was determined by Bradford reagent (Bio Rad, America), and equal amounts of protein were subjected to SDS-PAGE (Novex Wedgewell 10% Tris-Glycine Gel). Separated proteins were transferred to a nitrocellulose membrane (Amersham™ Protran®), which was then exposed to 5% nonfat milk TBST solution (Tris-buffered saline pH 8.0 + 1% Tween 20) for 1 h at room temperature and incubated with antibodies against KRAS (Proteintech, Germany) overnight at 4 ℃. The membranes were washed 3 times with 1% TBST and then incubated with horseradish peroxidase (HRP)-conjugated goat anti-rabbit antibodies (Proteintech, Germany) at 4 ℃ for about 7 hours. Chemiluminescence reagents were finally applied to the membrane and photographed immediately with the ChemiDoc imager (Bio-Rad, Feldkirchen, Germany). The membrane was then treated with stripping buffer for 15 min, washed with TBST, and blocked with 5% nonfat milk TBST solution, stained with a primary antibody against histone 3 (Santa Cruz Biotechnologies, Heidelberg, Germany) at 4 ℃ overnight, and then with an HRP-conjugated donkey anti-mouse antibody (Santa Cruz Biotechnologies, Heidelberg, Germany), before it was imaged in a GelDoc XR (Bio-Rad, Feldkirchen, Germany).

3. Results & Discussion

3.1 Synthesis and characterization of spermine-based poly(β-amino ester)s

To synthesize the target poly(β-amino ester)s, we first converted spermine to the monomer tri-Boc-spermine using a literature procedure.

Tri-Boc-spermine was then polymerized with 1,4-butanediol diacrylate. As shown in **Figure 1B**, the shift of the peak at 4.09 ppm (4.20 ppm in 1,4-butanediol diacrylate) and the new signal at 2.39 ppm indicated that tri-Boc-spermine was conjugated with 1,4-butanediol diacrylate. The peaks at 5.8 to 6.4 ppm belong to the terminal acrylate group. The peaks at 0.88 and 1.25 ppm belong to the residual n-hexane, which does not influence the next step and was further removed in vacuum before use. The product P(BSpBAE) was then analyzed by SEC, and a molar mass (M_n) of 3600 g/mol and a polydispersity of 1.73 were determined. The polymer was further treated with TFA to deprotect the Boc-protection groups, and the product P(SpBAE) as a TFA salt was obtained according to the ^{13}C NMR (**Figure S4**). As shown in **Figure 1C**, the disappearance of the peak at 1.43 ppm indicated that N-Boc groups were removed.

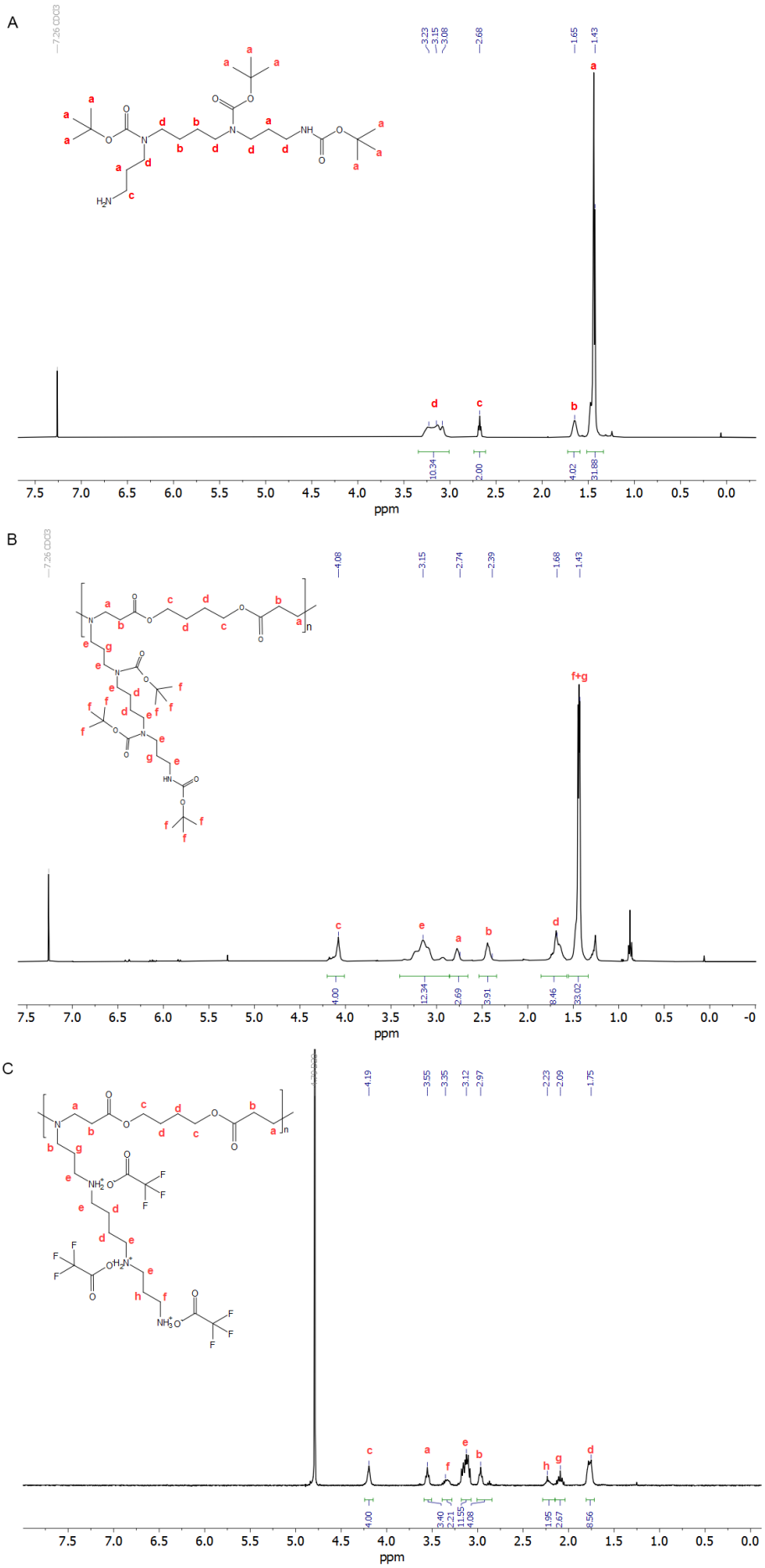
A
B
C
ppm

Figure 1. ^{1}H NMR of (A) tri-Boc-spermine in $CDCl_3$; (B) P(BSpBAE) in $CDCl_3$; (C) P(SpBAE) in D_2O

Polymer characteristics and results of the polymerization reactions in this study are summarized in **Table 1**.

Table 1. Step-growth polymerization (polyaddition) of tri-Boc spermine and 1,4-butanediol diacrylate and deprotection of the resulting polymer.

Polymer	Sol-vent	Time (h)	Yield (%)	M_n (Da)	Đ	Protonable unit
P(BSpAE) 5[a]	neat	15	83	3600[c]	1.73[c]	350
P(SpBAE) 6[b]	DCM	2	63	3800[d]	/	186

[a] reaction conditions: neat, 120 ℃, overnight, the molar ratio of spermine and 1,4-butanediol diacrylate is 1:1. [b]: reaction conditions: polymer 5, TFA, DCM, room temperature, 2 h. [c]: M_n and Đ was assessed via SEC (measurement relative to polystyrene and in chloroform at 30 ℃). [d]: molecular weight was calculated on the basis of SEC of polymer 5 (**Figure S3**) and the theoretical chemical structure of polymer 6.

Poly(β-amino ester)s (P(BSpBAE) and P(SpBAE)) were synthesized via Michael-addition-based step-growth polymerization. To obtain a high molecular weight polymer, the monomers must be pure and the stoichiometric ratio of the monomers should be 1:1.[153] Although different ratios of the monomers have been reported in the literature to obtain polymers with different terminal groups, according to the reaction kinetics, monomers with ratio 1:1 often lead to the highest molecular weight/conversion.[119, 154] The reaction temperature of synthesizing PBAEs in the literature ranged from 45 ℃ to 120 ℃, and the reaction time ranged from 5 hours to 5 days. High reaction temperature usually corresponds to short reaction time.[115, 120, 155] The widely used solvents for PBAE synthesis are dichloromethane (DCM), tetrahydrofuran (THF) and dimethyl sulfoxide (DMSO). Langer's group compared DCM and THF on the basis of the solubility of their monomers and found that the reaction in DCM yields higher molecular weight polymers.[112, 120] DMSO was also common for PBAEs synthesis due to the cytotoxicity of halogenated solvents, especially when the resulting PBAE was used directly without

further purification.[109, 156] In addition to optimizing solvents, a high concentration of monomers in the absence of solvents can also lead to high molecular weight PBAEs, shorter reaction time, and less intramolecular cyclization.[115, 155] Here, we synthesized P(SpBAE) without any additional solvents, as the reactions in DCM and THF does not lead to desired polymers, which could be due to the low boiling point of the two solvents and low reaction temperature, and the yield in DMSO was too low in our case (data not shown).

3.2 siRNA encapsulation efficiency

SYBR® Gold stain is a proprietary unsymmetrical cyanine dye that which can bind to double- or single-stranded DNA or RNA and exhibit high fluorescence intensity upon excitation. [150] Here we used the fluorescence of free siRNA as the negative control (100% free siRNA), and the free siRNA in other samples was calculated by dividing their fluorescence intensity by the negative control. As shown in **Figure 2**, in case of P(SpBAE) polyplexes, the siRNA was fully encapsulated from N/P 2 on, while P(BSpBAE) polyplexes encapsulated siRNA most efficiently at N/P 10. This observation can be explained by the primary amines and secondary amines in P(BSpBAE) being protected by the N-Boc groups. The amide usually does not contribute to encapsulation of siRNA, hence decreasing encapsulation efficacy on the basis of overall polymer weight.

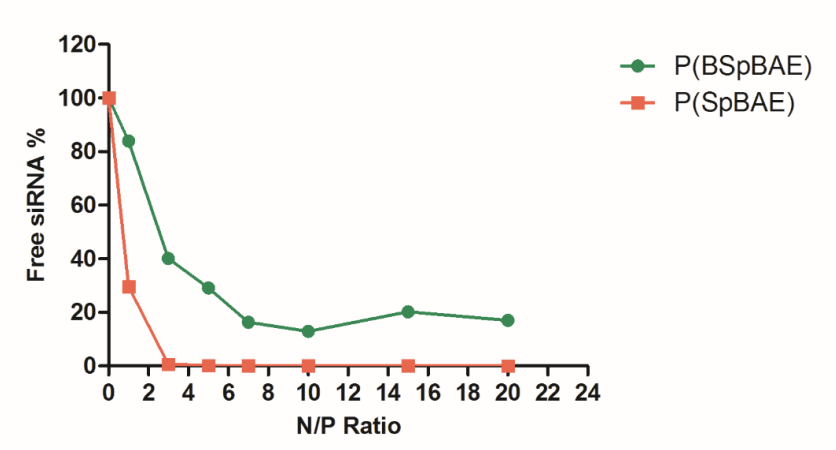

Figure 2. siRNA encapsulation profiles of polyplexes measured by SYBR Gold assays at various N/P ratios. 100% values (N/P = 0) are represented by the determined fluorescence of uncondensed free siRNA (data points indicate mean ± SD, *n* = 3).

In fact, despite their decreased encapsulation efficiency due to the lack of primary and secondary amines, the overall performance of poly(β-amino ester)s may not be affected negatively. Professor Langer's group published extensive research on the structure-function relationship of poly(β-amino ester)s. They found that the polymers synthesized from 1,4-butanediol diacrylate with 2-(piperidin-1-yl) ethan-1-amine and cyclohexane-1,4-diylbis(methylene) diacrylate with 4-aminol-1-butanol were most promising and had 4-8 times the transfection efficacy of poly(ethylene imine) (PEI).[119] In those polymers, the amines are mainly tertiary amines. Other poly(β-amino ester)s containing mainly tertiary amines were also synthesized and widely used by different groups. For example, Kim et al. utilized 4-amino-1-butanol to synthesize PBAE. They also modified the PBAE with PEG to enhance the stability and transfection efficiency of the polymer.[157] Kozielski and coauthors synthesized a bioreducible linear PBAE with 4-amino-1-butanol and bis(2-hydroxyethyl) disulfide reacted with acryloyl chloride. The repeating unit of the polymer contained only tertiary amines but achieved 92% GFP knockdown without measurable loss in metabolic activity in GBM 319 cells.[158]

3.3 Characterization of the polyplexes

As shown in **Figure 3**, the size (hydrodynamic diameter) and zeta potential of the polyplexes were measured by dynamic light scattering and laser Doppler anemometry. The N/P ratio has a significant influence on the size and zeta potential of the polyplexes. For P(SpBAE) polyplexes, the size ranged from 65.61 nm to 209.1 nm; for P(BSpBAE) polyplexes, the size ranged from 55.13 nm to 92.25 nm except the formulation at N/P 7 with a size of 764.1 nm.

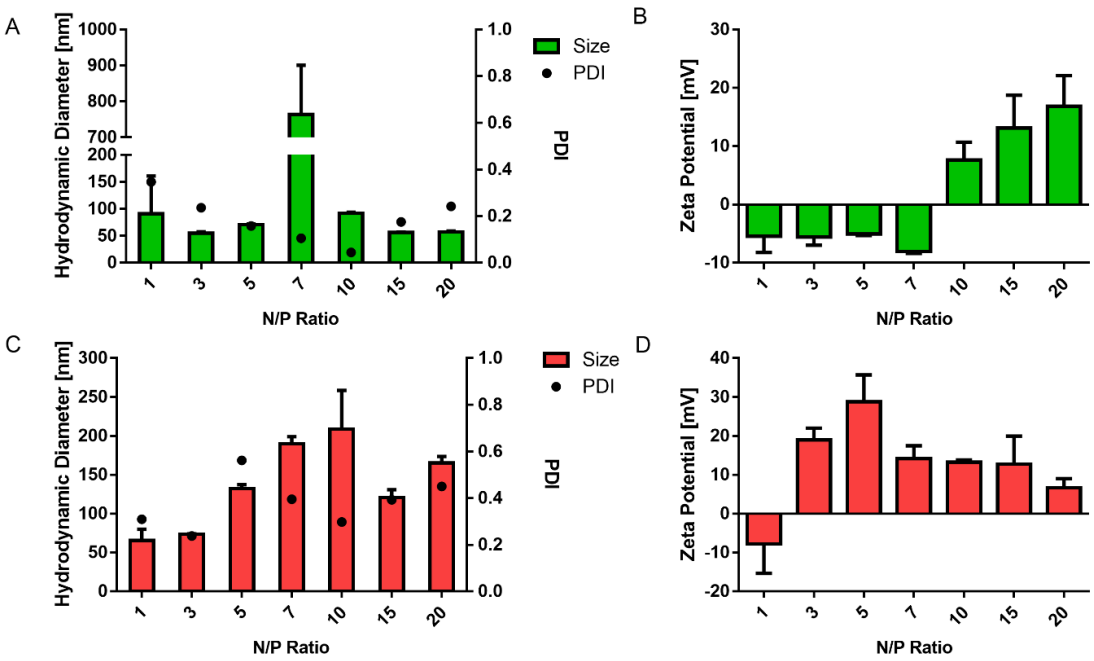

Figure 3. (A) Hydrodynamic diameter of P(BSpBAE) polyplexes; (B) Zeta potential of P(BSpBAE) polyplexes; (C) Hydrodynamic diameter of P(SpBAE) polyplexes; (D) Zeta potential of P(SpBAE) polyplexes. (Size and zeta potential, mean ± SD, n = 3, PDI, mean, n = 3).

The size of the polyplexes depends on the property of the polymer and the amount of polymer used in a formulation. siRNA cannot be condensed efficiently at low N/P ratios, while when the N/P ratio is too high, the free polymer may cause sedimentation. For both P(BSpBAE) and P(SpBAE), the polyplexes with the lowest PDI formed at the N/P ratio where the siRNA was just most efficiently encapsulated. For instance, according to the SYBR gold assay of P(BSpBAE), approximately 90% of the siRNA is encapsulated at N/P 10, and the PDI of polyplexes at N/P 10 was 0.044, which is the lowest for these polyplexes among the different N/P ratios tested. Similarly, for P(SpBAE), the siRNA was fully encapsulated at N/P 3, and the polyplexes of N/P 3 showed the lowest PDI 0.238. The size of P(BSpBAE) polyplexes at N/P 7 was large, which could be caused by aggregation of negatively and positively charged polyplexes present at N/P 7. From N/P 7 to N/P 10, the zeta potential of the polyplexes switches from negative to positive. It is therefore also possible that neutral polyplexes are formed whose net charge is insufficient to stabilize the polyplexes, resulting in aggregation.

3.4 In vitro compatibility

MTT assays were performed to investigate the polymers' and polyplexes' biocompatibility. As shown in **Figure 4**, PBAEs and PEI had comparable cell viability at low concentrations from 1 µg/mL to 5 µg/mL. However, above 10 µg/mL, PEI caused stronger cytotoxicity than the poly(β-amino ester)s P(SpBAE) and P(BSpBAE), confirming better biocompatibility of the poly(β-amino ester)s compared with PEI. All polyplexes mediated cell viability above 80% in H1299 cells, which indicated that the polyplexes were biocompatible. However, for the PBAE polyplexes, larger weight amounts of polymer are necessary, resulting in slight differences regarding polyplex biocompatibility.

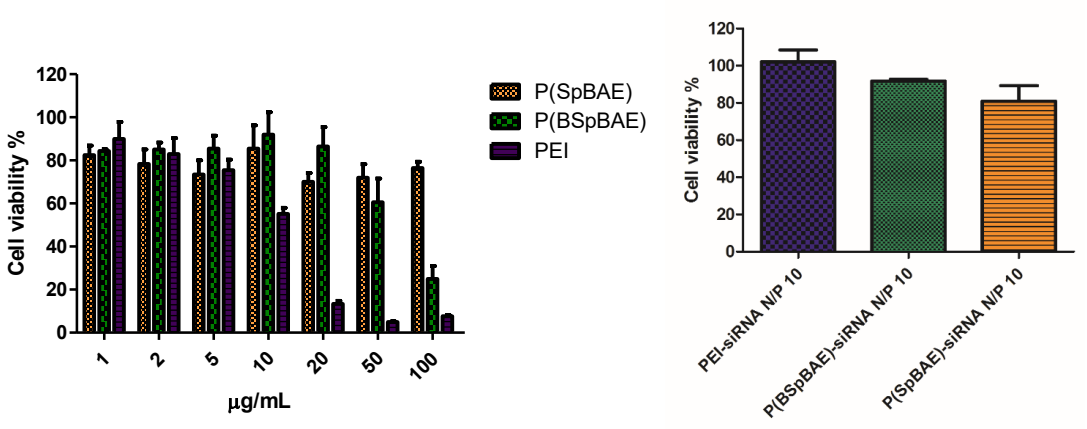

Figure 4. Cell viability of polymers and polyplexes determined by diemthylthiazolyl blue diphenyltetrazolium bromide (MTT) assay in H1299 cells.

3.5 Cellular uptake

The cellular uptake of P(BSpBAE) polyplexes and P(SpBAE) polyplexes was determined by flow cytometry with or without trypan blue quenching. As shown in **Figure 5**, there is no significant difference between unquenchend and quenched samples, which confirms cellular polyplex internalization, rather than adsorption on the surface of the cells. The uptake of P(SpBAE) polyplexes was 60 times higher than that of free AF488-siRNA (negative control), while the uptake of P(BSpBAE) polyplexes was 865 times higher than the negative control, 14 times higher than that of P(SpBAE) polyplexes, and 49 times higher than that of PEI polyplexes. The uptake of P(BSpBAE) polyplexes was even 2.77 times better than Lipofectamine ™ 2000 with the same amount of siRNA (50 pmol AF488-siRNA) for each well.

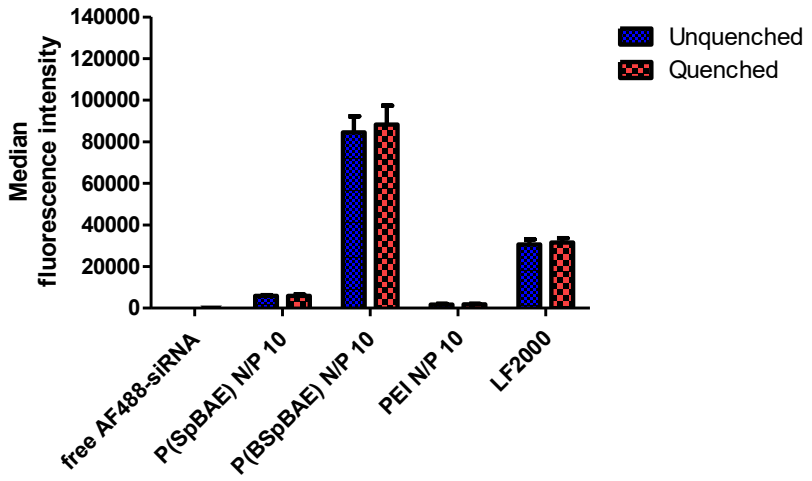

Figure 5. Cellular uptake of polyplexes quantified by flow cytometry and presented as median fluorescence intensity corrected by autofluorescence of untreated blank cells (H1299 cells, AF488-siRNA).

The uptake of P(SpBAE) polyplexes at N/P 1 to 20 was also determined (**Figure S1**). The cellular uptake depended on the N/P ratios, and higher N/P ratios often lead to higher cellular uptake regardless of the high PDI. This observation can be explained by the positive charge of the polyplexes enhancing the interaction with the negatively charged cell membrane. However, too much positive charge also leads to cytotoxicity and thus a lower cellular uptake in viable cells. Besides charge, the amphiphilicity of a polymer and its resulting polyplexes is crucial and has a significant influence on their cellular uptake. In this experiment, P(BSpBAE) is hydrophobic, while P(SpBAE) is hydrophilic. Although the siRNA encapsulation efficiency of P(BSpBAE) is lower than that of P(SpBAE) according to the SYBR gold assays (**Figure 3**), the P(BSpBAE) polyplexes still achieved much higher cellular uptake.

3.6 In vitro eGFP knockdown

To evaluate the gene silencing efficiency of such hydrophobic and hydrophlic polyplexes on the protein level, we utilized H1299/eGFP cells that stably express the enhanced green fluorescent protein reporter gene (eGFP). Chloroquine (CQ) used as an anti-malaria drug has been a focus of research for its contribution to the endosomal escape process, and it has been proposed to increase endosome escape through several mechanisms.[159] Chloroquine diffuses across the cell

membrane and into endosomes passively, as the pH drops in endosomes, it becomes protonated and trapped inside the endosome resulting in a dramatic increase in its endosomal concentration. It is thought to insert a hydrophobic motif into the lipid bilayer and lyse the endosome at a critical concentration.[160, 161] As shown in **Figure 6**, Lipofectamine™ 2000 (LF) was used as a positive control. In transfection experiments without chloroquine, P(SpBAE) polyplexes mediated only 4.91% of knockdown which is not significant in statistics, while P(BSpBAE) polyplexes had a knockdown efficiency of 58.48%. After chloroquine treatment, the knockdown efficiency of P(SpBAE) polyplexes was 86.56%, which indicates that the P(SpBAE) polyplexes were entrapped in endosome/lysosomes. However, the fluorescence intensity of cells transfected with P(SpBAE)-siNC polyplexes also decreased after treatment with chloroquine which might be a sign of cytotoxicity. The knockdown efficiency of P(BSpBAE) polyplexes, on the other hand, increased to 91.61% with the treatment of chloroquine without visible signs of increased cytotoxicity.

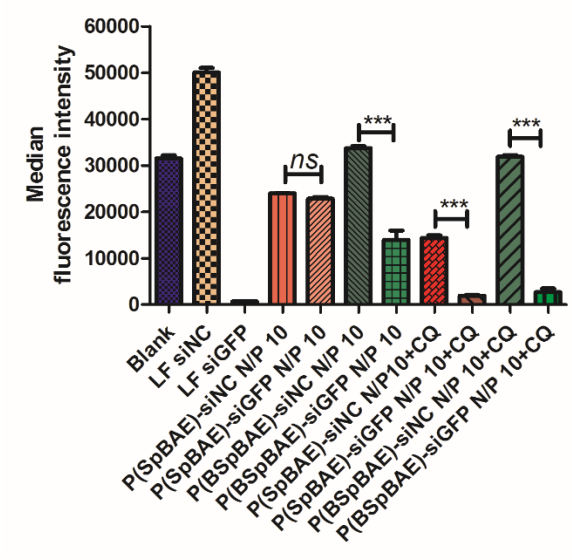

Figure 6. Enhanced green fluorescent protein (eGFP) knockdown of P(SpBAE) polyplexes and P(BSpBAE) polyplexes in H1299 cells expressing eGFP quantified by flow cytometry as median fluorescence intensity (Mean ± SD, n = 3, One-way ANOVA with Bonferroni multiple comparison test, $^{***}p < 0.001$, $^{ns}p > 0.05$).

Chloroquine enhanced the knockdown of P(BSpBAE) and P(SpBAE) polyplexes, which means both of the polyplexes are not released from the endosome efficiently. However, the GFP knockdown efficiency of P(SpBAE) polyplexes with

chloroquine was improved by a factor 17.6 times compared to the samples without chloroquine treatment. On the other hand, the knockdown efficiency of P(BSpBAE) polyplexes with chloroquine was only 1.57 times increased compared with samples without chloroquine treatment. This indicates that the P(BSpBAE) polyplexes may be less subject to endosomal entrapment than the P(SpBAE) polyplexes.

3.7 Endosome Entrapment

To find the mechanism behind the efficient knockdown of P(BSpBAE) polyplexes, the endosomal entrapment of the polyplexes was visualized via confocal laser scanning microscopy (CLSM). As shown in **Figure 7**, more AF488-siRNA P(BSpBAE) polyplexes seemed to reach the cytoplasm than P(SpBAE) polyplexes. This result is in line with the results obtained by flow cytometry. The P(BSpBAE) polyplexes were also distributed in other cell organelles. The colocalization of P(SpBAE) polyplexes with lysosomes (yellow dots in the merged figure) was more than that of P(BSpBAE) polyplexes, which indicates that the P(BSpBAE) polyplexes may have a better ability of endosomal escape. The colocalization coefficient was analyzed in Image J, which also confirmed that P(BSpBAE) polyplexes colocalized less with endosome/lysosomes than P(SpBAE) polyplexes.

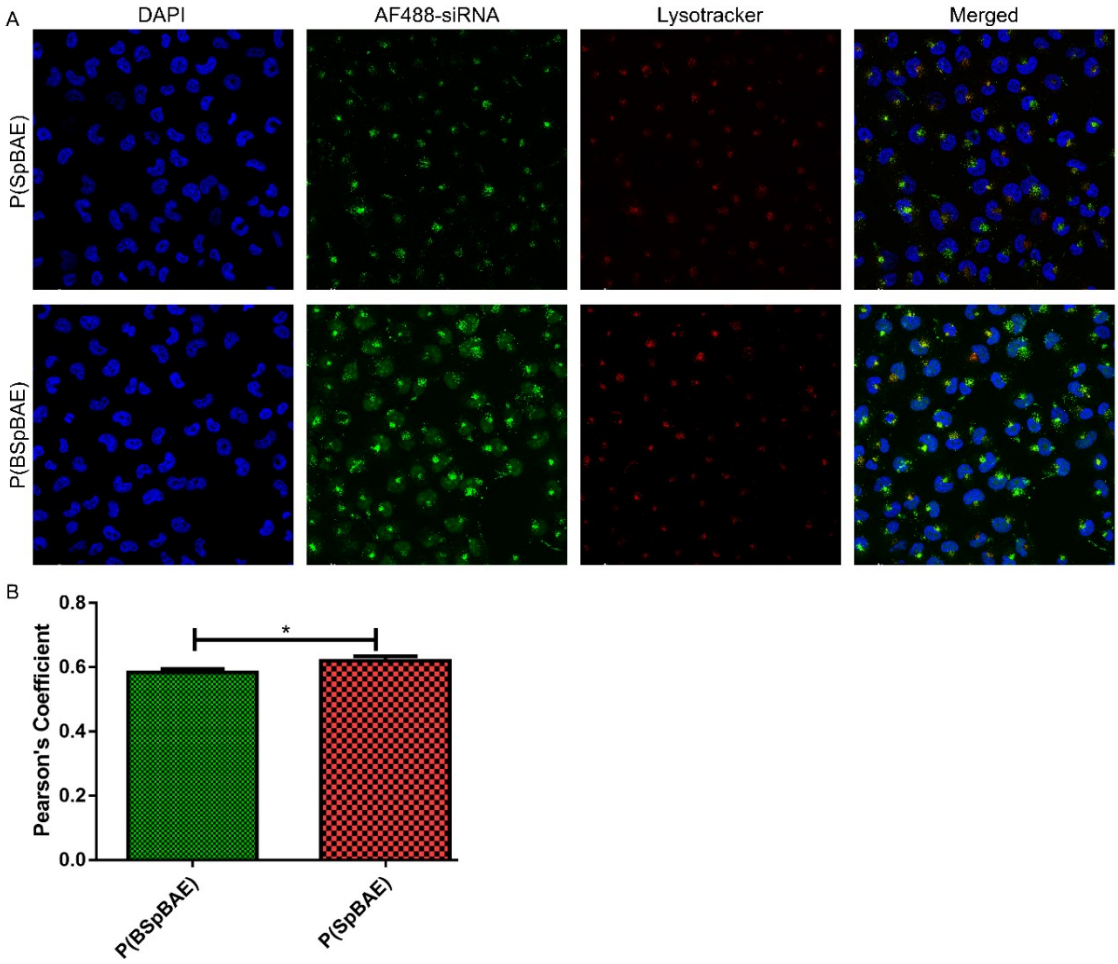

Figure 7. (A) Confocal images after treatment of H1299 cells with P(SpBAE) polyplexes and P(BSpBAE) polyplexes formulated with AF488-siRNA and stained with Lysotracker red^{TM} DND 99 and DAPI. (B) Pearson's coefficient analyzed via Image J (Mean ± SD, n = 3, Unpaired T test, $^{*}p < 0.05$).

Endosomal escape is one of the critical hurdles to successful intracellular delivery of nucleic acid-based therapeutics. Nanoparticles internalization must be followed by endosomal escape. Otherwise, endosomal entrapment renders the nanocarriers and their cargo useless as it is degraded via the endo/lysosomal pathway.[162, 163] One of the most common strategies for endosomal escape is the hypothesized "proton sponge effect". The sponges, which typically are polyamines, can absorb free protons in endosomes. As the absorbed protons accumulate, chloride will then begin to diffuse into the endosome as a compensation to restore the equilibrium potential which raises the osmotic pressure inside the vesicle. This causes the endosome/lysosome to swell and expand until a critical area

strain is passed, and finally the lipid bilayer membrane ruptures and the polyplexes are released without degradation.[164]

Interestingly, the P(BSpBAE) polyplexes seem to have a better endosomal escape ability although lacking amines. We assume that this may due to the partial removal of N-Boc groups in acidic endosome/lysosomes. N-Boc group is a common amine protecting group, which is stable in neutral to basic environment but is unstable and removable in an acidic environment. When N-Boc groups are removed in endosome/lysosomes, the amines can be protonated and thus enhance the “proton sponge effect”. The P(BSpBAE) polyplexes also achieved endosomal escape via other mechanisms. For example, the polyplex-mediated escape theory. In brief, the charged polyplexes interact directly with the anionic phospholipids of the inner membrane leaflet leading to membrane destabilization and nanoscale holes within the membrane and then vector escape from these holes.[35, 43] Another similar theory is that the endosomal escape could be a result from free polymer-mediated membrane permeability and nanoscale hole formation. It was hypothesized that there is a dynamic equilibrium between dissociated polymer chains and polyplexes, and free polymer chains intercalate in the membrane of endo-lysosomes and cause membrane disintegration and hole formation.[35, 165] It is also possible that due to the hydrophobicity of N-Boc groups, the polyplexes were internalized into the cells via a different pathway which results in less entrapment in endosome/lysosomes.

3.8 Cellular uptake pathway

Four cellular uptake inhibitors were applied in this experiment to investigate the cellular uptake pathway. Specifically, nystatin can inhibit the internalization of caveolae and lipid rafts through the depletion of cholesterol in the cell membrane; wortmannin can block macropinocytosis; methyl-β-cyclodextrin inhibits the lipid raft-dependent endocytic pathway by interfering with cholesterol synthesis and decomposing cholesterol; chlorpromazine blocks clathrin-mediated endocytosis through destroying cell surface clathrin and the AP2 complex.[149, 166] As shown in **Figure 8**, the P(SpBAE) polyplexes and P(BSpBAE) polyplexes showed different behavior after the treatment with these four inhibitors. Nystatin had almost no influence on the cellular uptake of P(SpBAE) polyplexes but decreased the uptake of P(BSpBAE) polyplexes’ by 70%; while wortmannin had no inhibition effect on the cellular uptake of P(BSpBAE) polyplexes, it inhibited the cellular uptake of

P(SpBAE) polyplexes by about 50%; Methyl-β-cyclodextrin strongly inhibited the uptake of both P(SpBAE) polyplexes and P(BSpBAE) polyplexes; Chlorpromazine decreased the uptake of P(SpBAE) polyplexes by 71.06% but that of P(BSpBAE) polyplexes only by only 32.97%.

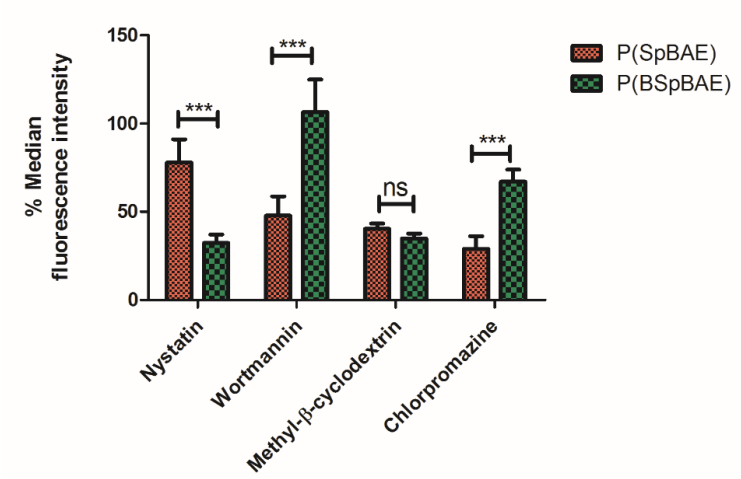

Figure 8. Cellular uptake of P(SpBAE) and P(BSpBAE) polyplexes (N/P = 10) after treatment with inhibitors nystatin, wortmannin, chlorpromazine, and methyl-β-cyclodextrin (M-β-CD). (Results are shown as mean ± SD as a percentage of median fluorescence intensity normalized to non-inhibited samples, n = 3, two-way ANOVA with Bonferroni post-hoc test, $^{***}p < 0.001$, $^{ns}p > 0.05$.)

These results indicate that P(SpBAE) polyplexes were mainly internalized via macropinocytosis, lipid raft-dependent, and clathrin-dependent endocytic pathways; P(BSpBAE) polyplexes, on the other hand were internalized mainly via caveolae and lipid raft-dependent endocytosis. Caveolae-dependent endocytosis is reported to have the potential to bypass lysosomes, and many pathogens including viruses and bacteria in fact select this pathway to avoid lysosomal degradation. Therefore, this route is believed to be beneficial for enhanced therapeutic effects.[167] While clathrin-dependent endocytosis usually leads to endosomal/lysosomal localization.[168] These differences in intracellular trafficking could explain why P(BSpBAE) polyplexes resulted in less endosomal entrapment and higher GFP knockdown efficiency.

3.9 Migration assay

KRAS (Kirsten rat sarcoma virus) is a gene that provides instructions for a protein called K-Ras, which relays signals from outside the cell to the nucleus. The

signals instruct the cell to grow and proliferate or to mature and differentiate. It is called KRAS because it was first identified as a viral oncogene in the Kirsten Rat Sarcoma Virus.[169] KRAS is the most frequently mutated gene associated with lung cancer, and the activating mutations in KRAS result in constitutive activation of the GTPase protein in the absence of growth factor signaling, resulting in a sustained proliferation signal within the cell which is related to the migration and invasion of cancer cells.[144] To achieve therapeutically relevant gene silencing, we used a siRNA sequence targeting a KRAS mutant, namely KRAS G12S. As shown in **Figure 9**, cells transfected with the siG12S encapsulated polyplexes showed less migration than cells transfected with the negative controls. Specifically, formulations with P(SpBAE)-siG12S inhibited about 32.57% of the migration, while P(BSpBAE)-siG12S inhibited about 55.11% of the migration.

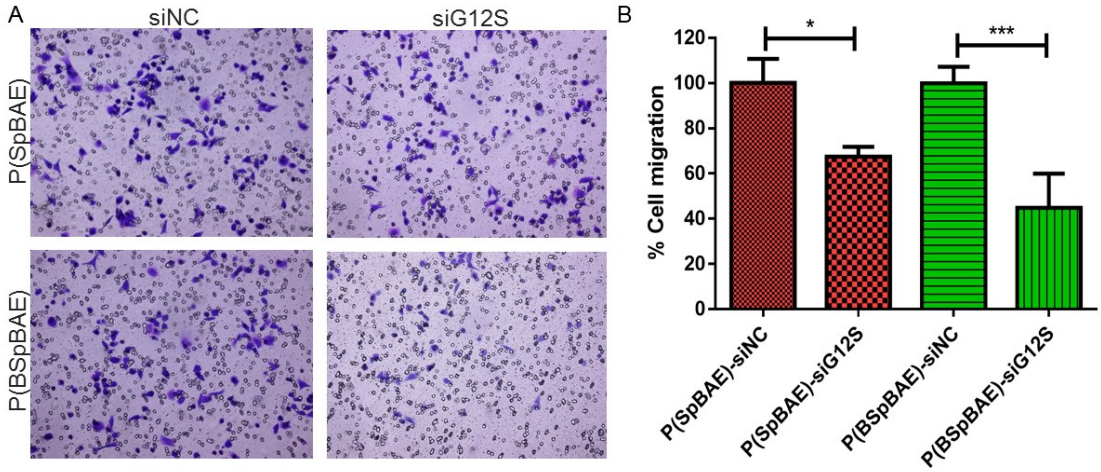

Figure 9. (A) The crystal violet staining of migrated A549 cells. (B) The percentage of the migrated cells was quantified by counting three fields per chamber and compared with controls (One way ANOVA, $n = 3$, $^{*}p < 0.05$, $^{***}p < 0.001$).

Interestingly, P(SpBAE) polyplexes did not mediate a significant GFP knockdown but were able to inhibit the migration of A549 cells. It was hypothesized that although P(SpBAE) polyplexes did not achieve a knockdown on protein level, they were yet able to change the status of the cells, for example, the signal transduction, thus leading to an inhibition of the migration. It is also possible that transfection of A549 cells with P(SpBAE) polyplexes was in general more efficient than transfection of H1299 cells or that a smaller gene silencing

effect of KRAS resulted in a more visible effect than eGFP silencing measured by flow cytomatry. The gene silencing efficiency is also related to the siRNA. It is thus possible that the siRNA against KRAS has a higher efficiency than the siRNA against GFP, thus the cytoplasmatically released siRNA delivered by P(SpBAE) polyplexes was able to achieved a KRAS knockdown and inhibited the migration of A549 cells. To observe the KRAS knockdown on protein level and investigate which assumption is correct, a western blot experiment was performed.

3.10 Western blot analysis

Western blot analysis was conducted to investigate if the P(SpBAE) polyplexes and P(BSpBAE) polyplexes can knock down KRAS on the protein level. As shown in **Figure 10**, both P(SpBAE) polyplexes and P(BSpBAE) polyplexes downregulated the expression of KRAS compared with the housekeeping gene Histone 3. P(SpBAE) polyplexes did not knock down GFP significantly but inhibited the expression of KRAS. To understand the underlying principles of this phenomenon, we determined the cellular uptake of P(SpBAE) and P(BSpBAE) polyplexes in A549 cells. PEI and Lipofectamine^{TM} 2000 were used as controls (**Figure S2**). The cellular uptake of P(BSpBAE) polyplexes was still higher than P(SpBAE) polyplexes. However, the cellular uptake of P(BSpBAE) polyplexes decreased compared with its behavior in H1299 cells, and the cellular uptake of P(SpBAE) polyplexes increased. This result could explain why P(SpBAE) polyplexes did not efficiently mediate GFP knockdown in H1299 cells but caused therapeutically relevant KRAS knockdown in A549 cells as shown in the migration assay. The phenomenon that nanoparticles show different behavior in different cell lines was also reported by other researchers. For example, Kim et al. investigated the transfection efficiency of DOTAP-liposomes with different DOTAP/DOPE ratios in different cell types including Huh7, AGS, COS7, and A549. They found that the formulation T1P0 and T3P1 showed higher luciferase activities than T1P1 or T1P3 in Huh7 and AGS cells. However, the transfection efficiencies of T3P1 and T1P1 were higher than those of T1P0 and T3P1 in COS7 cells. These results implied that specific cell lines can favor certain lipid compositions in gene delivery and the transfection efficiency is cell-line dependent.[170] The good performance of P(SpBAE)-siG12S polyplexes could also be due to the higher knockdown efficiency of the siRNA sequence siG12S. The knockdown

efficiency of siRNA is related to its length, nucleotide composition, and the distance of the target region to transcription start site.[171]

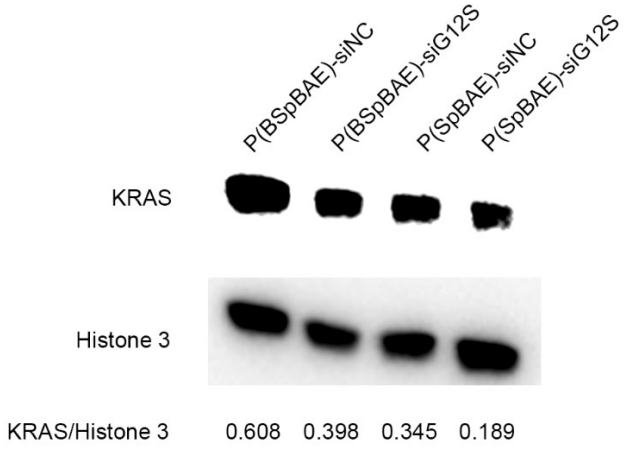

Figure 10. Western blot analysis of KRAS protein expression in A549 cells. Histone 3 was used as the loading control.

4. Conclusion

In this project, we have synthesized spermine-based poly(β-amino ester)s successfully. The PBAEs polymers were more biocompatible than PEI and were able to encapsulate siRNA and delivery siRNA efficiently. Interestingly, we observed that the PBAEs before removing the N-Boc protection groups P(BSpBAE) mediated much higher cellular siRNA uptake and GFP knockdown efficiency, benefiting from different cellular uptake mechanisms and lower endosomal entrapment. This indicates that the Boc-protection of the polymer could be beneficial for siRNA delivery and gene silencing efficiency. The PBAE polyplexes encapsulating siRNA against KRAS also showed promising results, which indicates the potential application of spermine-PBAEs for therapeutic purposes. Taken together, the spermine-based poly(β-amino ester)s are very promising for siRNA delivery and RNAi-based therapeutics.

ACKNOWLEDGMENTS

Yao Jin appreciates the financial support from China Scholarship Council (CSC 201906010329). This research was also funded by ERC-2014-StG – 637830 to Olivia Merkel.

Supporting information

Synthesis and application of spermine-based poly(β-amino ester)s for siRNA delivery

Yao Jin, Friederike Adams, Lorenz Isert, Domizia Baldassi, and Olivia M. Merkel*

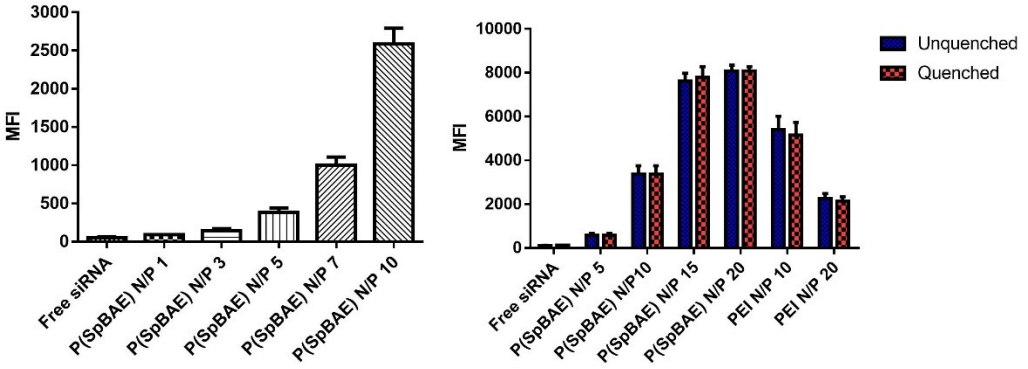

Figure S1. Cellular uptake of P(SpBAE) polyplexes quantified by flow cytometry and presented as median fluorescence intensity corrected by autofluorescence of untreated blank cells (H1299 cells, AF488-siRNA)

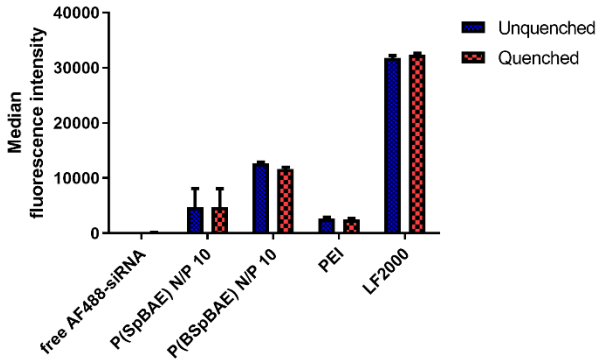

Figure S2. Cellular uptake of P(SpBAE) polyplexes quantified by flow cytometry and presented as median fluorescence intensity corrected by autofluorescence of untreated blank cells (A549 cells, AF488-siRNA)

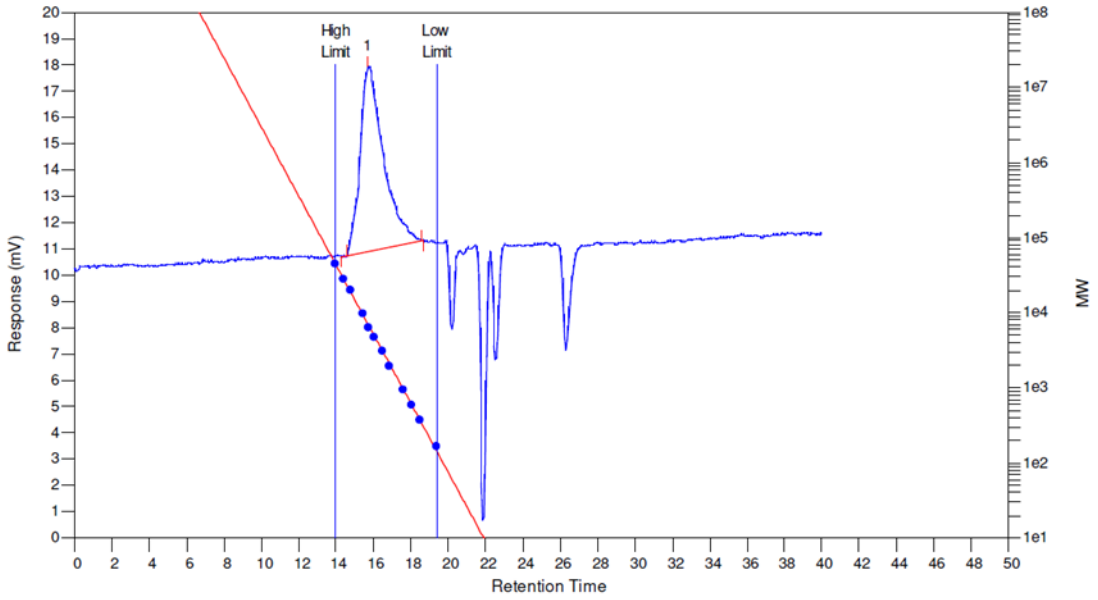

MW Averages

Peak No	*Mp*	*Mn*	*Mw*	*Mz*	*Mz+1*	*Mv*	*PD*
1	*7129*	*3565*	*6178*	*8630*	*10801*	*5814*	*1.73296*

Figure S3. Size exclusion chromatography (SEC) of P(BSpBAE).

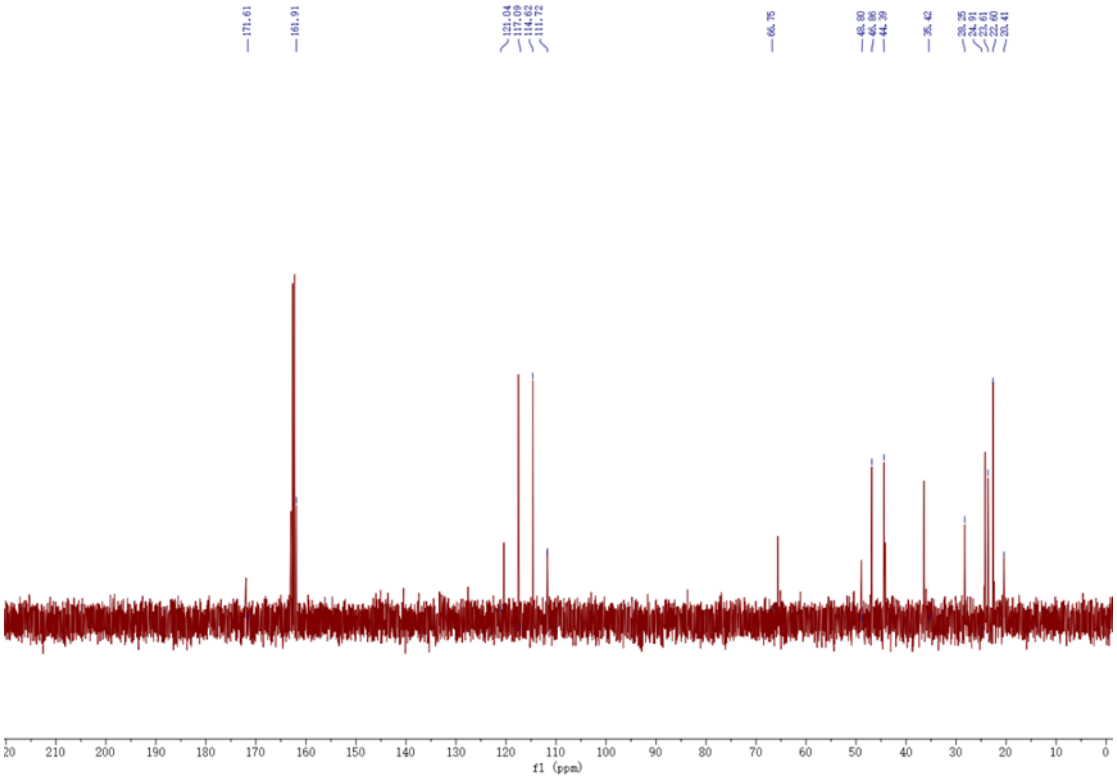

Figure S4. ^{13}C NMR of P(SpBAE) in D_2O. The peaks around 117 ppm and 162 ppm belong to the carbon of trifluoroacetate group.

Chapter II

Synthesis and application of spermine-based amphiphilic poly(β-amino ester)s for siRNA delivery

*Yao Jin, Friederike Adams, Olivia M. Merkel**

Ludwig-Maximilians-University Munich, Department of Pharmacy, Pharmaceutical technology and Biopharmaceutics, Butenandtstr. 5-13, 81377 Munich, Germany

KEYWORDS: poly(β-amino ester)s; siRNA delivery; spermine; PBAEs

ABSTRACT: Small interfering RNA (siRNA) can trigger RNA interference (RNAi) to therapeutically silence disease-related genes in human cells. The approval of siRNA therapeutics by the FDA in recent years generated a new hope in siRNA therapeutics. However, their therapeutic application is still limited by the lack of safe and efficient transfection vehicles. In this study, we successfully synthesized a novel amphiphilic poly(β-amino ester) characterized by ^{1}H NMR and gel permeation chromatography (GPC, Mn = 5987 Da). The polymer encapsulates siRNA quantitatively from N/P 5 on as assessed by fluorescence intercalation. Its biocompatibility and cellular delivery efficacy were also higher than those of commonly used cationic polymer polyethylenimine (PEI, 25 kDa). Optimized formulations mediated around 90% gene silencing in enhanced green fluorescence protein expressing H1299 cells (H1299-eGFP) as determined by flow cytometry. These results suggest that our spermine-based amphiphilic poly(β-amino ester) is a very promising candidate for efficient functional siRNA delivery.

1. Introduction

Small interfering RNA (siRNA) is a double-stranded macromolecule with a length of 19-21 nucleotides per strand used to trigger the innate RNA interference (RNAi) mechanism to degrade complementary mRNA molecules for a subsequent decrease in gene expression.[172] RNAi therapy has preclinically been demonstrated promising for the treatment for many diseases, for example,

chronic myeloid leukemia,[172]non-small cell lung cancer,[145] skin melanoma,[173] and many others. It also has the potential to treat COVID-19 caused by SARS-CoV-2 virus infections.[174, 175] Additionally, Several siRNA-based products are already approved by the FDA, and many additional siRNA-drugs are in different stages of clinical trials.[176] However, the physiochemical properties of siRNAs including their macromolecular characteristics, hydrophilicity, net negative charge, enzymatic degradation by serum endonucleases such as RNases, and rapid renal clearance of siRNA require the combination of bioactive sequences with effective delivery systems.[2, 7]

Cationic polymers have shown promise for nucleic acid delivery given their ability to self-assemble with anionic siRNA into condensed nanoparticles (polyplexes) with efficient encapsulation capacity. Various cationic polymers have been developed as nonviral nucleic acid vectors during the past three decades, for example, polyethylenimine (PEI), chitosan, inulin, poly-L-lysine, and many more.[8] Poly(β-amino ester)s (PBAE)s refer to polymers synthesized from acrylate compounds and amine-containing monomers by Michael addition-based step growth polymerization and have drawn people's attention after their first application for transfection in 2000 due to their inherent biocompatibility, biodegradability, and stimili-responsiveness.[112, 139] The first generation of PBAEs contains linear PBAEs (LPAEs), and a variety of LPAEs has been established and proven to be promising for gene delivery. However, the delivery of siRNA is bears new challenges in comparison to plasmid DNA because siRNA is linear and short with a rigid structure, which affords limited molecular entanglement points to electrostatically bind to cationic polymers.[177] Therefore, high polymer/siRNA weight ratios are reported to be required to fully condense siRNA and enable efficient transfection.[178] Hyperbranched and branched PBAEs (HPAEs) have a high density of branching linkers, and the resulting three-dimensional globular shape and multiple chain-end groups have the potential of high siRNA encapsulation efficiency. However, HPAEs with strong nucleic acid binding affinity may restrict the intracellular siRNA release, thus hampering siRNA-mediated gene silencing efficiency.[177] Environment responsive disulfide linkages containing HPAEs were thus designed and provided promising applications for anti-inflammatory siRNA delivery and for efficient cancer gene therapy in approaches of furthering HPAE efficacy. [177, 179]

Spermine is a naturally occurring, biocompatible polycation with primary and secondary amines spaced by methyl groups and has high affinity toward nucleic acids.[85, 154] The essential role of spermine in eukaryotic cells is to aid in packaging cellular DNA into a compact state.[79, 180] However, spermine shows a limited siRNA complexation ability and efficiency for transfecting nucleic acids because of its low molecular weight (~ 200 Da).[79] In addition, spermines yield limited endosomal escape despite of their good proton-buffering capacity.[83] The polymerization of spermine to increase its molecular weight can improve the products' buffering capacity as well as enhance the endosomal escape and transfection efficiency of spermine polyplexes.[82, 181] In this regard, Lote et al. synthesized a variety of oligospermines and found that the molecular weight of the linear oligospermines had a pronounced effect, while the molecular architectures influenced the siRNA encapsulation profiles.[85] Duan et al. synthesized a polyspermine imidazole-4,5-amide (PSIA), and the resulting PSIA-polyplexes were able to achieve high cellular uptake and efficient luciferase gene silencing.[181]

In this work, we synthesized a spermine-based poly(β-amino ester) combining the advantages of PBAEs with increased molecular weights of spermine macromolecules. Inspired by our previous research, we found that hydrophobic modification is important for the successful transfection and gene silencing of PBAEs polyplexes. Therefore, decylamine was polymerized together with spermine to give a brush-like poly(β-amino ester) with suitable amphiphilicity.

2. Materials and Methods

2.1 Materials

Spermine (Fisher Scientific, Acros, USA), 1,4-butanediol diacrylate (TCI, Japan), chloroform D (Eurisotop, Germany), hyperbranched polyethylenimine (Lupasol® WF, BASF, Germany), n-hexane, dichlorimethane, dimethyl sulfoxide (DMSO), are technically purely provided by Ludwig-Maximilians-University Munich.

Deuterium oxide, decylamine, HEPES (4-(2-hydroxylethyl)-1-piperazineethanesulfonic acid), thiazolyl blue tetrazolium bromide (MTT), RPMI-1640 medium, fetal bovine serum (FBS), Penicilin-Streptomycin solution, Dubecco's Phosphate Buffered Saline (PBS), trypsin-EDTA solution (0.05%), and Geniticin

(G418) disulfate solution were purchased from Sigma-Aldrich (Taufkirchen, Germany). SYBR Gold Dye, Lipofectamine™ 2000, AlexaFluor 488 (AF488) were bought from Life Technologies (Darmstadt, Germany).

Amine-modified eGFP siRNA (5´-pACCCUGAAGUUCAUCUGCACCACcg, 3´-ACUGGGACUUCAAGUAGACGGGUGGC) and scrambled siRNA (5´-pCGUUAAUCGCGUAUAAUACGCGUat, 3´-CAGCAAUUAGCGCAUAUUAUGCGCAUAp) were purchased from Integrated DNA Technologies (Leuven, Belgium). In the sequences, “p” represents a phosphate residue, lower case letters denote 2’-deoxyribonucleotides, capital letters express ribonucleotides, and underlined capital letters are 2’-O-methylribonucleotides.

2.2 Synthesis and characterization of amphiphilic poly(β-amino ester)s

2.2.1 Synthesis of tri-tert-Butyl Carbonyl Spermine

Tri-tert-Butyl Carbonyl Spermine abbreviated as tri-Boc-spermine was synthesized as described elsewhere with some modification.[148] In brief, spermine (1 eq) was dissolved in methanol and stirred at -78 °C, ethyl trifluoroacetate (1 eq) was added dropwise subsequently and stirred at -78 °C for 1 h, then 0 °C for 1 h. Without isolation, di-tert-butyl decarbonate (4 eq) was added dropwise to the solution and stirred at room temperature for 2 days. Finally, the solution was adjusted to a pH above 11 by 25% ammonia and stirred overnight to cleave the trifluoroacetamide protecting group. The mixture was then evaporated under vacuum, and the residue was diluted with dichloromethane (DCM) and washed with distilled water and saturated NaCl aqueous solution. The DCM phase was finally dried with $MgSO_4$ and concentrated to give the crude product. The crude product was purified by column chromatography (CH_2Cl_2\MeOH\NH_3, aq. 7:1:0.1, SiO_2, $KMnO_4$; R_f = 0.413). Tri-Boc-spermine was isolated and characterized by ^{1}H NMR. Yield: 37%.

^{1}H NMR, 400 MHz, $CDCl_3$: 1.43–1.48 [m, 31H, 6-CH_2, 7-CH_2, O–C–(CH_3)3×3, overlapping]; 1.65 (m, 6H, 2-CH_2, 11-CH_2, NH_2); 2.68 (t, 2H, 12-CH_2); 3.08–3.23 (m, 10H, 1-CH_2, 3-CH_2, 5-CH_2, 8-CH_2, 10-CH_2).

2.2.2 Synthesis of P(BSpDBAE)

For the synthesis of poly(tri-Boc-spermine and decylamine-based β-amino ester), abbreviated as P(BSpDBAE, tri-boc-spermine (1 eq), decylamine (1 eq) and 1,4-butanediol diacrylate (2 eq) were mixed and stirred at 120 ℃ overnight. The

crude product was then dissolved with 2 mL DCM and precipitated in 50 mL n-hexane at 4 ℃. The supernatant was discarded, and the product was dried in a vacuum oven for 2 days (50 ℃, 15 mbar). The product P(BSpDBAE) was finally obtained as brown semisolid and characterized via ^{1}H NMR and Gel Permission Chromatography (GPC, measurement relative to polystyrene and in chloroform at 30°C, 1 mg/mL). Yield: 44%.

^{1}H NMR (400 MHz, $CDCl_3$) δ 4.15 (d, 8H, $4CH_2$), 2.99 (d, J = 142.2 Hz, 23H), 1.72 (d, J = 18.6 Hz, 15H), 1.55 – 1.38 (m, 20H), 1.27 (d, J = 12.7 Hz, 17H), 0.93 – 0.81 (m, 4H).

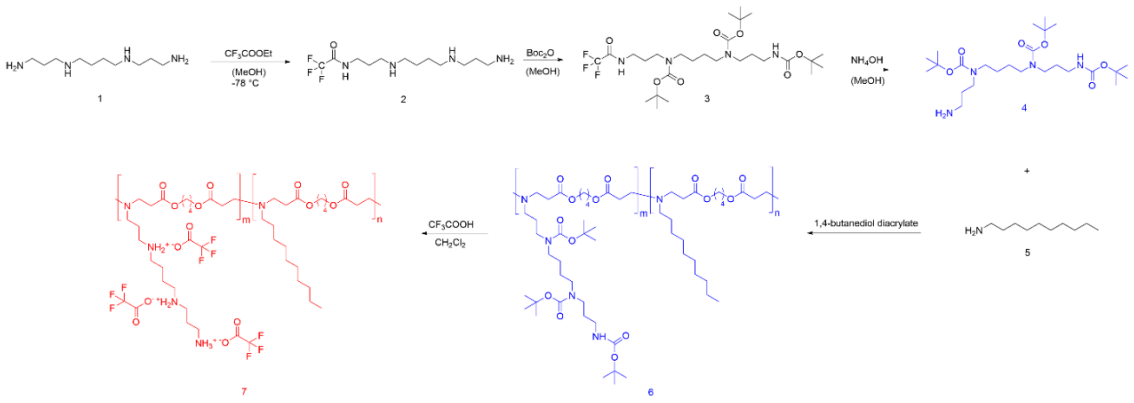

Scheme 1. Synthesis route of P(SpDBAE)

2.2.3 Synthesis of P(SpDBAE)

Deprotected P(SpDBAE) was synthesized by dissolving P(BSpDBAE) (130 mg) in 20 mL DCM and subsequently adding 1.2 mL TFA to the solution which was stirred at room temperature for 2 h. The solvents were then evaporated in a rotary evaporator and then dissolved with DCM and precipitated in n-hexane at 4 ℃. Finally, the product was dissolved with water and freeze-dried as a yellow semi-solid. The product was also characterized via ^{1}H NMR and named P(SpDBAE). Yield: 62%.

^{1}H NMR (500 MHz, D_2O) δ 4.16 (s, 8H), 3.54 (s, 6H), 3.34 (s, 2H), 3.12 (dt, *J* = 26.9, 8.1 Hz, 9H), 2.91 (d, *J* = 46.2 Hz, 6H), 2.23 (s, 1H), 2.08 (p, *J* = 8.3 Hz, 2H), 1.75 (d, *J* = 22.0 Hz, 15H), 1.26 (s, 21H), 0.85 (s, 5H).

2.3 Preparation and characterization of P(SpDBAE) polyplexes

To prepare P(SpDBAE) polyplexes (complexes of the polymer P(SpDBAE) and siRNA), P(SpDBAE) was first dissolved in water at a concentration of 1 mg/mL.

The amount of polymer required for each formulation was then calculated according to the N/P ratio and aliquoted in 50 µL 10 mM HEPES buffer (pH 5.3). Subsequently, siRNA in 50 µL 10 mM HEPES buffer was mixed with the corresponding polymer solution and incubated at room temperature for 2 h. The size and Zeta potential of the polyplexes in 10 mM HEPES buffer were assessed with a Zetasizer Nano ZS (Malvern Instruments, Malvern, UK).

The amount of polymer was calculated according to the following equation:

M (polymer in pg) = *n* siRNA (pmol) × 52 × N/P × Protonable unit (g/mol),

where 52 is the number of nucleotides of the 25/27mer siRNA; N/P ratio is the molar ratio of the polymer protonable amines (N) and the siRNA phosphate groups (P); The protonable unit was calculated by dividing the molar mass of repeating unit by the number of protonable amines in each repeating unit.

2.4 SYBR gold assay of P(SpDBAE) polyplexes

To determine the siRNA encapsulation efficiency of the polymer, SYBR gold assays were performed. In brief, the P(SpDBAE)-siRNA polyplex formulations from N/P 1 to 20 were prepared as described in section 2.3. Triplicates of 100 µL of the polyplexes were added to black 96-well plates, 30 µL 4X SYBR gold solution was added to each well subsequently, and the polyplexes were incubated with the intercalating dye at room temperature in the dark for 10 min. Finally, intercalation-based fluorescence was quantified in a microplate reader (TECAN, Switzerland, excitation: 485/20 nm, emission: 520/20 nm.). The fluorescence intensity of free siRNA (N/P = 0) was set as 100%.

2.4 In vitro cell compatibility of P(SpDBAE) and P(SpDBAE) polyplexes

The *in vitro* cell compatibility of P(SpDABE) and P(SpDBAE) polyplexes were evaluated via MTT assay. In brief, H1299 cells were seeded in 96-well plates (5000 cells/well) 24 h before use. P(SpDABE) diluted in RPMI-1640 complete medium in a concentration range from 1 µg/mL to 100 µg/mL was added to the plate (100 µL per well in triplicates). After incubation in the CO_2 incubator for 24 h, the polymer solution was discarded and replaced with MTT solution in serum-free RPMI-1640 and incubated for 4 h in the incubator. Finally, the MTT solution was discarded, 100 µL per well DMSO was added and incubated at room temperature for 30 min. The optical density was finally determined at 570 nm and

corrected with background measured at 680 nm using a microplate reader (TECAN, Switzerland).

For the MTT assay of P(SpDBAE) polyplexes, 10 µL polyplexes at N/P 5, 7 and 10 in 90 µL RPMI-1640 complete medium was incubated with H1299 cells the in CO_2 incubator for 24 h and treated with MTT solution and measured the same as described above. Hyperbranched polyethylenimine 25 kDa (hyPEI25K) and PEI polyplexes were used for comparison.

2.5 Cellular uptake of P(SpDBAE) polyplexes

The cellular uptake of P(SpDBAE) polyplexes was quantified by flow cytometry. The polyplexes were prepared as described in section 2.3 using Alexa Fluor 488 labeled siRNA (AF488-siRNA). Hyperbranched polyethylenimine 25 kDa (hyPEI25K) was used as control. H1299 cells were seeded in 24-well plates (50,000 cells in 1 mL medium/well). After incubation in the CO_2 incubator (37 ℃, 5% CO_2) for 24 h, polyplexes at N/P 5, 7 and 10 in RPMI-1640 complete medium were added (50 pmol AF488-siRNA/well) and incubated in the incubator for 24 h. Subsequently, the polyplex suspension was discarded, the cells were rinsed with PBS and detached with 0.05% Trypsin-EDTA. The detached cells were then washed with PBS for another 2 times and analyzed via flow cytometry (Attune NxT Acoustic Focusing Cytometer, Thermofisher, America) with or without quenching by Trypan blue.

2.6 GFP knockdown of P(SpDBAE) polyplexes

To determine the gene silencing ability of P(SpDBAE) polyplexes on the protein level, silencing of the enhanced green fluorescent protein reporter gene (eGFP) was quantified by flow cytometry. H1299/eGFP cells were seeded in 24-well plates (25000 cells in 500 µL medium/well), after growth in the CO_2 incubator (37 ℃, 5% CO_2) for 24 h, the cells were transfected with P(SpDABE) polyplexes composed of scrambled siRNA (siNC, 50 pmol/well) or siRNA against GFP (siGFP, 50 pmol/well). Lipofectamine™ 2000 formulated with siNC and siGFP were respective control groups. After incubation in the incubator for 48 h, the cells were detached with 0.05% Trypsin-EDTA and washed with PBS for flow cytometry measurements (Attune Cytometer, Thermo Fisher Scientific, Waltham, MA, USA).

3. Results and Discussion

3.1 Polymer synthesis

Tri-Boc-spermine was synthesized first. To obtain a pure product, it was purified by column chromatography. The purity of monomers is important for the following steps during polymer synthesis, and the chemical structure of the tri-Boc-spermine was therefore characterized by ^{1}H NMR (**Figure 1A**).

The polymer P(BSpDBAE) was synthesized by the Michael addition-based step-growth polymerization of tri-boc-spermine, decylamine and 1,4-butanediol diacrylate. As shown in **Figure 1B**, the peaks of the three monomers can be found in the spectrum. For instance, the peaks at 1.44 ppm, 1.70 ppm and 3.16 ppm belong to tri-boc-spermine; the peaks at 0.88 ppm and 1.26 ppm belong to decylamine; the peaks at 1.70 ppm, 2.46 ppm, 2.82 ppm and 4.11 ppm belong to 1,4-butanediol diacrylate. The peak at 4.11 ppm (4.20 ppm in 1,4-butanediol diacrylate) indicates that the conjugation of the monomers was successful. The molar ratio of the two monomers was calculated according to the integrations of peaks at 1.70 ppm and 0.88 ppm, and the ratio was approximately 1:1. The reaction was carried out without adding additional solvents, as high concentrations of monomers in the absence of solvents can produce PBAEs with high molecular weight, shorter reaction time and less intramolecular cyclization.[120, 155]

The polymer P(BSpDBAE) was then deprotected by TFA. As shown in **Figure 1C**, the disappearance of the peak at 1.44 ppm indicates that the N-Boc groups were removed successfully. The reaction conditions, yield, molecular weight, PDI and protonable unit of the polymers were summarized in Table 1.

Table 1. Step-growth polymerization (polyaddition) of tri-Boc spermine, decylamine and 1,4-butanediol diacrylate

Polymer	Solvent	Time (h)	Yield (%)	M_n (Da)	PDI	Protonable unit
6[a]	/	15	44	5987[c]	1.83[c]	/
7[b]	DCM	2	62	6217[d]	/	226

[a] reaction conditions: no solvents, 120 ℃, overnight. [b]: reaction conditions: polymer 6, TFA, DCM, room temperature, 2 h. [c]: M_n and PDI were tested via

GPC (measurement relative to polystyrene and in chloroform at 30 ℃). [d]: molecular weight was calculated on the basis of GPC of polymer 6 and the theoretical chemical structure of polymer 7 as TFA salt.

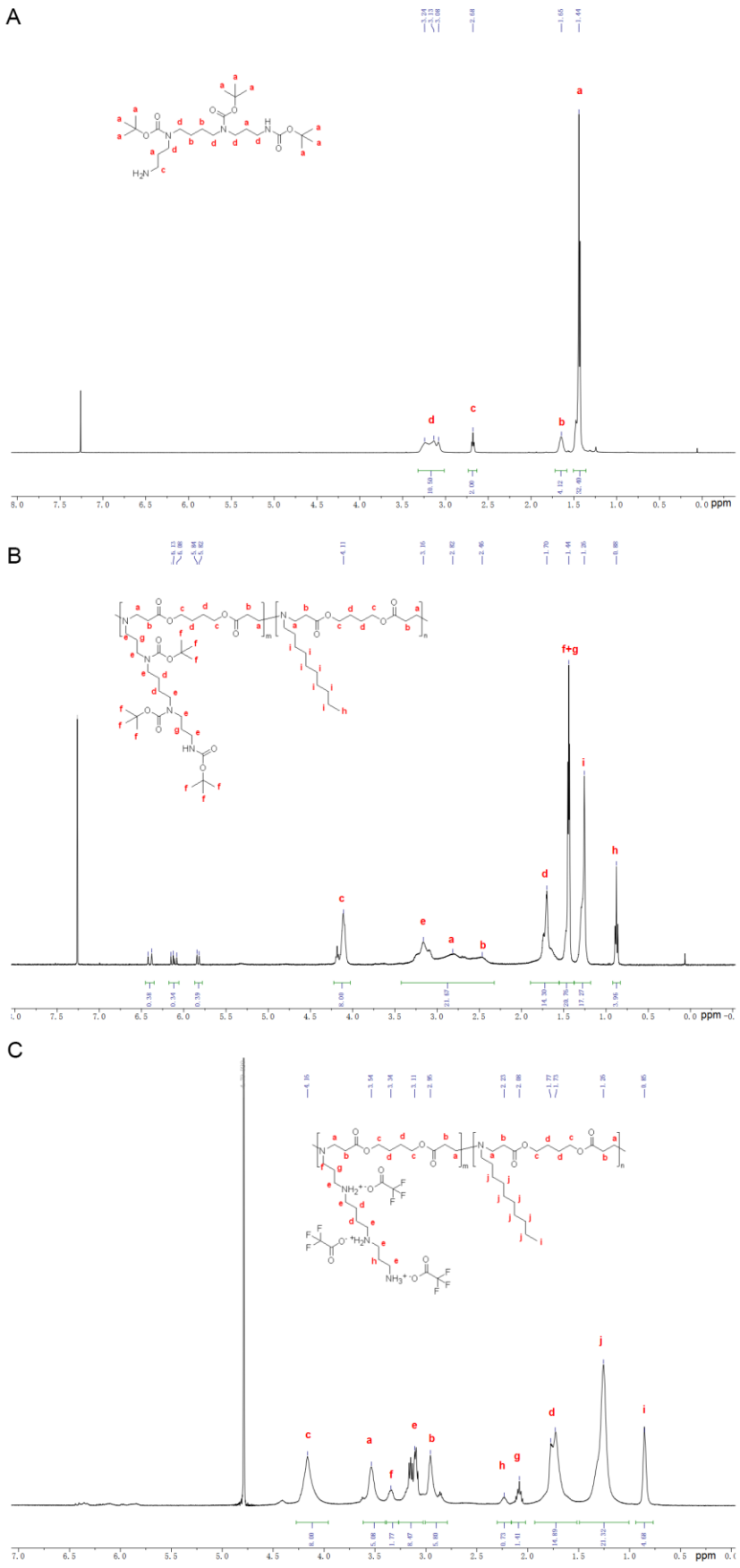

Figure 1. ^{1}H NMR of tri-Boc-spermine in $CDCl_3$ (A), P(BSpDBAE) in $CDCl_3$ (B) and P(SpDBAE) in D_2O (C).

3.2 Size and Zeta potential of P(SpDBAE) polyplexes

The hydrodynamic diameter (size) and polydispersity index of the polyplexes were measured by dynamic light scattering (DLS) and the Zeta potential of the polyplexes was determined by laser doppler anemometry (LDA). As shown in **Figure 2A**, the size of the polyplexes was dependent on the N/P ratios, the minimum size of the polyplexes was 36.81 nm at N/P 7 with a PDI of 0.179. It was hypothesized that the siRNA was not entirely encapsulated at N/P 1 and 3 as the Zeta potential was negative, and the observed sizes were comparably large. For the polyplexes at N/P 10 to 20, an excess of free polymer may form sedimentation, thus the PDI was comparably high. Size is an important factor for cellular uptake and transfection. Some reports indicate that nanoparticles with a size below 150 nm are required for the uptake in lung cells by endocytosis.[182] While there are also papers that report that spermine-based delivery systems with a larger size that have a good transfection efficiency in vivo.[183]

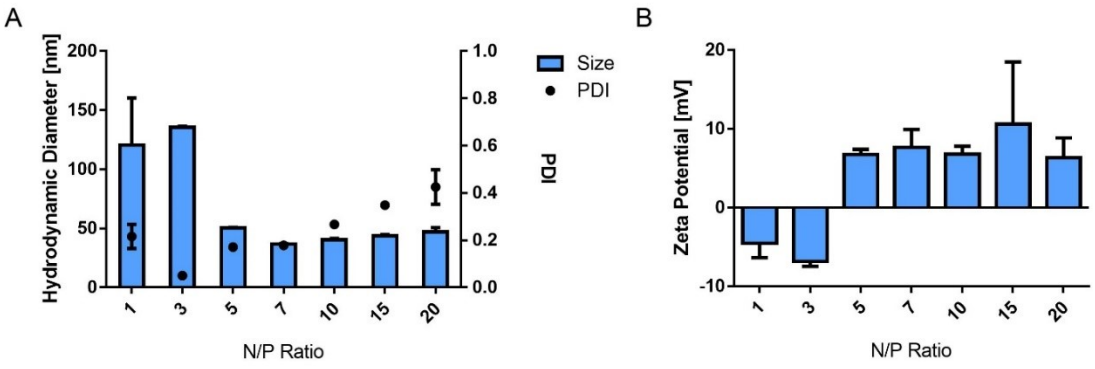

Figure 2. (A) Hydrodynamic diameter (size) and polydispersity index (PDI) of P(SpDBAE) polyplexes at various N/P ratios. (B) Zeta potential of P(SpDBAE) polyplexes at various N/P ratios. (Mean ± SD, *n* = 3)

3.3 SYBR Gold assay of P(SpDBAE)

SYBR® Gold stain is a high quantum yield proprietary unsymmetrical cyanine dye which can bind to free nucleic acids and exhibits high fluorescence intensity upon binding.[150] As shown in **Figure 3**, free siRNA was used as a negative control and its fluorescence intensity was set as 100%. The amount of free siRNA decreased with the increase of N/P ratio, which means the siRNA was encapsulated by the polymer in polyplexes. Almost all the siRNA can be encapsulated from N/P

5 on, which indicates that P(SpDBAE) can encapsulate siRNA efficiently. The SYBR gold result is also corresponding to the size and Zeta potential of the polyplexes. As shown in **Figure 3**, the siRNA was not fully encapsulated at N/P 1 and 3, and free siRNA attached to the surface of the polyplexes or remained in the solution, thus the zeta potentials of the polyplexes were negative (**Figure 2B**). The siRNA can be quantitatively encapsulated from N/P 5 on (**Figure 3**), which is corresponding to the positive Zeta potential of the formed polyplexes (**Figure 2B**).

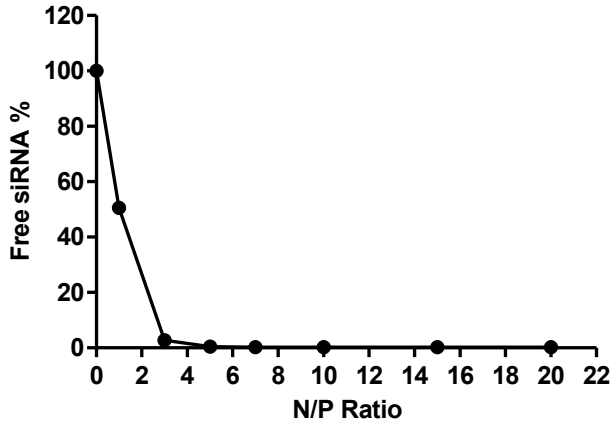

Figure 3. siRNA encapsulation profiles of P(SpDBAE) polyplexes measured by SYBR Gold assay at various N/P ratios. 100% values (N/P = 0) are represented by the determined fluorescence of uncondensed free siRNA (data points indicate Mean ± SD, *n* = 3).

3.4 In vitro compatibility of P(SpDBAE) and P(SpDBAE) polyplexes

The cell compatibility of P(SpDBAE) and P(SpDBAE) polyplexes was measured by MTT assay. MTT (diemthylthiazolyl blue diphenyltetrazolium bromide) is a yellow tetrazole, which can be reduced to purple formazan in living cells.[184] As shown in **Figure 4**, the treatment with polymer P(SpDBAE) leads to higher cell viability than PEI treatment in general. The cell viability of P(SpDBAE) polyplexes at N/P 5, 7 and 10 was 79.8%, 75.9% and 64.7% respectively. The cell viability of P(SpDBAE) polyplexes decreased from N/P 5 to 10 because of the increasing amount of excess free polymer. Interestingly, the cell viability of PEI polyplexes was better than P(SpDBAE) polyplexes. This observation was attributed to the smaller protonable unit of PEI than that of P(SpDBAE), resulting in smaller weight amounts of PEI necessary for preparing the polyplexes than the weight amount

of P(SpDBAE) in P(SpDBAE) polyplexes. Besides, the cellular uptake of P(SpDBAE) polyplexes was much higher than that of PEI polyplexes (**Figure 5**), which could also lead to stronger cytotoxicity. Although the cell compatibility of P(SpBAE) polyplexes seems not as good the compatibility of PEI polyplexes, the PBAE is biodegradable. PBAE degradation products are considered to be benign to mammalian cells and were reported to have limited influence on the metabolic activity of healthy cells.[109] When applied *in vivo*, several doses of polyplexes may be required to obtain a therapeutic effect and for improved long-term efficacy.[185] Therefore, we believe that the cumulative cytotoxicity of P(SpBAE) polyplexes will be improved compared to PEI polyplexes.

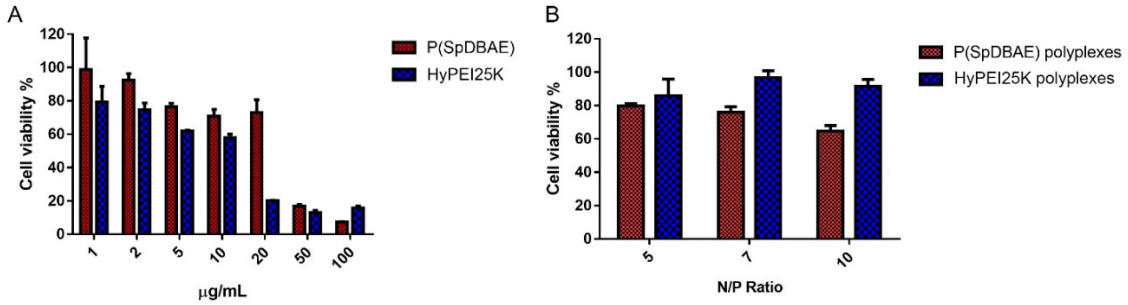

Figure 4. Cell viability of P(SpDABE) and P(SpDBAE) polyplexes determined by diemthylthiazolyl blue diphenyltetrazolium bromide (MTT) assay in H1299 cells.

3.5 Cellular uptake of P(SpDBAE) polyplexes

The cellular uptake of P(SpDBAE) polyplexes was quantified by flow cytometry and compared to hyperbranched polyethylenimine (hyPEI, 25 kDa) as a positive control and free AF488-siRNA as a negative control. Extracellular fluorescence associated with non-internalized polyplexes on the cell surface was quenched with 0.4% trypan blue. As shown in **Figure 5**, the median fluorescence intensities of all the formulations showed no significant difference before and after quenching with trypan blue, which confirms that the determined fluorescence stems from the polyplexes that were internalized into the cells. The uptake of P(SpDBAE) polyplexes at N/P 5 was 58.83 times higher than that of free AF488-siRNA (negative control) and 3.09 times higher than that of hyPEI25K poyplexes (positive control); the uptake of P(SpDBAE) polyplexes at N/P 7 was 87.19 times higher than the negative and 5.79 times higher than the positive control; the uptake of P(SpDBAE) polyplexes at N/P 10 was 132.6 times higher than negative and

12.49 times higher than positive control. The cellular uptake of P(SpDBAE) polyplexes increased from N/P 5 to 10, while the uptake of hyPEI25K polyplexes decreased from N/P 5 to 10.

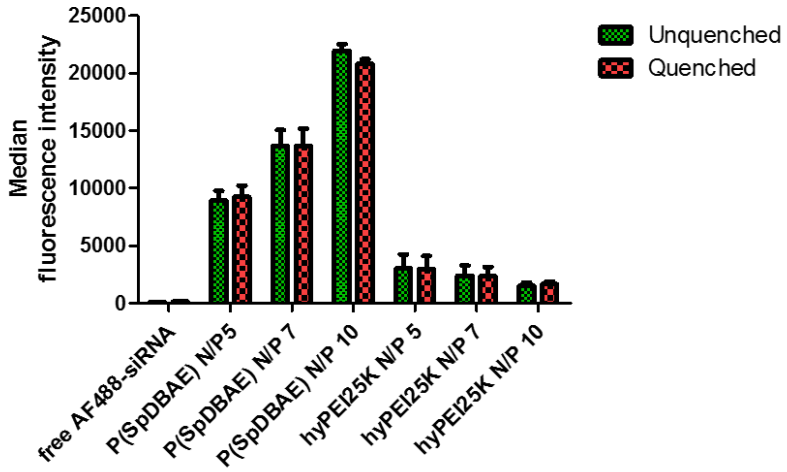

Figure 5. Cellular uptake of P(SpDBAE) polyplexes quantified by flow cytometry and presented as median fluorescence intensity corrected by autofluorescence of untreated blank cells (H1299 cells, AF488-siRNA, Mean ± SD, *n* = 3).

The cellular uptake of the polyplexes was determined from N/P 5 where the siRNA is quantitatively encapsulated according to the SYBR gold assay (**Figure 3**). The highest N/P ratio chosen in this experiment was N/P 10 to avoid any possible cytotoxicity at higher N/P ratios. Interestingly, the cellular uptake of P(SpDBAE) polyplexes increased as the N/P ratio increased from N/P 5 to 10, regardless of the PDI of the polyplexes; while for PEI polyplexes, the cellular uptake decreased from N/P 5 to 10, which may not be attributed by the cytotoxicity of PEI according to the MTT assay, but could indicate that the size of the PEI polyplexes was too disperse at high N/P ratios.

3.6 GFP knockdown of P(SpDBAE) polylexes

To determine the gene silencing efficiency of P(SpDBAE) polyplexes on the protein level, we did a GFP knockdown assay using enhanced green fluorescence protein expressing cells (H1299-eGFP) and quantified the median fluorescence intensity via flow cytometry. Lipofectamine^{TM} 2000 (LF) was used as positive control and LF and P(SpDBAE) were used to encapsulate scrambled siRNA (siNC) as well as negative control. As shown in **Figure 6**, the knockdown efficiency of P(SpDBAE) polyplexes at N/P 5, 7 and 10 was 89.73%, 90.35% and

94.33% respectively. Higher cellular uptake of P(SpDBAE) polyplexes led to higher levels of GFP knockdown.

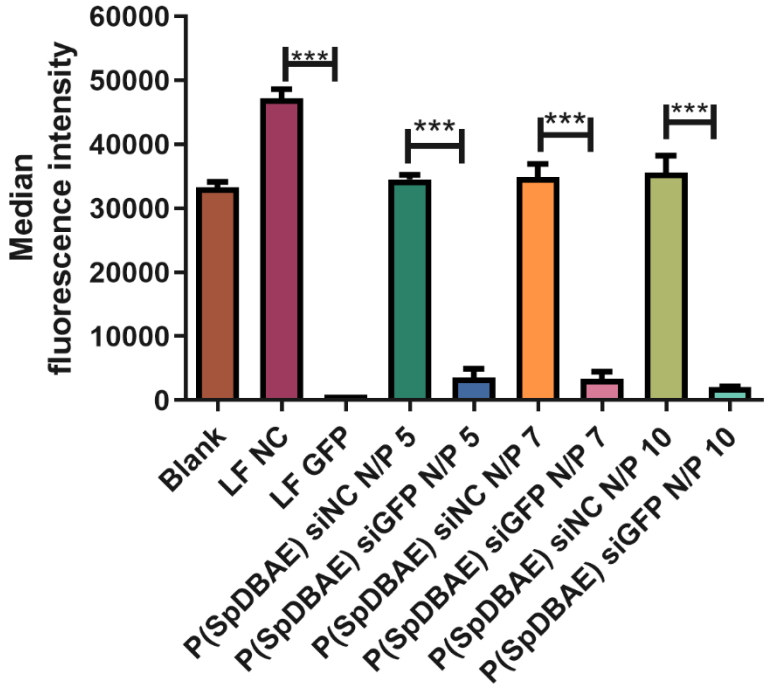

Figure 6. Enhanced green fluorescent protein (eGFP) knockdown of P(SpDBAE) polyplexes in H1299 cells expressing eGFP quantified by flow cytometry as median fluorescence intensity, LF: Lipofectamine™ 2000 (Mean ± SD, n = 3, One-way ANOVA with Bonferroni multiple comparison test, $^{***}p < 0.001$).

In fact, the cellular uptake and knockdown does not always show a positive correlation. For example, Dosta et al. synthesized a group of PBAEs. Although the cholesterol-modified polymers showed lower siRNA uptake than the unmodified hexylamine and hexadecylamine pendant polymers, the GFP knockdown efficiency of cholesterol-modified polymers was still comparable with the unmodified PBAEs.[186]

In our case, higher cellular uptake led to more efficient gene silencing efficiency. As far as we understand, the correlation between cellular uptake and gene knockdown mainly depends on the endosomal escape ability of the polyplexes.[7] If the polyplexes can escape from the endosomes and lysosomes successfully, high cellular uptake means efficient gene silencing. However, if the polyplexes have poor ability to escape from endosomes or lysosomes, most of the polyplexes will be entrapped in latter compartment, and the siRNA will be degraded in the end. In that case, high cellular uptake does not correlate with efficient gene silencing.

In addition, the polyplexes should not be too cytotoxic, otherwise the polyplexes cannot silence genes successfully but may cause off-target effects.[187] For the same polyplexes with different N/P ratios, the formulations with high cellular uptake usually means high gene silencing efficiency. However, when comparing polyplexes with and without modification, the modified polyplexes may have low cellular uptake but high gene silencing efficiency.[186] Kwon et al. modified PEI with a membrane-lytic peptide called HGP taken from the endodomain of HIV gp41. The PEI-HGP polyplexes showed slightly lower cellular uptake than PEI but the transfection efficiency of PEI-HGP polyplexes was significantly higher than PEI. This effect was explained by the enhanced endosomal escape mediated by the HGP peptide.[49]

The gene silencing efficacy of polyplexes also strongly depends on the polymers. After the first use of PBAEs for gene delivery by Langer's group[112], a lot of PBAEs were synthesized and researchers tried to understand the relationship between the properties and the chemical structures of PBAEs.[119, 188] It was found that amine-terminated PBAEs are more suitable for gene delivery, and the transfection potential of PBAEs can also be effected by molecular weight.[115] For example, PBAEs with molecular weight less than 11 kDa were unable to form stable polyplexes even at a high 150:1 polymer to DNA weight ratio, however, PBAEs at molecular weight more than 13 kDa (Mw = 13100 and 13400) were able to stably complexes DNA even at polymer to DNA weight ratio as low as 10:1, and showed the highest luciferase expression.[115] In addition, low molecular weight PBAEs (Mw < 8 kDa) only poorly transfect DNA compared with higher molecular weight versions, which is the same trend as observed for PEI.[115, 119, 189] However, we found that for siRNA formulation and delivery investigated here, the molecular weight of PBAEs does not necessarily need to be higher than 8 kDa. Instead, a suitable amphiphilicity could be the determining factor.[186]

P(SpDBAE) polyplexes mediated efficient gene silencing at N/P 5 (polymer/siRNA weight ratio 3.5). Compared with polyplexes prepared from cross-linked PEI 800, which achieved gene silencing efficiency 46.63% at N/P 115.05,[190] and another PBAE polyplexes with 92 ± 1% GFP knockdown at polymer/siRNA weight ratio 445,[158] the N/P ratio of our polyplexes is rather low and gene silencing is highly efficient. Low N/P ratios are expected to cause less cyto-

toxicity or side effects when applied *in vivo*. In the case of intravenous administration, polyplexes encounter a complex environment, especially interaction with hundreds of serum proteins. Negatively charged proteins may attach to the polyplexes and form the so-called “protein corona”, which can alter the endocytic pathway of the polyplexes and lower the transfection efficiency due to the reduced endo/lysosomal escape.[191, 192] P(SpDBAE) polyplexes can be effectively applied in complete cell culture medium regardless of the presence of proteins in serum. Although the serum concentration in cell culture is lower than the serum concentration in full blood, our results still indicate the potential application of the polyplexes *in vivo*.

4. Conclusion

Safe and efficient transfection of siRNA has remained a challenge for many years. In this study, we successfully synthesized a novel poly(β-amino ester) composed of decylamine and spermine. The free polymer has higher biocompatiblity than the commonly used cationic polymer PEI, and its polyplexes achieved a high cellular uptake and around 90% GFP knockdown at low N/P ratios in complete cell culture medium. These results suggest that this new PBAE P(SpDBAE) is very promising for siRNA delivery and it could be one of the most efficient PBAEs for siRNA delivery reported so far.

AUTHOR INFORMATION

Corresponding author

*Prof. Dr. Olivia M. Merkel

E-Mail: olivia.merkel@lmu.de

Present Addresses

Friederike Adams University of Stuttgart, Institute of Polymer Chemistry, Chair of Macromolecular Materials and Fiber Chemistry, Pfaffenwaldring 55, 70569 Stuttgart, Germany University Eye Hospital Tübingen, Center for Ophthalmology, Elfriede-Aulhorn-Straße 7, 72076 Tübingen, Germany

Author Contributions

Conceptualization, Yao Jin, Friederike Adams, and Olivia M. Merkel; methodology and investigation, Yao Jin and Friederike Adams; original manuscript preparation, Yao Jin; review and editing, Olivia. M. Merkel; funding acquisition, Olivia M. Merkel.

ACKNOWLEDGEMENT

Yao Jin appreciates the financial support from China Scholarship Council (CSC201906010329). This project was funded by ERC-2014-StG – 637830 to Olivia Merkel.

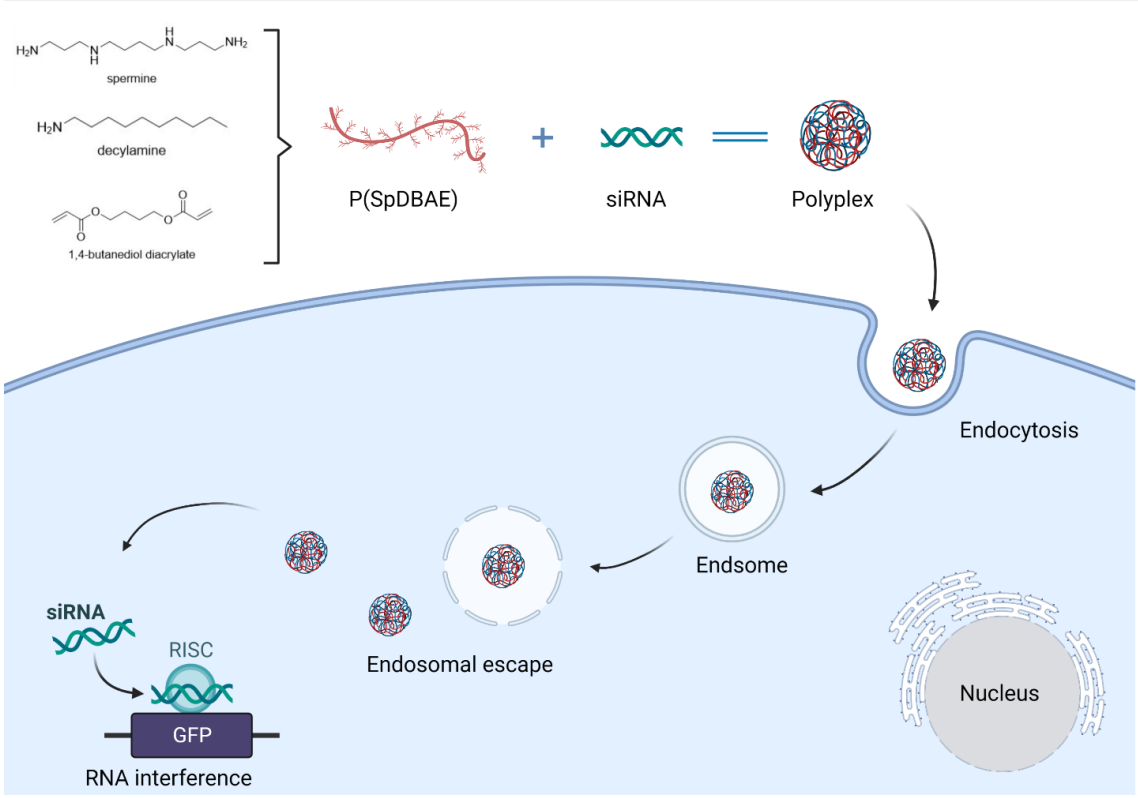

Graphical abstract. Created with BioRender.com

Chapter III

Hydrophobic modification of spermine-based poly(β-amino ester)s and its role in siRNA delivery

Yao Jin, Xiaoxuan Wang, Friederike Adams, Thi My Hanh Ngo, and Olivia M. Merkel*

Contributions: I and Xiaoxuan Wang performed the experiments with support of the coauthors and I wrote the manuscript.

Abstract

After RNAi was first discovered over 20 years ago, siRNA-based therapeutics are finally becoming reality. However, the delivery of siRNA has remained a challenge. In our previous research, we found that the spermine-based poly(β-amino ester)s are very promising for siRNA delivery. However, the role of hydrophobic modification in siRNA delivery of spermine-based poly(β-amino ester)s is not fully understood yet. In this research, we synthesized spermine-based poly(β-amino ester)s composed of different percentages of oleylamine side chains, named P(SpOABAE). The chemical structures of the polymers were characterized by ^{1}H NMR. The polymers showed efficient siRNA encapsulation determined by SYBR gold assays. The hydrodynamic diameters of the P(SpOABAE) polyplexes from N/P 1 to 20 were 30 – 100 nm except for aggregation phenomena observed at N/P 3. The cellular uptake of the polyplexes was determined by flow cytometry in H1299 cells, and all the polyplexes showed significantly higher cellular uptake than hyperbranched polyethylenimine (hyPEI, 25 kDa). The P(SpOABAE) polyplexes were able to achieve more than 90% GFP knockdown in H1299/eGFP cells and Sp0.7/OA0.3 polyplexes at N/P 5 mediated a similar GAPDH knockdown as the commercial transfection reagent Lipofectamine™ 2000 in 16HBE14o- cells.

Keywords

siRNA delivery; hydrophobic modification; poly(β-amino ester)s; spermine; oleylamine

1. Introduction

RNA interference (RNAi) refers to a process of post-transcriptional gene silencing that is triggered by small, double-stranded regulatory RNA molecules (dsRNAs).[1] Endogenously expressed long dsRNAs are cleaved by Dicer into short (~ 21-nt) duplexed RNAs, termed small interfering RNAs (siRNAs). Dicer associates with a dsRNA-binding protein R2D2 in Drosophila and HIV, and with transactivating response RNA-binding protein (TRBP) in mammalian cells to determine the orientation of siRNA loading onto Argonaute 2 (Ago2), the catalytic core of the RNA-induced silencing complex (RISC).[5, 6] Once assembled into RISC, the passenger strand of the siRNA duplex is cleaved and released, leaving the guide strand to direct the activated RISC toward the complementary sequence in the target mRNA. The target mRNA is finally endonucleotyically cleaved and the gene expression is inhibited.[7]

The approval of siRNA therapeutics by the FDA in recent years brings new hope to siRNA therapeutics. However, the therapeutic use of siRNA is still limited by the delivery of siRNA, as siRNAs are negatively charged macromolecules, membrane-impermeable and highly unstable in systemic circulation due to the degradation by endogenous enzymes and the elimination through the kidneys.[2] The half-life of most naked or unmodified siRNA is around 5-10 min.[193]

Cationic polymers are one of the main categories of non-viral vectors for siRNA delivery. After the first successful mammalian gene delivery experiments based on spermine in the early 1960s by Szybalska and Szybalski,[194] many polycations were developed such as poly(ornithine),[195] poly(arginine),[196] poly(l-lysine),[197] and poly(ethylene imine).[30] Poly(β-amino ester)s abbreviated as PBAEs or PAEs refer to polymers synthesized from acrylates and amines by Michael addition. PBAEs were first introduced for nucleic acid delivery by Lynn and Langer in 2000.[112] PBAEs are biocompatible, biodegradable, and pH-responsive.[109] These properties make them very promising materials for siRNA delivery. Spermine is a linear tetramine and an important component of nucleic acid delivery vehicles. Endogenous spermine is naturally occurring, safe, and aids in packaging cellular DNA into a compact state, which is essential during cell growth in eukaryotic cells.[79, 180] However, the siRNA delivery efficiency of spermine is limited due to

its low molecular weight (202.34 g/mol).[79] In addition, spermine has a limited endosomal escape ability despite its good proton-buffering capacity.[83] Polymerization of spermine to increase its molecular weight has been shown an effective strategy to enhance its siRNA delivery efficiency.

We have synthesized spermine-based poly(β-amino ester)s in our lab, but several of them did not mediate efficient gene silencing of green fluorescence protein in a cell model, which was found to be caused by endosomal entrapment. Research from other groups also indicates the same problem: for example, Benns et al. synthesized N-Ac-poly(L-histidine)-graft-poly(L-Lysine) to deliver plasmid DNA, but only inclusion of chloroquine enhanced the transfection efficiency.[198]

In fact, endosomal entrapment is one of the biggest barriers to siRNA delivery. According to previous reports, only 3.5% or even less than 1% of internalized siRNA can escape from the endosome and be incorporated into RISC to mediate gene silencing.[161, 199] Thus, a carrier for better disruption of the endosomal membrane is critical for successful endosomal escape and gene silencing by siRNA. The strategies that have been developed to promote endosomal escape include the use of polymers with high buffering capacity, for example, polyethylenimine (PEI) which has been hypothesized to mediate endosomal release by the 'proton sponge effect'; fusogenic proteins such as cell-penetrating peptides (CPP);[200] endocytosed photosensitive molecules (photosensitizers) which after activating by light can release singlet oxygen to damage the endosomal membrane,[7, 201] and some small molecules such as chloroquine can also be employed to avoid endosomal entrapment.[202]

According to our experience, hydrophobic modification can be beneficial for more quantitative endosomal escape and subsequent gene silencing efficiency of polyplexes. Many reports also point out that increasing the hydrophobicity of polyplexes improves the transfection efficiency and stability. For example, Alshamsan et. al modified polyethylenimine with oleic acid and stearic acid, and the hydrophobically modified polymers resulted in 3-fold increased siRNA delivery than the parent PEI, and revealed a more pronounced reduction of integrin α levels.[203] Thanou et al. synthesized trimethylated chitosan for gene delivery. The trimethylated derivatives appeared to enhance the stability of the polyplexes and the trans-

fection efficiency was not affected in the presence of serum.[204] In addition, unsaturated hydrophobic fragments were reported to enhance the gene silencing efficiency of siRNA. For example, MacLachlan and colleagues prepared lipoplexes with hydrophobic tails including different numbers of double bonds. They found that lipoplexes containing unsaturated cationic lipids enhanced luciferase gene knockdown compared with those containing saturated cationic lipids.[51]

In this research, we therefore co-polymerized spermine and 1,4-butanediol diacrylate with different amounts of oleylamine which is an unsaturated fatty amine. By changing the ratio of cationic fragment spermine to hydrophobic fragment oleylamine, we aimed to find out the relationship between a balanced hydrophobic modification, endosomal escape, and gene knockdown efficiency and finally give rational design guidelines of PBAEs for siRNA delivery.

2. Materials and methods

2.1 Materials

Spermine, Oleylamine, and trifluoroacetic acid were purchased from Acros Organics (Thermo Fisher Scientific), and 1,4-butanediol diacrylate was purchased from Tokyo chemical industry Co., Ltd. (TCI, Japan). n-hexane, dichloromethane, dimethyl sulfoxide (DMSO), and methanolare technically purely provided by Ludwig-Maximilians-University Munich.

Deuterium oxide, decylamine, HEPES (4-(2-hydroxyethyl)-1-piperazineethanesulfonic acid), thiazolyl blue tetrazolium bromide (MTT), RPMI-1640 medium, Eagle's minimum essential medium (EMEM), fetal bovine serum (FBS), Penicillin-Streptomycin solution, Dulbecco's Phosphate Buffered Saline (PBS), trypsin-EDTA solution (0.05%), and Geneticin (G418) disulfate solution were purchased from Sigma-Aldrich (Taufkirchen, Germany). SYBR Gold Dye, Lipofectamine™ 2000, and Alexa Fluor 488 (AF488) were bought from Life Technologies (Darmstadt, Germany).

Amine-modified eGFP siRNA (5´-pACCCUGAAGUUCAUCUGCACCACcg, 3´-ACUGGGACUUCAAGUAGACGGGUGGC) and scrambled siRNA (5´-pCGUUAAUCGCGUAUAAUACGCGUat, 3´-CAGCAAUUAGCGCAUAUUAUGCG-

CAUAp), and siRNA against GAPDH (5´-pGGUCGGAGUCAACGGAU-UUGGUCgt, 3´-UUCCAGCCUCAGUUGCCUAAA-CCAGCA) were purchased from Integrated DNA Technologies (Leuven, Belgium). “p” denotes a phosphate residue, lower case letters are 2’-deoxyribonucleotides, capital letters are ribonucleotides, and underlined capital letters are 2’-O-methylribonucleotides.

2.2 Synthesis and characterization of the polymers

2.2.1 synthesis of tri-Boc-spermine

Tri-tert-Butyl Carbonyl Spermine abbreviated as tri-Boc-spermine was synthesized as described elsewhere.[147, 148] In brief, spermine (1 eq) was dissolved in methanol and stirred at -78 °C, ethyl trifluoroacetate (1 eq) was added dropwise subsequently and stirred at -78 °C for 1 h, then at 0 °C for 1 h. Without isolation, di-tert-butyl decarbonate (4 eq) was added dropwise to the solution and stirred at room temperature for 2 days. Finally, the solution was adjusted to a pH above 11 by 25% ammonia and stirred overnight to cleave the trifluoroacetamide protecting group. The mixture was then evaporated under vacuum and the residue was diluted with dichloromethane (DCM) and washed with distilled water and saturated NaCl aqueous solution. The DCM phase was finally dried by $MgSO_4$ and concentrated to give the crude product. The crude product was purified by column chromatography (CH_2Cl_2\MeOH\NH_3, aq. 7:1:0.1, SiO_2, $KMnO_4$; R_f = 0.413). Tri-Boc-spermine was isolated and characterized by ^{1}H NMR. Yield: 37%.

2.2.2 Synthesis of P(BSpOABAE)

Tri-Boc-spermine (0.9 eq) and oleylamine (0.1 eq) were first mixed, and 1,4-butanediol diacrylate (1 eq) was then added and stirred at 120 °C overnight. The product was dissolved in 2 mL dichloromethane (DCM) and precipitated in 50 mL n-hexane. The precipitation was dried under vacuum (50 °C, 20 mbar) for 2 days and finally characterized by ^{1}H NMR. The target product has 10% oleylamine side chains. To obtain the polymers with 30% and 50% oleylamine units, tri-Boc-spermine (0.7 eq), oleylamine (0.3 eq) and tri-Boc-spermine (0.5 eq), oleylamine (0.5 eq) were reacted with 1,4-butanediol diacrylate (1 eq) under the same conditions. All of the products were named poly(tri-Boc-spermine and oleylamine-based β-amino ester)s, abbreviated as P(BSpOABAE).

2.2.3 Synthesis of P(SpOABAE)

The N-Boc groups of P(BSpOABAE) were removed to give the final product P(SpOABAE). To give an example, 100 mg P(BSpOABAE) was dissolved in 20 mL DCM and reacted with 1 mL trifluoroacetic acid (TFA) at room temperature for 2 h. The polymers, DCM, and TFA were always used in the same ratios as described above. The reaction solution was then evaporated by a rotary evaporator and the product was dissolved with 2 mL methanol and precipitated in 50 mL n-hexane. The precipitation was dried under vacuum (50 °C, 20 mbar) for 2 days to afford the final product. The product was then characterized by ^{1}H NMR. The product with 10% oleylamine repeating units was named Sp0.9/OA0.1; the product with 30% oleylamine units was named Sp0.7/OA0.3; and the product with 50% oleylamine units was named Sp0.5/OA0.5.

The reaction conditions, molecular weight, yield, and protonable unit of the polymers are summarized in Table 1.

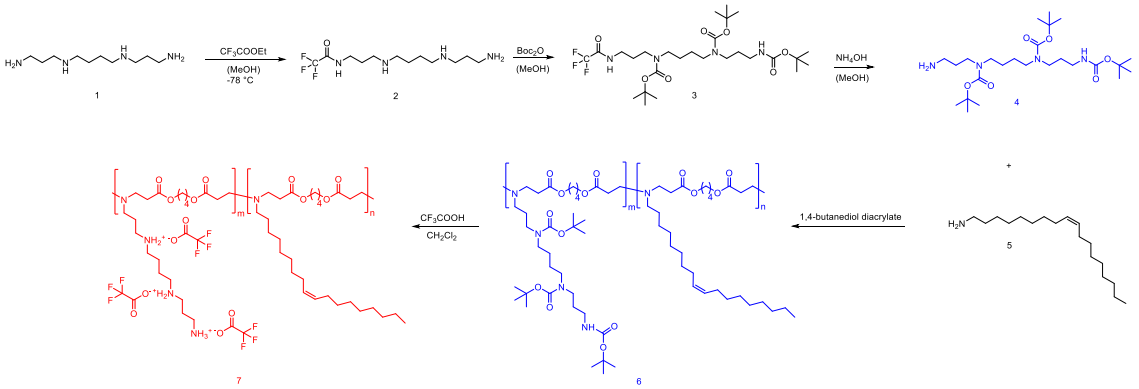

Scheme 1. The synthesis route of spermine and oleylamine-based poly((β-amino ester)s P(SpOABAE)

Table 1. Step-growth polymerization of tri-Boc-spermine, oleylamine, and 1,4-butanediol diacrylate

Polymers	Solvents	Time (h)	Yield (%)	Protonable unit (g/mol)
BSp0.9/OA0.1[a]	/	15	89%	/
BSp0.7/OA0.3[a]	/	15	70%	/
BSp0.5/OA0.5[a]	/	15	91%	/
Sp0.9/OA0.1[b]	DCM	2	76%	196

Sp0.7/OA0.3[b]	DCM	2	91%	213
Sp0.5/OA0.5[b]	DCM	2	91%	246

[a] P(BSpOABAE) reaction conditions: no solvents, 120 °C, overnight. [b]: P(SpOABAE) reaction conditions: TFA, DCM, room temperature, 2 h.

2.3 Preparation and characterization of polyplexes

To prepare polyplexes, the polymers were dissolved in high-purity water at a concentration of 1 mg/mL as a stock solution, and the siRNA stock solution is 100 μM. The amounts of polymers were calculated according to the following equation:

$$m\ (\text{polymer in pg}) = n\ \text{siRNA (pmol)} \times 52 \times \text{N/P} \times \text{Protonable unit (g/mol)},$$

where 52 is the number of nucleotides of the 25/27mer siRNA; N/P ratio is the molar ratio of the protonable polymer amine groups (N) and the siRNA phosphate groups (P). The protonable unit was calculated by dividing the molar mass of the repeating unit by the number of protonable amines in each repeating unit.

P(SpOABAE) and siRNA in an equal volume of 10 mM HEPES buffer (pH 5.3) were mixed and incubated at room temperature for 30 min. The P(SpOABAE) polyplexes were then characterized using a Zetasizer Nano ZS (Malvern Instruments, Malvern, UK). For instance, 100 μL polyplexes in 10 mM HEPES were added to a disposable microcuvette (Malvern Instruments, Malvern, UK) and measured for 15 runs 3 times for each sample. The polyplexes suspension was then diluted with 10 mM HEPES to 700 μL and filled into a Zeta Cell (Zetasizer Nano series, Malvern, UK) to measure the Zeta potential.

2.4 siRNA encapsulation efficiency

SYBR gold assays were used to evaluate the capacity of the P(SpOABAE)s to condense siRNA at various N/P ratios (0 - 20). In brief, P(SpOABAE) polyplexes were prepared as described in section 2.3. The polyplexes were then transferred to a black 96-well plate of 100 μL for each sample. Subsequently, 30 μL SYBR gold (4X) was s added to each well and incubated at room temperature in the dark for 10 min. The fluorescence was then measured using a plate reader (TECAN, Männedorf, Switzerland, excitation: 485/20 nm, emission: 535/20 nm.). The fluorescence intensity of free siRNA (N/P = 0) was set as 100%.

2.5 Cellular uptake

H1299 cells were seeded in 24-well plates at a density of 50 000 cells/well, and the plates were incubated at 37 °C and 5% CO_2 for 24 h. Polyplexes were prepared as described above with 50 pmol Alexa Fluor AF488-labeled siRNA (AF488-siRNA) at N/P ratios of 5, 7, and 10. Free AF488-siRNA and hyperbranched PEI 25 kDa (HyPEI25K) were used as negative control and positive control, respectively. Cells were incubated with the polyplexes in complete RPMI1640 medium for 24 h. The polyplexe suspension was then discarded and the cells were rinsed with PBS and treated with 0.05% trypsin-EDTA (100 µL/well) for 4 min to detach the cells. Fresh Medium (500 µL/well) was added to deactivate the trypsin. Samples were then transferred to microcentrifuge tubes and washed with PBS 2 times. Fluorescence was quantified by flow cytometry by exciting with a 488 nm laser and detection with a BL1 filter (530/30 nm) (Attune NxT Acoustic Focusing Cytometer, Thermo Fisher Scientific, Darmstadt, Germany) with or without quenching by trypan blue.

2.6 GFP knockdown

H1299/eGFP cells were seeded in 24-well plates at a density of 25 000 cells per well and cultured in a CO_2 incubator (37 °C, 5% CO_2) for 24 h before transfection. P(SpOABAE) polyplexes at N/P 5, 7, and 10 were prepared as described above in section 2.3 using siRNA against GFP (siGFP) and scrambled siRNA (siNC) as negative control. Lipofectamine™ 2000 encapsulated with siNC and siGFP were used as controls. Polyplexes and lipoplexes were added with 50 pmol siNC or siGFP to each well and incubated with the cells for 48 h. The medium was finally discarded and the cells were washed with PBS and treated with 0.05% trypsin-EDTA. The cells were collected and washed with PBS twice and measured by flow cytometry by exciting with a 488 nm laser and detection with a BL1 filter (530/30 nm) ((Attune NxT Acoustic Focusing Cytometer, Thermo Fisher Scientific, Darmstadt, Germany).

2.7 GAPDH gene knockdown

16HBE14o- cells were seeded in 24-well plates at a density of 50,000 cells/well, and the plates were incubated at 37 °C and 5% CO_2 for 24 h. P(SpOABAE) polyplexes were prepared as described above with siNC and siGAPDH at N/P 5, 7,

and 10. Cells were transfected with P(SpOABAE) polyplexes for 48 h (100 pmol siNC or siGAPDH/ well). Lipofectamine™2000 encapsulated with the same amount of siRNA was used as a positive transfection control. Subsequently, cells were washed with PBS and detached with 0.05% trypsin-EDTA. The harvested cells were then lysed with lysis buffer (Purelink RNA mini kit, Thermo Fisher Scientific, Darmstadt, Germany). Total RNA was then isolated from cells according to the manufacturer's protocol with supplementary DNase digestion, reverse transcribed to cDNA, and cDNA was amplified in a one-step protocol using Brilliant III SYBR green qRT-PCR master mix. Hs_GAPDH primers (Qiagen, Hilden, Germany) were used to quantify the gene expression of hGAPDH. Hs_β-actin primers (Qiagen, Hilden, Germany) were used as a standard to evaluate the relative gene expression of GAPDH using a QuantStudio real-time PCR system (Thermo Fisher Scientific). Cycle threshold (Ct) values were obtained with the cloud dashboard of Thermo Fisher Connect™.

2.8 Cell viability

The cell viability of the polymers P(SpOABAE) and the polyplexes were determined by MTT assays. In brief, H1299 cells were seeded in 96-well plates at a density of 5000 cells/well and incubated at 37 °C, 5% CO_2 for 24 h. P(SpOABE) and hyPEI25K were diluted with RPMI1640 complete cell culture medium in a range of 1 µg/mL to 100 µg/mL and incubated with the cells for 24 h. After the incubation, the medium was discarded and MTT solution prepared in serum-free RPMI1640 medium was added to the plate (0.5 mg/mL, 100 µL/well) and incubated for 4 h in the CO_2 incubator. Subsequently, the cell culture medium was removed and DMSO (100 µL/well) was added and incubated at room temperature for 30 min. The optical absorbance was measured at 570 nm and corrected with background measured at 680 nm via plate reader (TECAN, Männedorf, Switzerland).

Polyplexes at N/P 5, 7, and 10 were prepared as described in section 2.3. Subsequently, 10 µL polyplexes containing 5 pmol siRNA were added to each well with 90 µL complete RPMI1640 cell culture medium and incubated in the CO_2 incubator for 24 h. The plates were then treated and measured as described above for the polymers. HyPEI25K polyplexes were used as control.

2.9 Endosomal entrapment

Endosomal entrapment was determined by confocal laser scanning microscopy (CLSM). In brief, H1299 cells were seeded on 13-mm microscope cover glasses (VWR, Allison Park, PA, USA) in each well (24-well plate, 50 000 cells/well) 24 h before use. The Sp0.9/OA0.1, Sp0.7/OA0.3, and Sp0.5/OA0.5 AF488-siRNA polyplexes were prepared (N/P =10) and incubated with the cells in the same way as described in section 2.5. Subsequently, the polyplex-containing medium was discarded and incubated with 75-nm Lysotracker Red™ DND 9 in RPMI1640 complete medium at 37 °C for 1 h. The cells were then washed with PBS twice and fixed with 4% paraformaldehyde (PFA) at room temperature for 15 min. After washing with PBS twice more, the cells were stained with DAPI (1 μg/mL) at room temperature for 20 min. Finally, the cells were washed with PBS 5 times and mounted with FluorSave™ reagent (Sigma-Aldrich, Darmstadt, Germany). The fluorescence images were acquired using a confocal laser scanning microscope with excitation by diode laser (405 nm), and argon laser (488 nm and 552 nm), and detection in the blue channel for DAPI (627 nm – 750 nm), green channel for AF488 (750 nm – 755 nm), and red channel (755 nm – 760 nm) for lysotracker, respectively. (Leica SP8 inverted, software: LAS X, Leica microsystems GmbH, Wetzlar, Germany).

3. Results and discussion

3.1 Synthesis and characterization of P(SpOABAE)

As shown in Scheme 1, the polymer synthesis started with spermine, which was protected with ethyl trifluoroacetate and di-tert-butyl decarbonate. Then the trifluoroacetate group was removed to give the monomer tri-tert-Butyl carbonyl spermine (tri-Boc-spermine), and the chemical structure was characterized by ^{1}H NMR (**Figure 1A**). The peak at 4.73 ppm belongs to the solvent residual peak of heavy water.

Tri-Boc-spermine was then co-polymerized with oleylamine and 1,4-butanediol diacrylate to give the polymer 6 (Scheme 1) P(BSpOABAE). As shown in **Figure 1A**, the peaks at 0.83 ppm, 1.25 ppm, and 5.35 ppm are the representative peaks belonging to the oleylamine units, and the peaks around 1.45 ppm and 3.15 ppm belong to tri-Boc-spermine. The peaks around 2.43 ppm, 2.36 ppm, and 4.08 ppm

belong to 1,4-butanediol diacrylate. The appearance of these peaks indicates the presence of the three monomers in the product, and the polymers with different amounts of oleylamine units were calculated according to the integrations of peak k (5.35 ppm) and peak c (4.08 ppm) and named BSp0.9/OA0.1, BSp0.7/OA0.3 and BSp0.5/OA0.5 respectively.

P(BSpOABAE) was finally treated with TFA and to obtain the target product P(SpOABAE). As shown in **Figure 1B**, the disappearance of the peak at 1.45 ppm indicates that the N-Boc groups were removed successfully. The molar ratio of the repeating units of spermine and oleylamine units was calculated according to the integrations of the peaks at 5.31 ppm and 4.19 ppm. The P(SpOABAE)s with 10%, 30%, and 50% of oleylamine were named Sp0.9/OA0.1, Sp0.7/OA0.3, and Sp0.5/OA0.5, respectively.

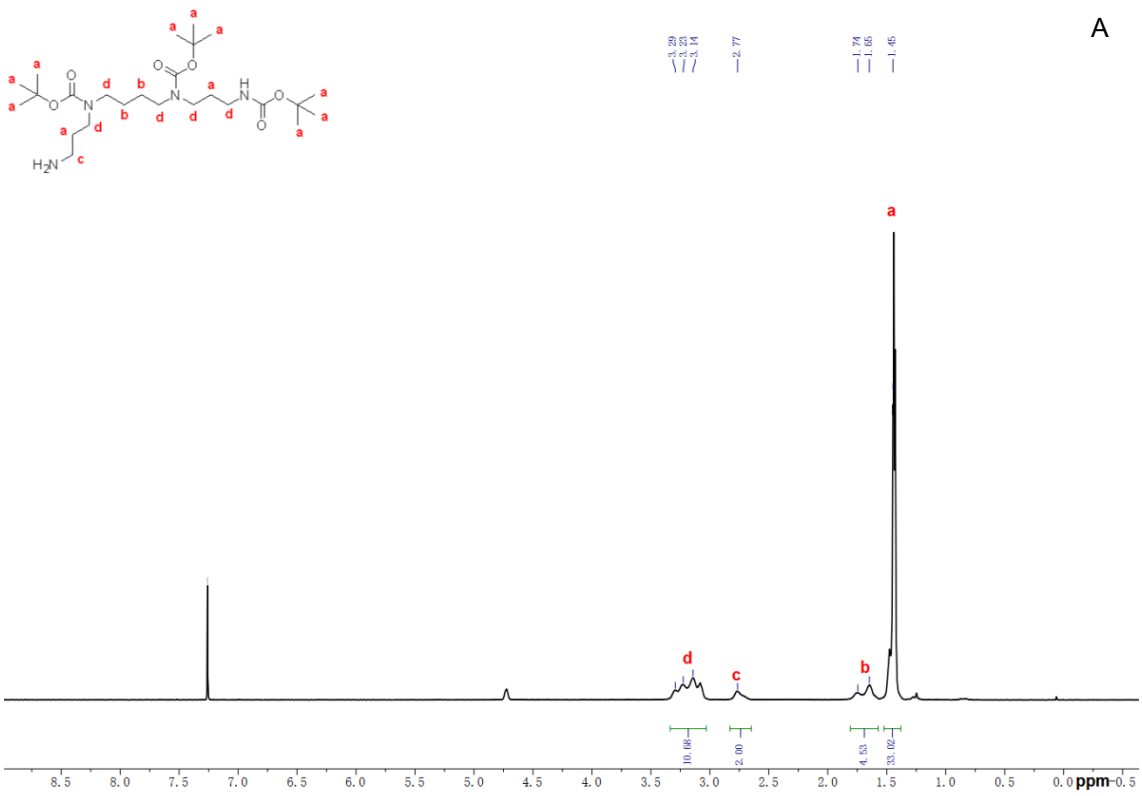

B

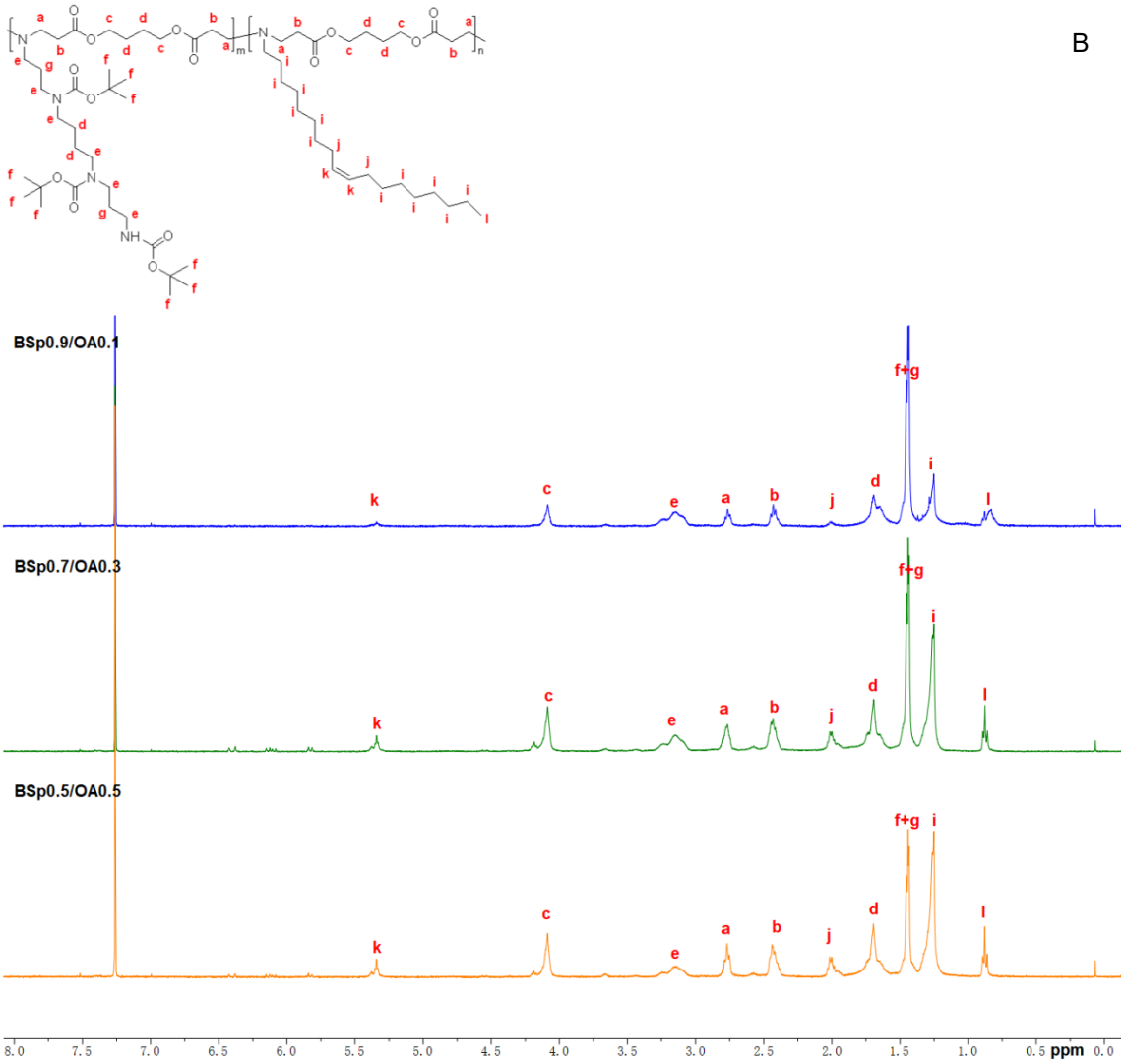
BSp0.9/OA0.1
BSp0.7/OA0.3
BSp0.5/OA0.5
f+g
k
c
e
a
b
j
d
i
l
8.0
7.5
7.0
6.5
6.0
5.5
5.0
4.5
4.0
3.5
3.0
2.5
2.0
1.5
1.0
0.5
ppm
0.0

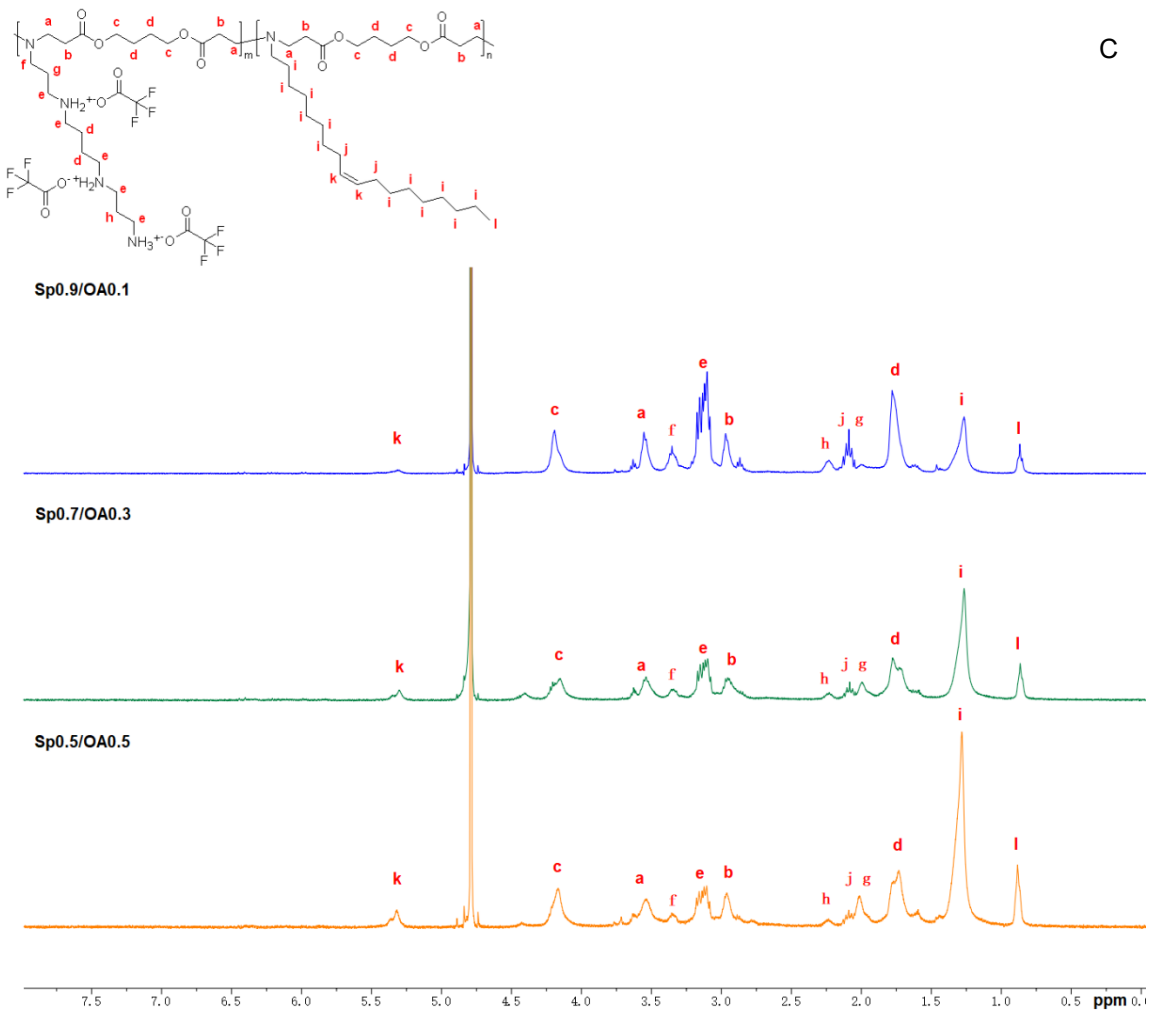

Figure 1. ^{1}H NMR of tri-Boc-spermine in $CDCl_3$ supplemented with D_2O (A), P(BSpOABAE) in $CDCl_3$ (B), and P(SpOABAE) in D_2O (C) (The spectra of polymers with 10% oleylamine are blue and named BSp0.9/OA0.1 and Sp0.9/OA0.1 before and after deprotection; the spectra of polymers with 30% oleylamine are green and named BSp0.7/OA0.3 and Sp0.7/OA0.3 before and after deprotection; The spectra of polymers with 50% oleylamine are orange and named BSp0.5/OA0.5 before and after deprotection.)

3.2 siRNA encapsulation efficiency

The siRNA encapsulation efficiency of the three PBAEs was measured by SYBR gold assay. In this assay, free siRNA is accessible to the intercalating dye SYBR gold and is quantified based on the fluorescence emitted. As shown in **Figure 2**, SP0.9/OA0.1 had the highest siRNA encapsulation efficiency at N/P 1, SP0.5/OA0.5 had the lowest encapsulation efficiency, and SP0.7/OA0.3 had intermediate encapsulation efficiency according to the percentage of spermine,

containing primary amines and secondary amines. All of the PBAEs encapsulated siRNA quantitatively from N/P 5 on. These results indicate that the three PBAEs can encapsulate siRNA efficiently.

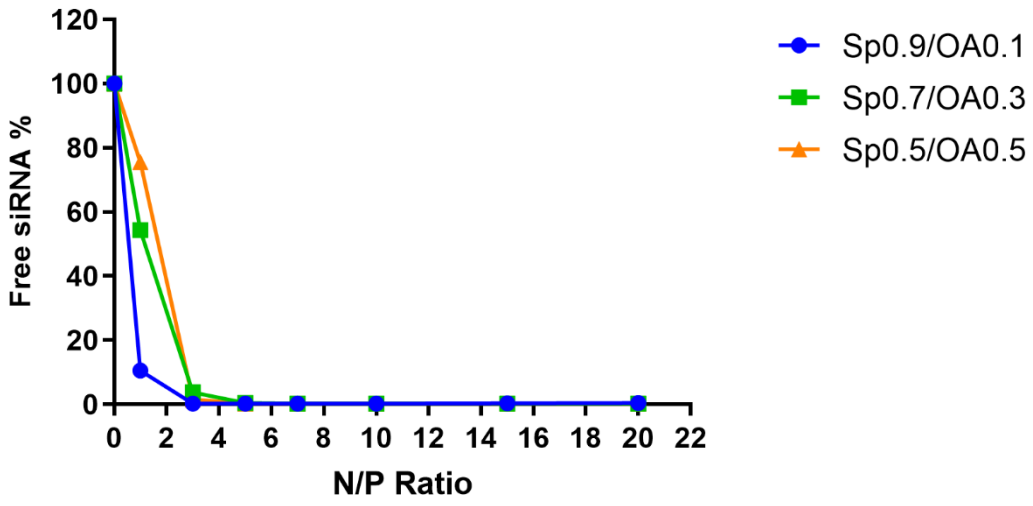

Figure 2. siRNA encapsulation profiles of poly(β-amino ester)s composed of different percentages of spermine and oleylamine. Sp: the repeating unit of spermine, OA: the repeating unit of oleylamine. Sp0.9/OA0.1: P(SpOABAE) with 10% of oleylamine, Sp0.7/OA0.3: P(SpOABAE) with 10% of oleylamine, Sp0.5/OA0.5: P(SpOABAE) with 50% of oleylamine. (Data points indicate Mean ± SD, *n* = 3)

3.3 Size and zeta potential of the polyplexes

The hydrodynamic diameter (size) and polydispersity index (PDI) of the polyplexes was measured by dynamic light scattering (DLS) and the zeta potential of the polyplexes was measured by laser Doppler anemometry (LDA). As shown in **Figure 3**, the sizes of the polyplexes were below 100 nm except for the Sp0.7/OA0.3 and the Sp0.5/OA0.5 polyplexes at N/P 3. The large sizes of the two formulations may be caused by the lack of stabilizing charge of the polyplexes thus leading to aggregation. The zeta potential of the polyplexes corroborates the SYBR gold assay results: when the siRNA is not fully encapsulated, the Zeta potential is negative because siRNA is attached on the surface of the polyplexes. For example, Sp0.9/OA0.1 polyplexes at N/P 1 and Sp0.7/OA0.3 polyplexes at N/P 1, 3 and the Sp0.5/OA0.5 polyplexes at N/P 1, 3 present accessible siRNA on their surfaces as reflected in measurable fluorescence and negative zeta potentials. When siRNA is fully encapsulated, the zeta potential turned to positive.

The PDI of the polyplexes was lowest when the siRNA is quantitatively encapsulated, while an excess free polymer or free siRNA led to higher PDIs.

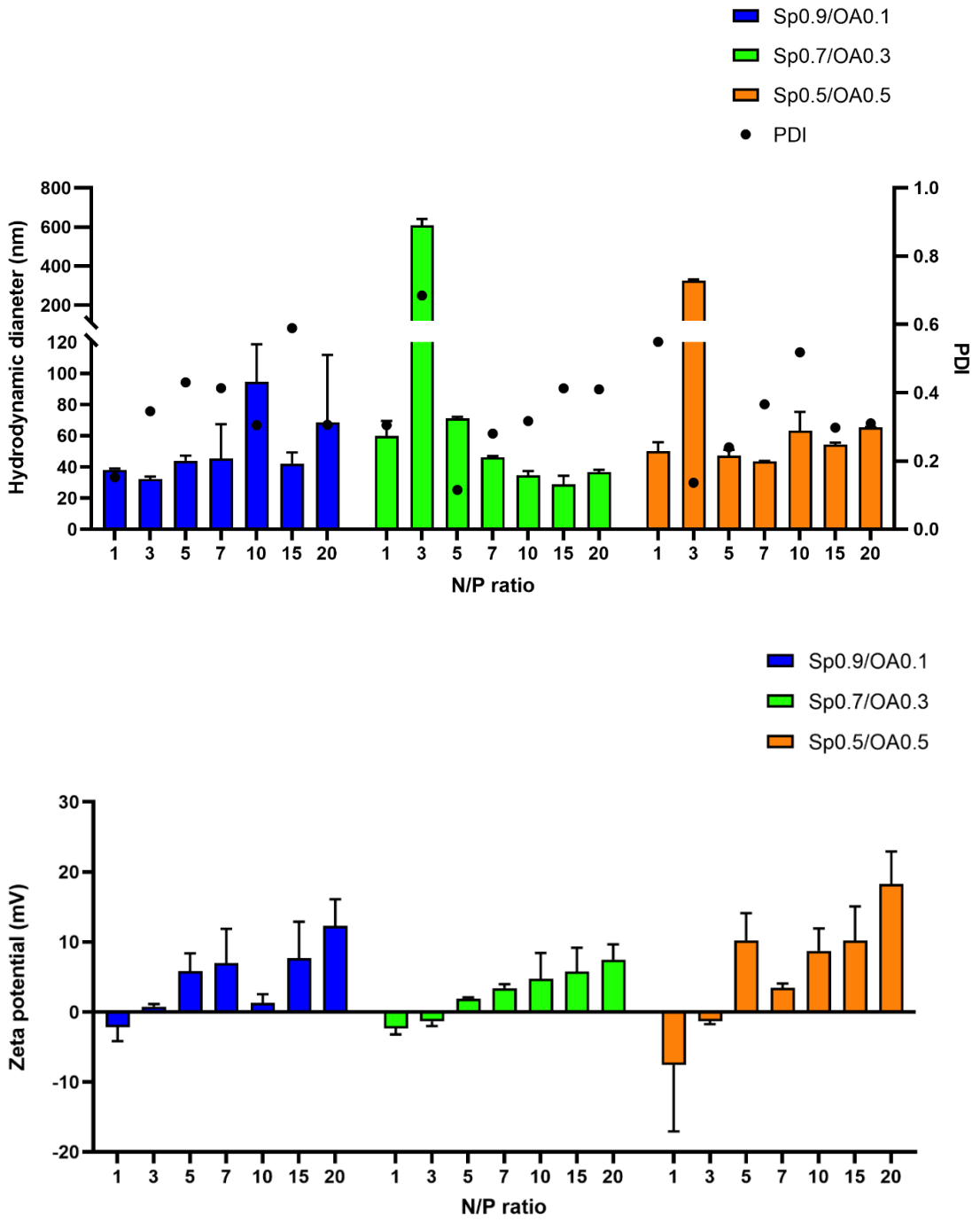

Figure 3. Size and size distribution of the P(SpOABAE) polyplexes and the Zeta potential (Data points indicate Mean ± SD, *n* = 3) Sp0.9/OA0.1: P(SpOABAE) with 10% of oleylamine, Sp0.7/OA0.3: P(SpOABAE) with 30% of oleylamine, Sp0.5/OA0.5: P(SpOABAE) with 50% of oleylamine.

3.4 Cellular uptake

The cellular uptake was quantified by flow cytometry and compared to hyPEI25K polyplexes as a positive control and free AF488-siRNA as a negative control. P(SpOABAE) polyplexes with 50 pmol AF488-siRNA at N/P 5, 7, and 10 were compared as the siRNA can be fully encapsulated from N/P 5 on according to the SYBR gold assays (**Figure 2**). Polyplexes at higher N/P ratios were not used due to the possible cytotoxicity. In half of the samples, 0.4% trypan blue was used to quench the extracellular fluorescence associated with polyplexes that bind to the surface of the cells but are not internalized. As shown in **Figure 4**, the fluorescence intensity of the quenched and unquenched groups did not significantly differ, which means the polyplexes were internalized into the cells. Among the P(SpOABAE) polyplexes with different percentages of oleylamine, the formulations with 50% oleylamine units (Sp0.5/OA0.5) achieved the highest cellular uptake, and the formulations with 30% oleylamine units (Sp0.7/OA0.3) had the lowest cellular uptake with the cellular uptake of the formulations with 10% oleylamine units (Sp0.9/OA0.1) resulting in intermediate values. These interesting results were explained by the different cellular uptake mechanisms of the polyplexes for mainly cationic vs. more hydrophobic polyplexes. However, all the P(SpOABAE) polyplexes showed higher cellular uptake than hyPEI25K. Regardless of the size and PDI of the polyplexes, the cellular uptake of P(SpOABAE) polyplexes increased from N/P 5 to N/P 10.

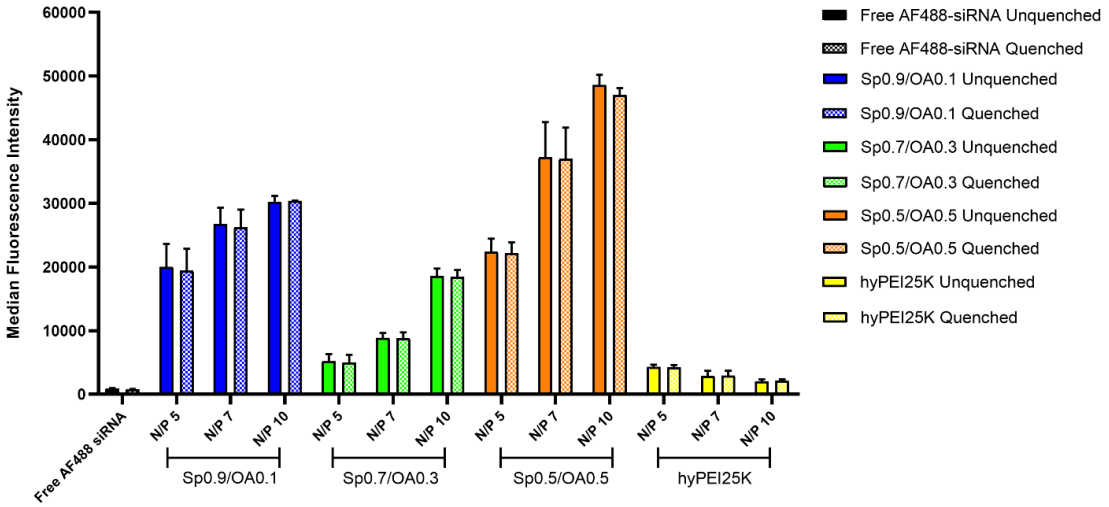

Figure 4. Cellular uptake of Sp0.9/OA0.1, Sp0.7/OA0.3, and Sp0.5/OA0.5 polyplexes at N/P ratios of 5, 7, and 10 was quantified by flow cytometry after 24 h

incubation. The results are presented as median fluorescence intensity (MFI) with and without trypan blue quenching. Negative control: cells treated with free AF488-siRNA. Positive control: cells treated with hyPEI25K. (Data points indicate Mean ± SD, *n* = 3)

3.5 GFP knockdown

To investigate whether high cellular uptake also correlates with corresponding gene silencing, an enhanced green fluorescence protein (eGFP) knockdown assay was performed in stably expressing H1299/eGFP cells to assess the gene silencing efficiency of the P(SpOABAE) polyplexes on the protein level. P(SpOABAE) polyplexes with 10%, 30%, and 50% oleylamine units at N/P 5, 7, and 10 were compared for the knockdown experiment. As shown in **Figure 5**, the P(SpOABAE) polyplexes with 10% oleylamine units (Sp0.9/OA0.1) although resulted in high cellular uptake but could not achieve an efficient GFP knockdown. On the other hand, P(SpOABAE) polyplexes with 30% oleylamine (Sp0.7/OA0.3), despite less efficient cellular uptake than Sp0.9/OA0.1, mediated higher GFP knockdown efficiency than Sp0.9/OA0.1. The P(SpOABAE) polyplexes had been taken up intracellularly most efficiently and also achieved the highest GFP knockdown efficacy. These results could be explained by the different endosome escape abilities of the P(SpOABAE) polyplexes. The high cellular uptake of Sp0.9/OA0.1 could be due to its relatively high amount of primary and secondary amines, which enhanced the permeability of the polyplexes. However, due to the problem of endosome escape, the polyplexes did not achieve an efficient GFP knockdown. Polymers Sp0.7/OA0.3 and Sp0.5/OA0.5 are expected to have higher endosomal escape ability due to their more amphiphilic nature. As a result, the higher cellular uptake of Sp0.5/OA0.5 polyplexes led to very high GFP knockdown.

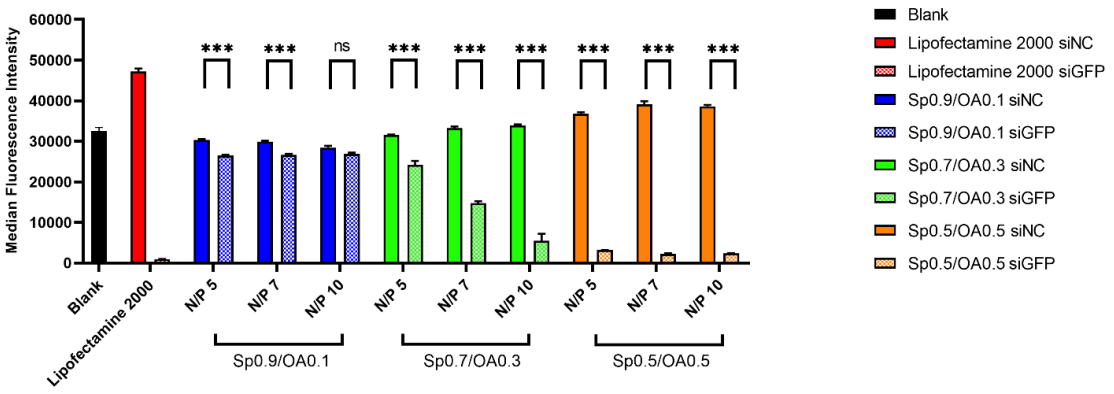

Figure 5. Enhanced green fluorescent protein (eGFP) knockdown efficiency in H1299-eGFP cells quantified by flow cytometry as median fluorescence intensity (MFI) after transfection with Sp0.9/OA0.1, Sp0.7/OA0.3, and Sp0.5/OA0.5 polyplexes at N/P 5, 7 and 10 with siGFP or siNC for 48 h. Positive control: Lipofectamine™ 2000 formulated with siGFP and siNC. Blank controls are cells without any treatment. Data points indicate Mean ± SD, n = 3, One-way ANOVA with Bonferroni post-hoc test, $^{ns}p > 0.05$, $^{***}p < 0.001$.

Many studies have shown that the incorporation of hydrophobic chains can enhance internalization and improve nucleic acid delivery efficiency. For example, Azahara Rata-Aguilar et al. found that the inclusion of small hydrophobic fragments into the polycation backbone improves the stability and transfection efficiency of plasmid DNA.[205] Alshamsan et al. modified branched PEI with oleic acid and stearic acid and observed higher cellular uptake and more pronounced reduction of integrin levels.[203] In addition, incorporation of lipophilic or hydrophobic groups into the polymers should also affect interactions with endo/lysosomal membranes resulting in a more efficient escape.[206] Oleylamine contains an unsaturated double bond in its structure which is similar to the so-called fusogenic lipid DOPE. The unsaturation of the hydrocarbon chains is one of the conditions for inducing the transition from the lamellar to the fusogenic phase and thus rapidly fusing with anionic membranes.[7] Heyes et al. compared the fusogenicity of lipid nanoparticles with different numbers of double bonds in the hydrophobic tails.[51] They found that lipoplexes containing unsaturated cationic lipids enhanced luciferase gene knockdown compared with those containing saturated cationic lipids. The improvement in efficiency was correlated with the extent of unsaturation of the cationic lipid hydrophobic domain and the fusogenicity of the delivery system.

3.6 Cell viability

Polycations can protect siRNA from replacement of the polyplex by other polyanions and degradation by enzymes. However, the trade-off is that the positive charges can interact with cell membranes, inhibit crucial biological processes, and lead to cytotoxic effects.[207] The cell viability of the polymer P(SpOABAE) and polyplexes was measured by MTT (3-(4,5-dimethylthiazol-2-yl)-2,5-diphenyltetrazolium bromide) assays. Hyperbranched polyethylenimine 25kDa (hyPEI25K) was used as control. As expected, with the increase in the concentration of the polymers, the cell viability decreased. As shown in **Figure 6A**, the free polymer P(SpOABAE) was more biocompatible than hyPEI25K at higher concentrations than 20 µg/mL. P(SpOABAE)s at a concentration less than 10 µg/mL were even a bit more toxic than hyPEI25K, which could be attributed to the hydrophobic fusogenic lipid that enhances the cell permeability of the polymer. However, the P(SpOABAE)s did not cause strong cytotoxicity and they are still considered biocompatible.

The cell biocompatibility of the P(SpOABAE) polyplexes at N/P 5, 7, and 10 was also determined. The hyPEI25K polyplexes were used as a control. As shown in **Figure 6B**, the cytotoxicity of P(SpOABAE) polyplexes was comparable with hyPEI25K. The Sp0.9/OA0.1 polyplexes were a bit more toxic than the other P(SpOABAE) polyplexes, which could be caused by the higher content of primary and secondary amines in this polymer.

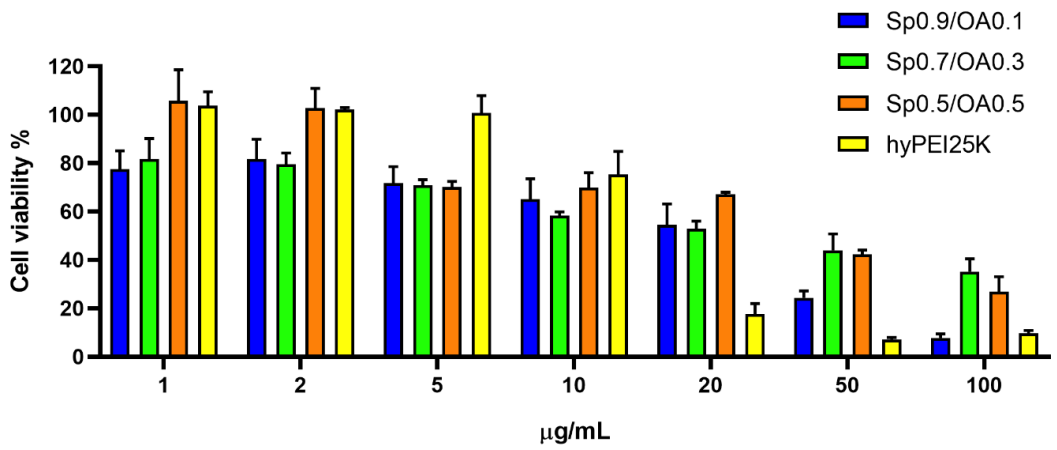

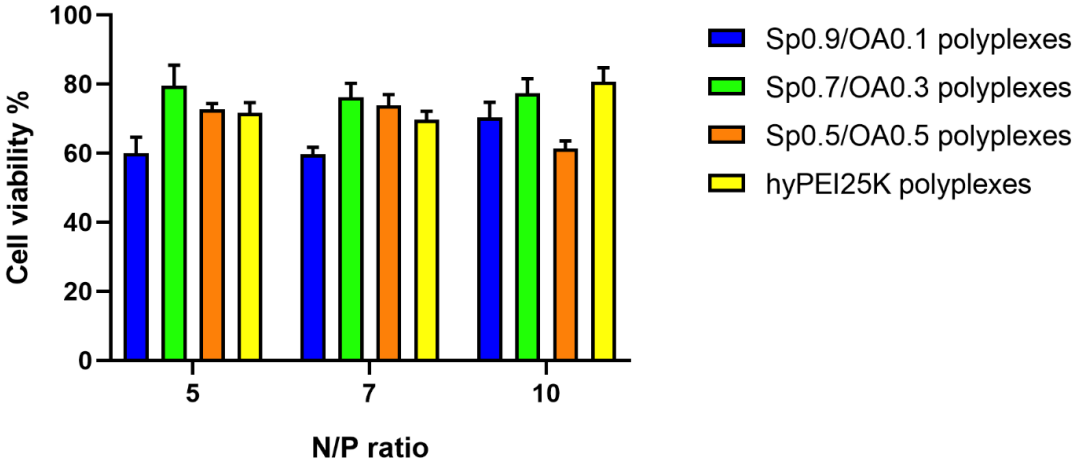

Figure 6. Cell viability measured by MTT assay for P(SpOABAE) and P(SpOABAE) polyplexes with different N/P ratios. Untreated cells represent 100% viability. (Data points indicate Mean ± SD, *n* = 3).

3.7 GAPDH knockdown

As the P(SpOABAE) polyplexes achieved excellent GFP knockdown, their ability to silence endogenous genes in other cell lines was assessed. Polar, differentiated epithelial cells with tight junctions are difficult to transfect compared with less differentiated, nonpolar cells.[208] We used 16HBE14o- cells, a human bronchial epithelial cell line, to evaluate the gene knockdown efficiency ofP(SpOABAE) polyplexes. As shown in **Figure 5**, the P(SpOABAE) polyplexes with 10% oleylamine units (Sp0.9/OA0.1) did not achieve highly efficient GFP knockdown a and were therefore excluded for this assay. Sp0.7/OA0.3 and Sp0.5/OA0.5 polyplexes were used to silence the housekeeping gene GAPDH. Lipofectamine™ 2000 was used as a positive control. All formulations were also applied containing scrambled siRNA (siNC) as a negative control. As shown in **Figure 7**, GAPDH expression was normalized to β-actin. Sp0.7/OA0.3 polyplexes at N/P 5 were able to achieve slightly better (50.14%) knockdown than Lipofectamine™ 2000 (48.38% silencing efficacy). Interestingly, the Sp0.7/OA0.3 polyplexes at N/P 7 and 10, although they had achieved efficient GFP knockdown in H1299/eGFP cells (**Figure 5**), did not mediate significant GAPDH knockdown in 16HBE14o- cells. The different behavior of the polyplexes can be attributed to the different cell lines. 16HBE14o- cells possess the capacity to secrete mucus via the airway-specific mucin protein, MUC5AC.[209, 210] Mucus is composed of water, glycoproteins, ions,

and lipids that constitute a physiological barrier that protects the apical surfaces of the respiratory.[211] It is possible that Sp0.7/OA0.3 polyplexes at higher N/P ratio were either not stable in presence of this mucus or were entrapped in it.

Besides the nanocarriers, the cell type can also determine the transfection efficiency of the nanoparticles.[212] Kim et al. investigated the transfection efficiency by DOTAP-liposomes with different DOTAP/DOPE ratios and cell types including Huh7, AGS, COS7, and A549. They found that the formulation T1P0 and T3P1 showed higher luciferase activities than T1P1 or T1P3 in Huh7 and AGS cells. However, the transfection efficiencies of T3P1 and T1P1 were higher than those of T1P0 and T3P1 in COS7 cells. These results implied that specific cell lines can favor certain lipid compositions in gene delivery and the transfection efficiency is cell-line dependent.[170] We did not get a consistent result with the polymer Sp0.5/OA0.5, so the data was not shown here. It is possible that the cell density, siRNA amount, incubation time, etc. for GAPDH knockdown still need to be optimized for better results.

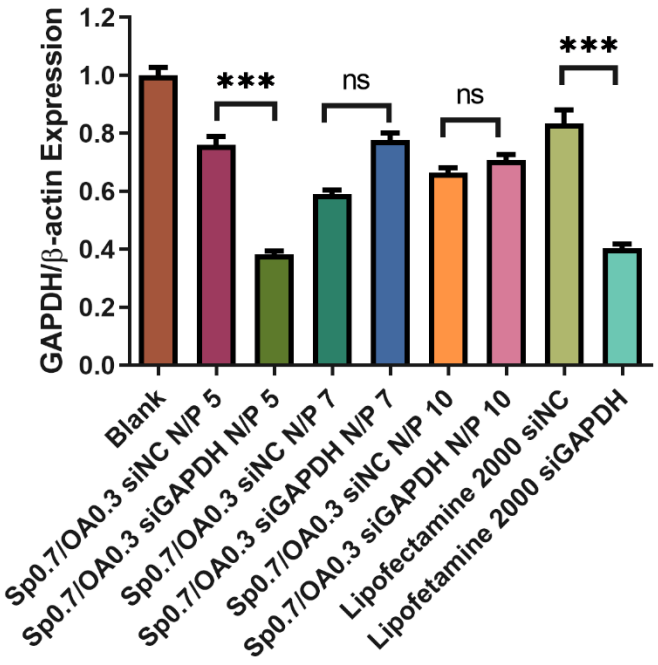

Figure 7. GAPDH knockdown of SpOA0.7/OA0.3 of different N/P ratios in 16HBE14o- cells after treatment with siRNA against GAPDH (siGAPDH) or scrambled siRNA (siNC) as a negative control. (Data points indicate Mean ± SD, n = 3; one-way ANOVA with Bonferroni post-hoc test, $^{***}p < 0.001$, $^{ns}p > 0.05$).

3.8 Endosomal entrapment

The endo/lysosomal entrapment of the polyplexes was visualized by confocal laser scanning microscopy (CLSM). Endosomal entrapment of polyplexes and other nanoparticles is one of the main barriers to siRNA delivery with non-viral carriers.[2] Normally, the nanoparticles entrapped in endosomes follow the endosomal-lysosomal route, which is a series of organelles in the endocytic pathway and a dynamic, interconnected vesicular network.[213] The endocytotic vesicles fuse with pre-existing early endosomes within seconds which mature into late endosomes and finally fuse with lysosomes.[12]

As shown in **Figure 8**, we utilized polyplexes prepared using AF488-siRNA in green, and lysosomes were stained with lysotracker in red. The merged picture indicates the colocalization of polyplexes with endosomes. The Sp0.5/OA0.5 polyplexes have the highest cellular uptake widely distributed in each cell, which indicates that the polyplexes escaped from endo/lysosomes. This result confirms that the modification with oleylamine can help the endosomal escape of polyplexes and explains its high GFP knockdown efficiency. Oleylamine shares a similar structure with so-called fusogenic lipids containing an unsaturated double bond in its structure, which can enhance the interaction with endosomal membranes thus promoting endosomal escape.[7] The Sp0.7/OA0.3 polyplexes did not show a significant difference from Sp0.9/OA0.1 polyplexes, probably due to the overall lower cellular uptake of Sp0.7/OA0.3 polyplexes. Hence, the escaped polyplexes were also less as reflected in the image.

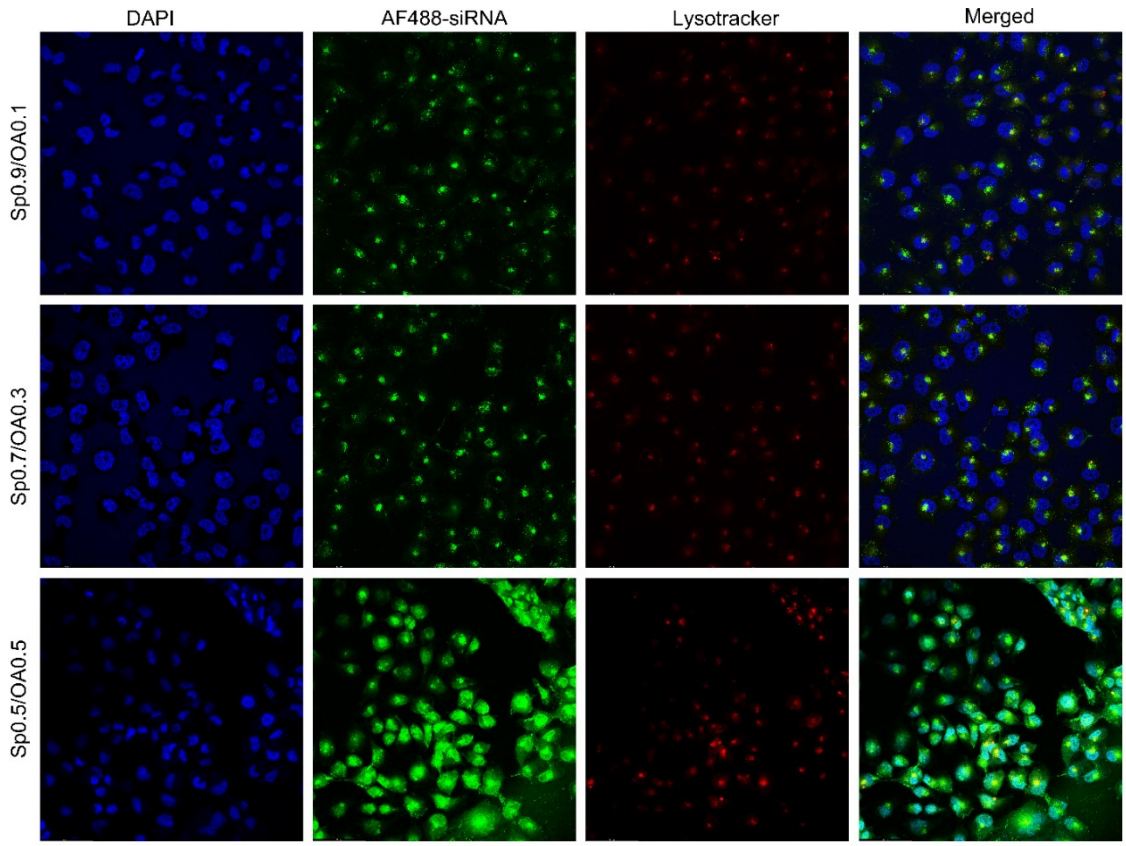

Figure 8. CLSM images of colocalization of Sp0.9/OA0.1, Sp0.7/OA0.3, and Sp0.5/OA0.5 polyplexes encapsulated with AF488-siRNA and endo/lysosomes (Lysotracker). The cell nuclei were stained with DAPI shown in blue.

4. Conclusion

Amphphilic spermine-based poly(β-amino ester)s have been shown to be promising materials for siRNA delivery. However, the hydrophobic modification of poly(β-amino ester)s and its role in siRNA delivery were not fully understood. In this study, we synthesized several poly(β-amino ester)s with different ratios of spermine and oleylamine side chains and constructed polyplexes that can achieve more than 90% GFP knockdown. We found that the hydrophobic modification with oleylamine can enhance siRNA delivery efficiency and gene silencing efficiency of the spermine-based poly(β-amino ester)s, and this gene silencing efficiency of the polyplexes could be cell-line dependent. This study therefore provides guidelines for the rational design of materials for nucleic acid delivery and established excellent polyplexes for siRNA delivery.

Acknowledgment

Yao Jin appreciates the financial support from China Scholarship Council (CSC201906010329). The project was funded by ERC-2014-StG – 637830 to Olivia Merkel.

Supplementary information

Oleic acid modified spermine-based poly(β-amino ester)s

In fact, before the modification by oleylamine, as described in Chapter 3, oleic acid (9-Octadecenoic acid) was tried to conjugate with P(SpBAE).

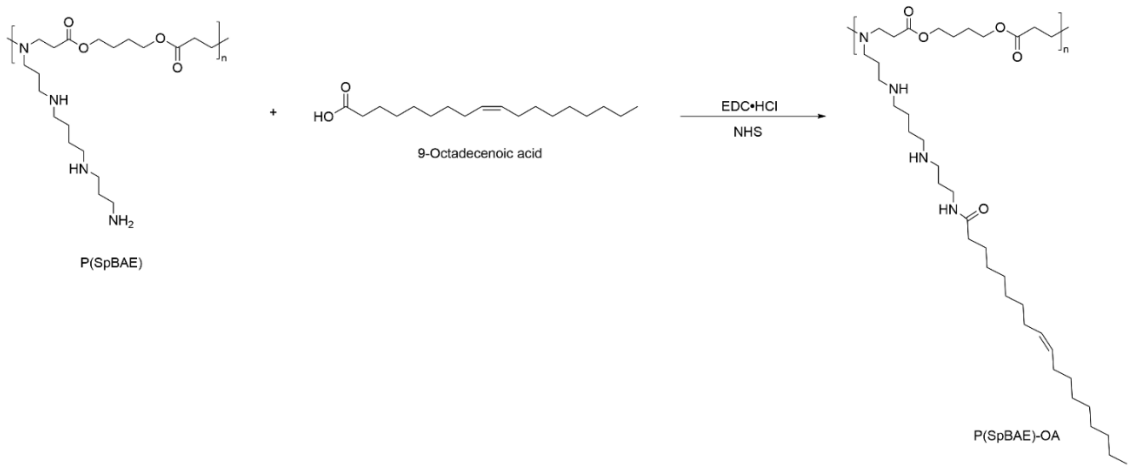

Scheme S1. The synthesis route of modification P(SpBAE) with oleic acid

As shown in Scheme 1, oleic acid was conjugated to P(SpBAE) under the catalysis of EDC-HCl (1-(3-Dimethylaminopropyl)-3-ethylcarbodiimide hydrochloride) and NHS (N-Hydroxysuccinimide). In brief, oleic acid (1 eq.) was dissolved in absolute ethanol, EDC-HCl (3 eq.) and NHS (3 eq.) were dissolved in ethanol and added to the oleic acid solution, and 2 M NaOH was applied to provide a basic environment. After reaction at room temperature for 30 min, P(SpBAE) in high-purity water was added dropwise and stirred at room temperature for 24 h. The product was finally transferred to a dialysis kit (MWCO 1 kDa) and dialyzed for 3 days and finally freeze-dried to get the product as yellow to brown semisolid.

The chemical structure of the product was confirmed by ^{1}H NMR. As shown in **Figure S1**, the peaks around 5.5 ppm and 0.8 ppm indicate that oleic acid was conjugated to P(SpBAE) successfully. However, the coupling ratio of oleic acid estimated according to the ^{1}H NMR was more than 100%.

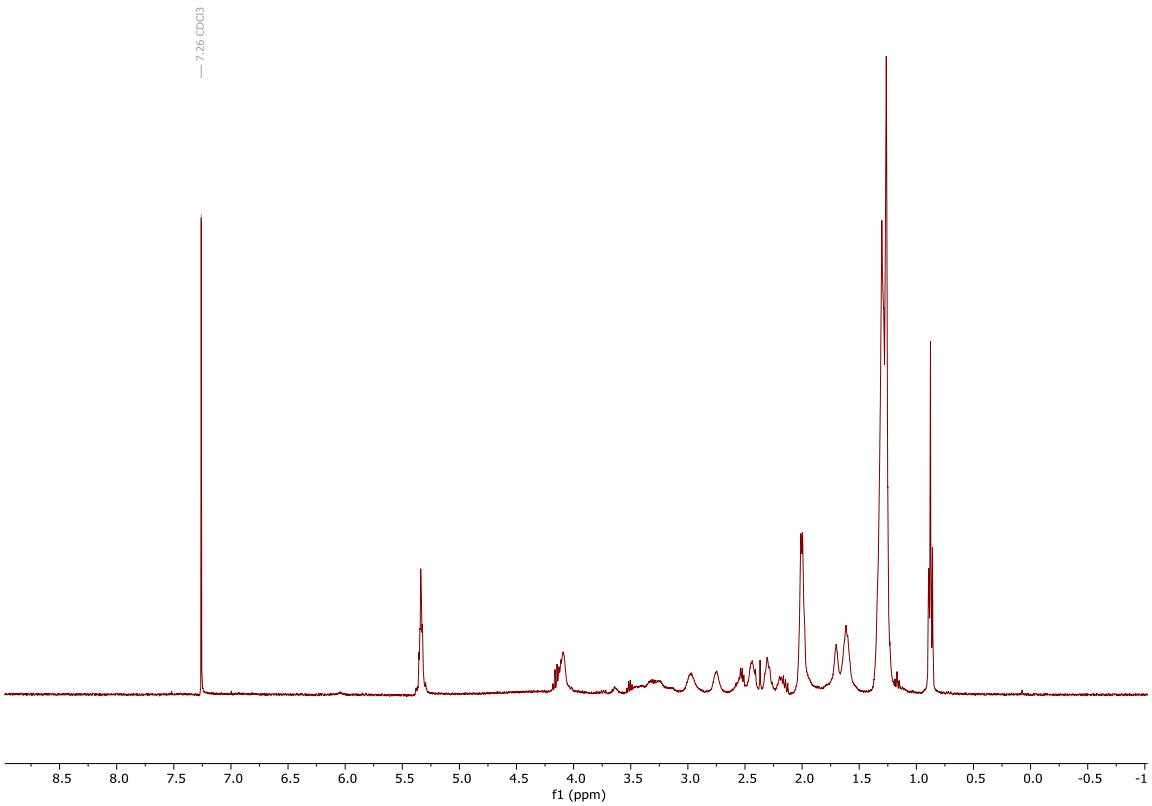

Figure S1. ^{1}H NMR of P(SpBAE)-OA in $CDCl_3$

The siRNA encapsulation efficiency of P(SpBAE)-OA was determined by SYBR gold assay. As shown in **Figure S2**, about 95.7% of the siRNA can be encapsulated from N/P 5, which indicates that the polymer can encapsulate siRNA efficiently.

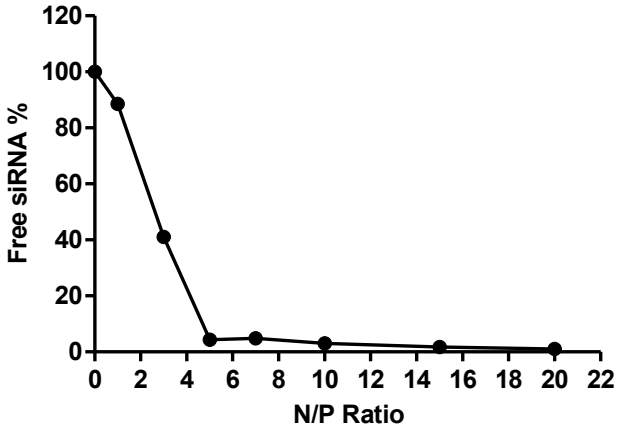

Figure S2. siRNA encapsulation profiles of P(SpBAE)-OA polyplexes measured by SYBR Gold assay at various N/P ratios. 100% values (N/P = 0) are represented by the determined fluorescence of uncondensed free siRNA (data points indicate mean, *n* = 3)

The size (hydrodynamic diameter) and zeta potential of the polyplexes were determined by Zetasizer NanoZS (Malvern Instruments, Malvern, UK). As shown in **Figure S3**, the sizes of the polyplexes at different N/P ratios were around 100 nm except the one at N/P 5 with a size of 402.6 nm, which could be due to the aggregation of the polyplexes because of the insufficient net charge of the polyplexes for stabilization. The trend of the zeta potential was in parallel with the SYBR gold assay, when there was much negatively charged free siRNA (N/P 1 and N/P 3), the zeta potential was negative, while when the siRNA was fully encapsulated, the zeta potential was positive.

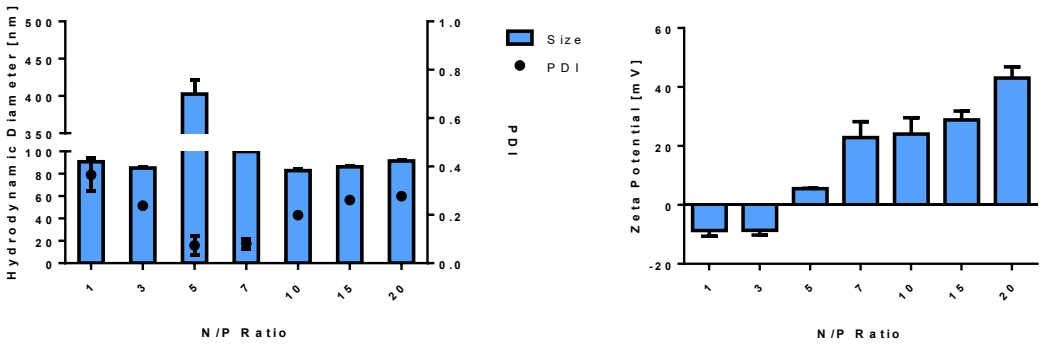

Figure S3. Hydrodynamic diameter (size), polydispersity index (PDI), and zeta potential of P(SpBAE)-OA polyplexes at various N/P ratios.

The cellular uptake of the polyplexes at N/P 5, 7, and 10 was determined by flow cytometry. As shown in **Figure S4**, the P(SpBAE)-OA polyplexes at N/P 7 showed the highest cellular uptake but still less than hyperbranched polyethylenimine (hyPEI25K), P(SpBAE)-OA at N/P 10 showed less cellular uptake than P(SpBAE)-OA polyplexes at N/P 5 which could be due to the cytotoxicity.

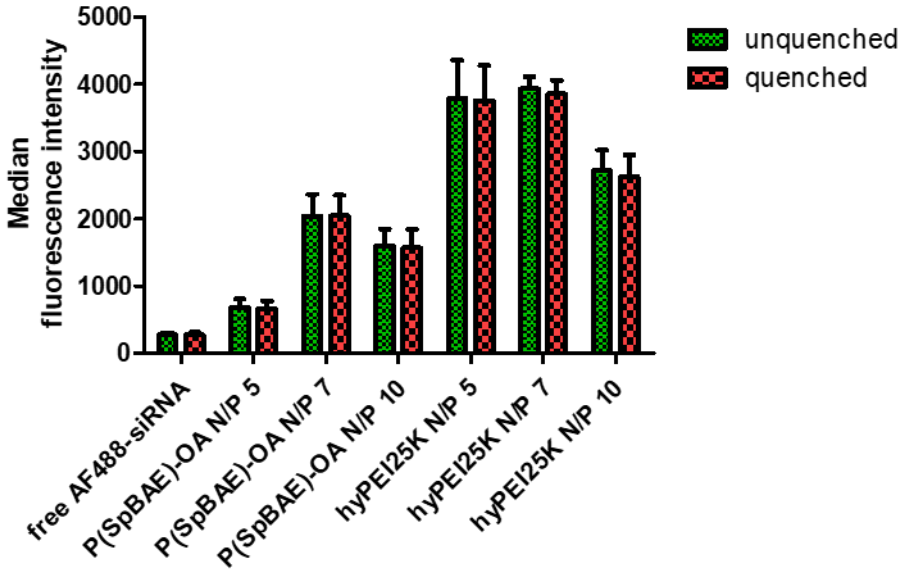

Figure S4. Cellular uptake of polyplexes quantified by flow cytometry and presented as median fluorescence intensity corrected by autofluorescence of untreated blank cells (H1299 cells, AF488-siRNA, *n* = 2)

Since the P(SpBAE)-OA polyplexes showed the highest cellular uptake at N/P 7, the polymer was then encapsulated with siGFP (siRNA against green fluorescence protein) to determine the gene silencing efficiency. As shown in **Figure S5**, compared with polyplexes encapsulated with siNC (scrambled siRNA), P(SpBAE)-OA siGFP polyplexes achieved a significant GFP knockdown statistically but only 10%. The gene knockdown efficiency was low could be due to the low cellular uptake of the polyplexes, and the low cellular uptake could be attributed to the excessive hydrophobic modification of oleic acid.

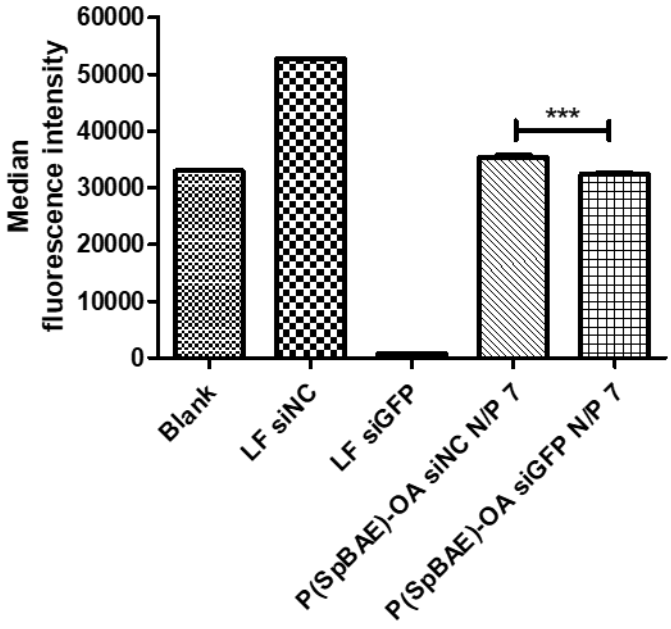

Figure S5. Enhanced green fluorescent protein (eGFP) knockdown of P(SpBAE)-OA polyplexes in H1299 cells expressing eGFP quantified by flow cytometry as median fluorescence intensity (Mean ± SD, *n* = 2, One-way ANOVA with Bonferroni multiple comparison test, ***p < 0.001)

Chapter IV

Synthesis and application of low molecular weight PEI-based copolymers for siRNA delivery with smart polymer blends

*Yao Jin, Friederike Adams, Judith Möller, Lorenz Isert, Christoph M. Zimmermann, David Keul, Olivia M. Merkel**

Y. Jin, Dr. F. Adams, J. Möller, L. Isert, C. M. Zimmermann, D. Keul, Prof. Dr. O. M. Merkel

Ludwig-Maximilians-University Munich, Department of Pharmacy, Pharmaceutical Technology and Biopharmaceutics, Butenandtstr. 5-13, 81377 Munich, Germany

*Corresponding author:

Prof. Dr. Olivia M. Merkel

Email: Olivia.Merkel@lmu.de

C. M. Zimmermann

University of Bern, Department for Chemistry, Biochemistry and Pharmacy, Freiestrasse 3, 3012 Bern, Switzerland

Dr. F. Adams

Current address: University of Stuttgart, Institute of Polymer Chemistry, Chair of Macromolecular Materials and Fiber Chemistry, Pfaffenwaldring 55, 70569 Stuttgart, Germany; University Eye Hospital Tübingen, Center for Ophthalmology, Elfriede-Aulhorn-Strasse 7, 72076 Tübingen, Germany

Contributions: I performed the experiments with support of the coauthors and I wrote the manuscript.

Keywords: siRNA delivery, low molecular weight PEI, PEG-PCL, nanoprecipitation

Abstract

Polyethylenimine (PEI) is a commonly used cationic polymer for small-interfering RNA (siRNA) delivery due to its high transfection efficiency at low commercial cost. However, high molecular weight PEI is cytotoxic and thus, its practical application is limited. In this study, we investigated different formulations of low molecular weight PEI (LMW-PEI) based copolymers PEI-PCL (800 Da-40 kDa) and PEI-PCL-PEI (5 kDa-5 kDa-5 kDa) blended with or without PEG-PCL (5 kDa-4 kDa) to prepare nanoparticles via nanoprecipitation using a solvent displacement method with sizes around 100 nm. PEG-PCL can stabilize the nanoparticles, improve their biocompatibility, and extend their circulation time *in vivo*. The nanoparticles composed of PEI-PCL-PEI and PEG-PCL showed higher siRNA encapsulation efficiency than PEI-PCL/PEG-PCL based nanoparticles at low N/P ratios, higher cellular uptake, and a gene silencing efficiency of around 40% as a result of the higher molecular weight PEI blocks. These results suggested that the PEI-PCL-PEI/PEG-PCL nanoparticle system could be a promising vehicle for siRNA delivery at minimal synthetic effort.

1. Introduction

After RNA interference (RNAi) was discovered over 20 years ago,[1] the field of RNAi-based therapeutics is now growing rapidly. The first siRNA-based drug patisiran (Onpattro®) was approved by the U.S. FDA in 2018 for polyneuropathy of hereditary transthyretin-mediated amyloidosis, and givosiran (Givlaari®) was approved in 2019 for acute hepatic porphyria.[214, 215] In 2020, lumasiran (Oxlumo®) was approved for the treatment of primary hyperoxaluria type 1 (PH1).[216] In 2021, inclisiran (Leqvio®) was approved and the latest approved siRNA agent is vutrisiran (Amvuttra®). Additional siRNA-based drugs are in the pipelines. The approval of siRNA-based drugs fostered a new interest from industrial and academic groups in RNAi therapeutics.[215] However, the delivery of siRNA, which is a double-stranded siRNA with 21-25 nucleotides and can induce RNAi, remains a challenge. As siRNA molecules are hydrophilic, anionic macromolecules, they

cannot cross cell membranes by passive diffusion for efficient cellular uptake; also, due to enzymatic degradation, and its fast renal clearance, the half-life of naked siRNA in blood circulation is very short.[2]

Among the vast family of non-viral nucleic acid delivery systems, polyethylenimine (PEI) and its derivatives have taken a prominent position due to their high encapsulation efficiency at low commercial cost.[99] However, the transfection efficiency and cytotoxicity of PEI are strongly dependent on the molecular weight.[217] PEI with high molecular weight (HMW-PEI), such as the commonly used branched PEI with a molecular weight of 25 kDa, exhibits both higher transfection efficiency and higher cytotoxicity than smaller PEIs.[137, 218] In addition, high molecular weight PEI may accumulate during *in vivo* application, since there is no degradation pathway or a mechanism of excretion known for such molecules.[218] Low molecular weight PEI (LMW-PEI, <22 kDa) is non-cytotoxic and can also be eliminated from systemic circulation through the kidneys.[219] However, the lower molecular weight also causes low transfection efficiency due to weak nucleic acid binding abilities and insufficient protection from nucleases.[217] To circumvent the low transfection efficiency of LMW-PEI, researchers have adopted various strategies, for example, crosslinking LMW-PEI to form biodegradable HMW-PEI,[97, 220] modifying with polyethylene glycol (PEG), targeting peptides and hydrophobic groups.[221] In particular, hydrophobic group conjugation to LMW-PEI has been proven to be an effective strategy to improve nucleic acid delivery, which may be due to the improved cellular uptake, endosomal escape, and the unpacking of polyplexes intracellularly.[222-224] For example, Zheng et al. conjugated lipoic acid to PEI (Mw 1800 Da) and increased the transfection efficiency in 293T cells and Hela cells.[222]

Amphiphilic polymer structures containing polycaprolactone (PCL) as hydrophobic segments grafted onto PEI could in principle form micelles exhibiting a core-corona structure with improved colloidal stability in aqueous dispersion and biological fluids. Also, the micelle-like architecture could potentially promote the transmembrane transport, thus enhancing the transfection efficiency.[225, 226] Moreover, the core-corona architecture could offer the possibility of multi-functionality whereby the co-delivery of siRNA in the corona by electrostatic interaction and hydrophobic chemicals (e.g. quantum dots, paclitaxel) in the core due to the hydrophobic interaction could be achieved.[105]

The main goal of this study is to develop an efficient and safe siRNA delivery system based on LMW-PEI. To this extent, we compared LMW-PEI-based copolymers PEI-PCL (800 Da-40 kDa) and PEI-PCL-PEI (5 kDa-5 kDa-5 kDa) with varying amounts of cationic and hydrophobic ratios and block structures and separately blended each copolymer with PEG-PCL (5 kDa-4 kDa) to prepare nanoparticles via nanoprecipitation (solvent displacement). PEG-PCL functions as a stabilizer in the nanoparticles, where the PEG section can shield the positive charge of PEI to improve the nanoparticles' biocompatibility; PEG can also counteract protein absorption while maintaining suspension stability and extending the circulation time in blood.[103] Three methods were compared to optimize the preparation of nanoparticles for optimized size and zeta potential of the nanoparticles, siRNA encapsulation efficiency, cellular uptake, and GFP knockdown efficiency.

2. Results & Discussion

2.1 Size and zeta potential of NPs-siRNA complexes

The commercially available polymer PEI-PCL (800 Da-40 kDa) was initially used to prepare nanoparticles. Because of the poor solubility of this polymer in water due to a high hydrophobic polymer ratio, the NPs-siRNA complexes were prepared by nanoprecipitation methods. The typical procedure for nanoprecipitation is to dissolve the polymers in water-miscible organic solvents (organic phase) and to add the organic phase to a nonsolvent of polymer (aqueous phase). The PEI-PCL is not soluble in acetone or ethanol but soluble in THF. Therefore, THF was chosen for all experiments with PEI-PCL and three different methods were evaluated for the formation of NPs-siRNA at various N/P ratios Method 1 is a common method, where the blank NPs are prepared first and then loaded with siRNA. As shown in **Figure 1**, the NPs-siRNA prepared by methods 1 and 2, in general, had smaller sizes (around 100 nm) than the ones prepared by method 3. However, the sizes of NPs-siRNA prepared with method 1 at N/P 7 and 10 were large. It was hypothesized that the net charges of the nanoparticles were not sufficient to stabilize the nanoparticles as reflected by the neutral zeta potential. The large sizes of NPs-siRNA obtained with method 2 at N/P 6 can also be explained by aggregation and insufficient siRNA encapsulation due to the same reasons.

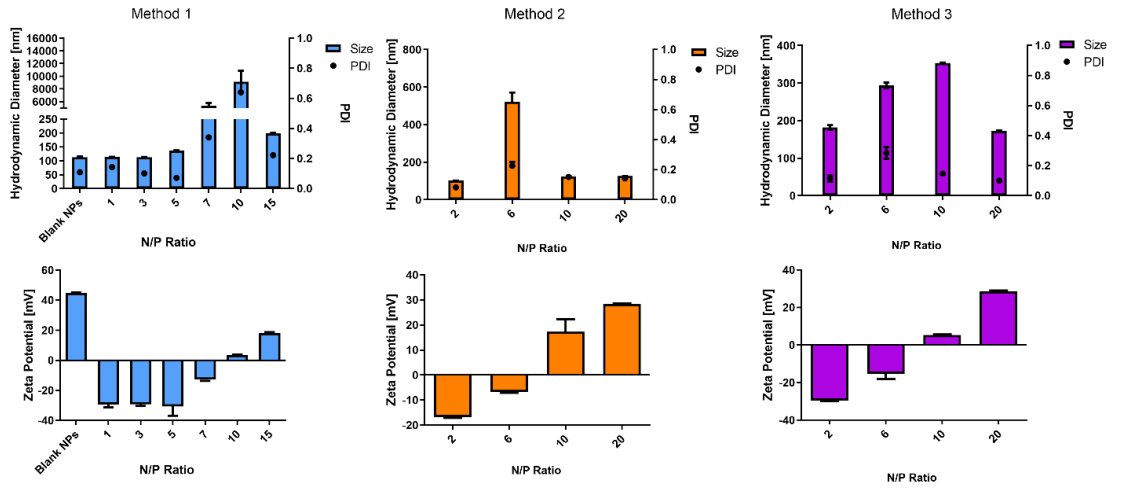

Figure 1. Hydrodynamic diameter (Size), polydispersity index (PDI) and zeta potential of NPs-siRNA prepared by methods 1 (blue), 2 (orange) and 3 (purple).

Nanoprecipitation (solvent displacement) is one of the most commonly used methods for preparing biodegradable submicron particles.[227] Different mechanisms have been proposed to explain particle formation of the solvent displacement technique. Vitale and Katz proposed the “ouzo effect” in 2003.[228] On mixing with water, the oil becomes supersaturated, which results in the nucleation of oil droplets. Oil immediately begins to diffuse to the nearby droplets, until the supersaturation decreases and no further nucleation occurs.[229]

Various parameters can influence nanoprecipitation. For instance, the stirring rate can influence the size and entrapment efficiency of the nanoparticles. A low stirring speed rate leads to high drug entrapment efficiency,[230] while a high stirring speed can produce nanoparticles of smaller size.[231] The size of the nanoparticles is also related to the polymer concentration in the organic phase, where lower concentrations could produce smaller nanoparticles.[232] Besides, the system temperature and organic phase addition method can also influence the characteristics of the nanoparticles.[227] The organic phase can be added to the aqueous phase dropwise[233] or rapidly dispersed[234] or added at a constant speed.[235] Here, we added the organic phase (THF solution) dropwise which is a commonly used method.

The amphiphilic diblock copolymer PEG-PCL is rationally used as a stabilizer in this experiment. The aqueous suspensions of hydrophobic solute NPs are non-

equilibrium systems, and the high interfacial surface area renders such systems prone to aggregation. Thus a stabilizer is necessary unless the surface is charged, or modified through adsorption of ionic surfactants or polymers.[232, 236] PEG-PCL offers several advantages: during NPs formation, it can arrest solute particle growth and provide stabilization before aggregation; PEG can prolong the circulation time *in vivo*; as a diblock copolymer, PEG-PCL has lower critical micelle concentration (CMC) than small-molecule surfactants, which enhances the stability of nanoparticles and offers longer protection from opsonization *in vivo*.[232, 236]

2.2 SYBR gold assay of PEI-PCL/PEG-PCL nanoparticles

The siRNA encapsulation efficiency of the nanoparticles prepared by methods 1, 2 and 3 were all determined by SYBR gold assays. In this assay, free or unbound siRNA is accessible to the intercalating dye SYBR gold, and is quantified based on the fluorescence emitted.[79] The data is reported as the ratio of the formulation's fluorescence to free siRNA. As shown in **Figure 2**, the nanoparticles prepared by method 1 where siRNA is added to pre-formed particles cannot encapsulate siRNA quantitatively even at N/P 15, while the nanoparticles prepared by methods 2 and 3 can almost fully encapsulate the siRNA from N/P 6 on. The siRNA encapsulation efficiency of particles prepared by methods 2 and 3 is better than that of particles prepared by method 1. This observation can be explained by the siRNA more adequately interacting with PEI-PCL in a small volume and before the NPs are formed. The siRNA encapsulation trends of the particles prepared with the three different methods are corresponding to the zeta potential of the nanoparticles: when the siRNA was fully encapsulated, the zeta potential was positive possibly with PEI-PCL on the surface. However, when free siRNA was present on the surface, the zeta potential was negative. For NPs-siRNA prepared by method 2 and method 3 at N/P 6, still 1-2% of free siRNA was left, resulting in a negative zeta potential. Additionally, the PEG segment is also slightly negative in buffer, adding another explanation for the zeta potential of NPs-siRNA at N/P 6.

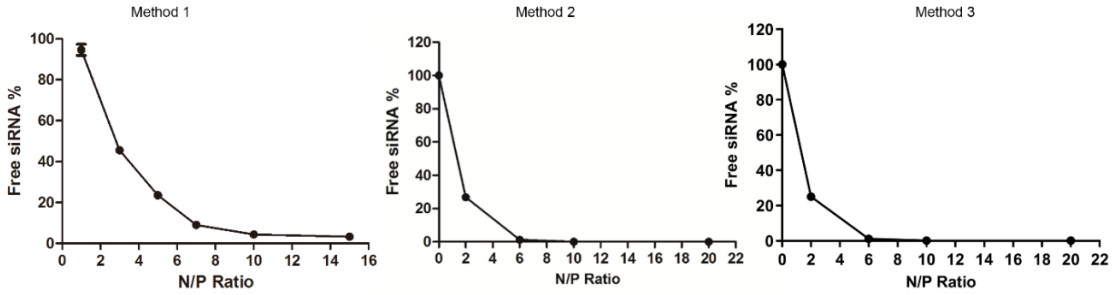

Figure 2. siRNA encapsulation efficiency of PEI-PCL/PEG-PCL nanoparticles prepared by methods 1, 2 and 3 measured by SYBR gold assay. The fluorescence of free siRNA was set as 100% fluorescence value. Data points indicate Mean ± SD, *n* = 3.

2.3 Cellular uptake of PEI-PCL/PEG-PCL nanoparticles

The cellular uptake of the NPs-siRNA complexes at various N/P ratios was determined by flow cytometry. Alexa Fluor 647 labeled siRNA (AF647-siRNA) was used for this experiment, as the fluorescence of AF647 seems more stable than AF488 when stirred for 3 h and exposed to light. As shown in **Figure 3**, compared with LMW-PEI (PEI 1.3 kDa in method 1, PEI 800 Da and 1.3 kDa in method 2), the LMW-PEI-based nanoparticles showed significantly higher cellular uptake, which can be explained by enhanced colloidal stability of the nanoparticles and improved serum resistance. Particles prepared by method 2 showed higher cellular uptake than particles obtained with method 1, which is expected to be a result of higher siRNA encapsulation efficiency of the NPs prepared by method 2 as indicated by the SYBR gold assays. The NPs-siRNA complexes prepared by method 3 showed the highest cellular uptake, which is also assumed to result from the higher siRNA encapsulation efficiency of the latter nanoparticles. In method 3, the siRNA was incubated with PEI-PCL/PEG-PCL polymer in THF solution first, and the siRNA can bind with PEI-PCL during the incubation. It was also hypothesized that the siRNA can be encapsulated into the core of the nanoparticles when the polymer solution is added to the aqueous phase, thus efficiently protecting the siRNA from release. Similarly, Kly et al. first complexed pDNA with PCL-*b*-P2VP (poly(ε-caprolactone)-block-poly(2-vinyl pyridine)) in a dioxane/acetic acid/water mixture and then added PCL-PEG and extra water.

The nanoparticles finally formed with a “polyplexes-in-hydrophobic-core” architecture.[237] To prove our assumption, heparin competition assays were performed. Despite the efficient encapsulation, the cellular uptake of nanoparticles prepared with methods 2 and 3 was still much lower than the uptake observed with higher molecular weight PEI (Mn = 10 kDa) polyplexes. However, the high positive charge density of PEI 10K on the one hand is expected to encapsulate siRNA even more efficiently. And on the other hand, the high charge density can enhance the interaction of polyplexes with the cell membrane and thus promote cellular uptake.

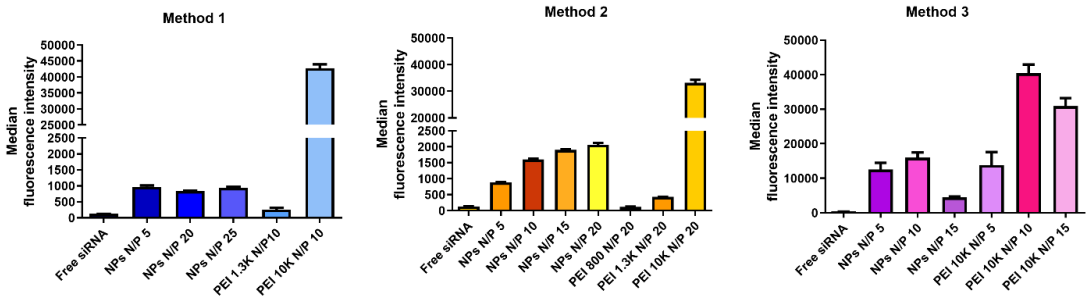

Figure 3. Cellular uptake of NPs loaded with AF647-siRNA prepared by method 1, method 2 and method 3 in H1299 cells as determined by flow cytometry. (Mean ± SD, *n* = 3)

2.4 Heparin competition assay of PEI-PCL/PEG-PCL nanoparticles

To evaluate the stability of the NPs-siRNA complexes and have a deeper understanding of the different behavior of the nanoparticles prepared by different methods, heparin competition assays were evaluated. For nonviral vectors, complex stability is important and is influenced by the presence of competing anions in the cell membrane or serum.[238-240] The heparin competition assay was performed in the neutral (pH 7.4) and acidic (pH 4.5) buffer to mimic the environment of cytoplasm and endo/lysosomes, respectively. The nanoparticles prepared by method 2 and method 3 were selected because of their relatively higher cellular uptake. As shown in **Figure 4**, the stability of all NPs-siRNA complexes decreased with increasing heparin concentration, and siRNA was released due to the competition with heparin polyanions. The release of siRNA at pH 4.5 was a bit higher than at pH 7.4, which could be due to the further protonation of PEI and the repulsion of

the PEI molecules which loosens the PEI layer and thus promotes the siRNA release.[149, 241] The nanoparticles prepared by method 3 are more stable in presence of heparin, which may explain the higher cellular uptake of these nanoparticles. While polyplexes on the one hand need to be stable to protect the siRNA from the competition with other polyanions and degradation from enzymes, on the other hand, the siRNA has to be released to the cytoplasm to induce RNAi. If the siRNA molecules are bound too tightly in the particles with too little release, the gene silencing efficiency of the nanoparticles can be limited as well. Finding a balance between the nanoparticles' stability and release property is still a major hurdle in the field of non-viral RNA vectors.

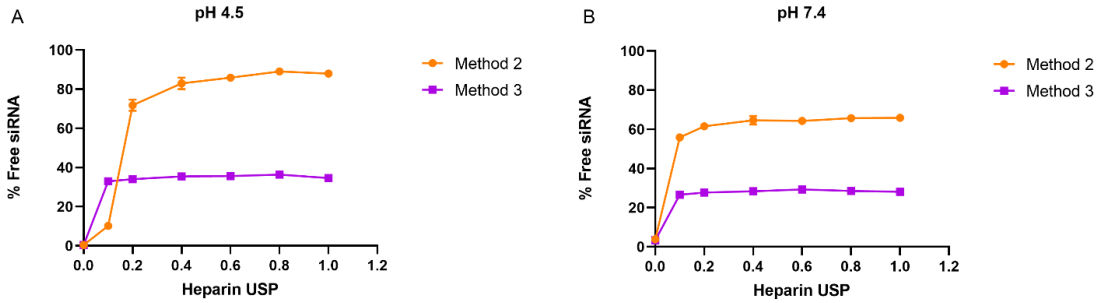

Figure 4. Release profiles of siRNA from NPs-siRNA complexes (N/P = 10) prepared by methods 2 and 3 in presence of heparin at pH 4.5 (A) and pH 7.4 (B). Results are given as mean normalized fluorescence (Mean ± SD, *n* =3).

Taking the results of the SYBR gold assays, cellular uptake and heparin assays together, the binding capacity of the nanoparticles seems important. Optimizing the formulation technique of the nanoparticles improved the cellular uptake. However, the formed NPs are still not as efficient as PEI with higher molecular weight. Therefore, we decided to synthesize a polymer using an intermediate molecular weight of PEI (5 kDa).

2.5 Synthesis of PEI5K-PCL5K-PEI5K

Polyethylenimine (branched PEI, 5 kDa) was conjugated to polycaprolactone-diacrylate (PCL-diacrylate, 5 kDa) via Michael addition reaction, and the unconjugated polymer was removed by dialysis. As shown in the ^{1}H NMR spectra in **Figure S1**, the peaks around 5.83 ppm, 6.12 ppm and 6.36 ppm belonging to the

acrylate group of PCL-diacrylate disappeared in the spectrum of PEI-PCL-PEI, which confirms successful conjugation of PEI and PCL-diacrylate. The peaks between 2.5 ppm to 2.9 ppm belong to PEI, the peaks at 1.38 ppm, 1.64 ppm, 3.30 ppm, and 4.06 ppm belong to PCL.

2.6 Characterization of PEI-PCL-PEI/PEG-PCL nanoparticles

The hydrodynamic diameter (size) and zeta potential of the PEI-PCL-PEI/PEG-PCL nanoparticles were characterized by dynamic light scattering (DLS) and laser doppler anemometry (LDA). As shown in **Figure 5**, increasing amounts of PEG-PCL were used in different batches. The sizes of the nanoparticles were all around 60 nm: in the first batch, the nanoparticles without PEG-PCL (PPP) were 63.69 nm, and the nanoparticles with 2 µL PEG-PCL (PPP + 2 µL PP) were 63.10 nm in hydrodynamic diameter. In the second batch, the nanoparticles with 2 µL, 4 µL and 8 µL PEG-PCL (5 mg/mL) were all around 56 nm small. These results indicate that the nanoprecipitation method is reproducible. The amount of PEG-PCL did not have a visible influence on the size of the nanoparticles. There is a slight difference from batch to batch, which might be due to the speed of adding organic solvents or the variation of room temperature. However, the sizes of the nanoparticle were all in the range of 50 nm – 100 nm, which is not expected to lead to big differences regarding the *in vitro* performance.[242] The zeta potentials of all the nanoparticles without loading siRNA were around 40 mV. When loaded with siRNA at different N/P ratios, the sizes of the NPs-siRNA complexes differed depending on the N/P ratio, and ranged from 61.1 nm (PPP/PP NPs-siRNA N/P 3) to 108.7 nm (PPP NPs-siRNA N/P 1). For PEI5K-PCL5K-PEI5K, we assume that the higher molecular weight of PEI is sufficient enough to encapsulate siRNA. Therefore, we prepared blank nanoparticles first and loaded them with siRNA afterwards (method 1). Acetone was used instead of THF because of its lower boiling point for evaporation and removal. Also, acetone is better tolerated by cells and tissues.[243] Indeed, acetone was also initially chosen for the polymer PEI-PCL (800 – 40 kDa), however, due to its insolubility in acetone, THF was used as an alternative. Not surprisingly, we did observe cytotoxicity with THF, which cannot be eliminated by overnight evaporating under fume hood, in vacuo or dialysis, but can only be removed by freeze-drying (**Figure S2**). When distilled

water was used for the preparation of PEI-PCL based nanoparticles, the sizes of the nanoparticles were not reproducible. Hence, 10 mM HEPES was used for the PEI-PCL based nanoparticles, while for PEI5K-PCL5K-PEI5K based nanoparticles we did not have this problem using distilled water. This could be due to the different net charge of the PEI segments in the polymers leading to different colloidal stability. Methods 2 and 3 were not used with PEI-PCL-PEI, because on one hand, the content of PEI of the triblock copolymer was much higher than that of PEI-PCL. Additionally, to prepare nanoparticles with method 2 and method 3, a lot of siRNA was necessary, and the produced micelleplexes are unstable and uneconomical for storage. For method 1, the blank NPs can be simply stored at 4 °C. On the other hand, for method 2 and 3, there might be possible degradation of siRNA during the solvent evaporation process over 3 h. In fact, the PEI-PCL/PEG-PCL nanoparticles prepared by method 3, did not mediate significant GFP knockdown (**Figure S3**) although they showed a relatively high cellular uptake. One possible explanation could be degradation of siRNA during preparation or storage, or a limited release of siRNA, of course.

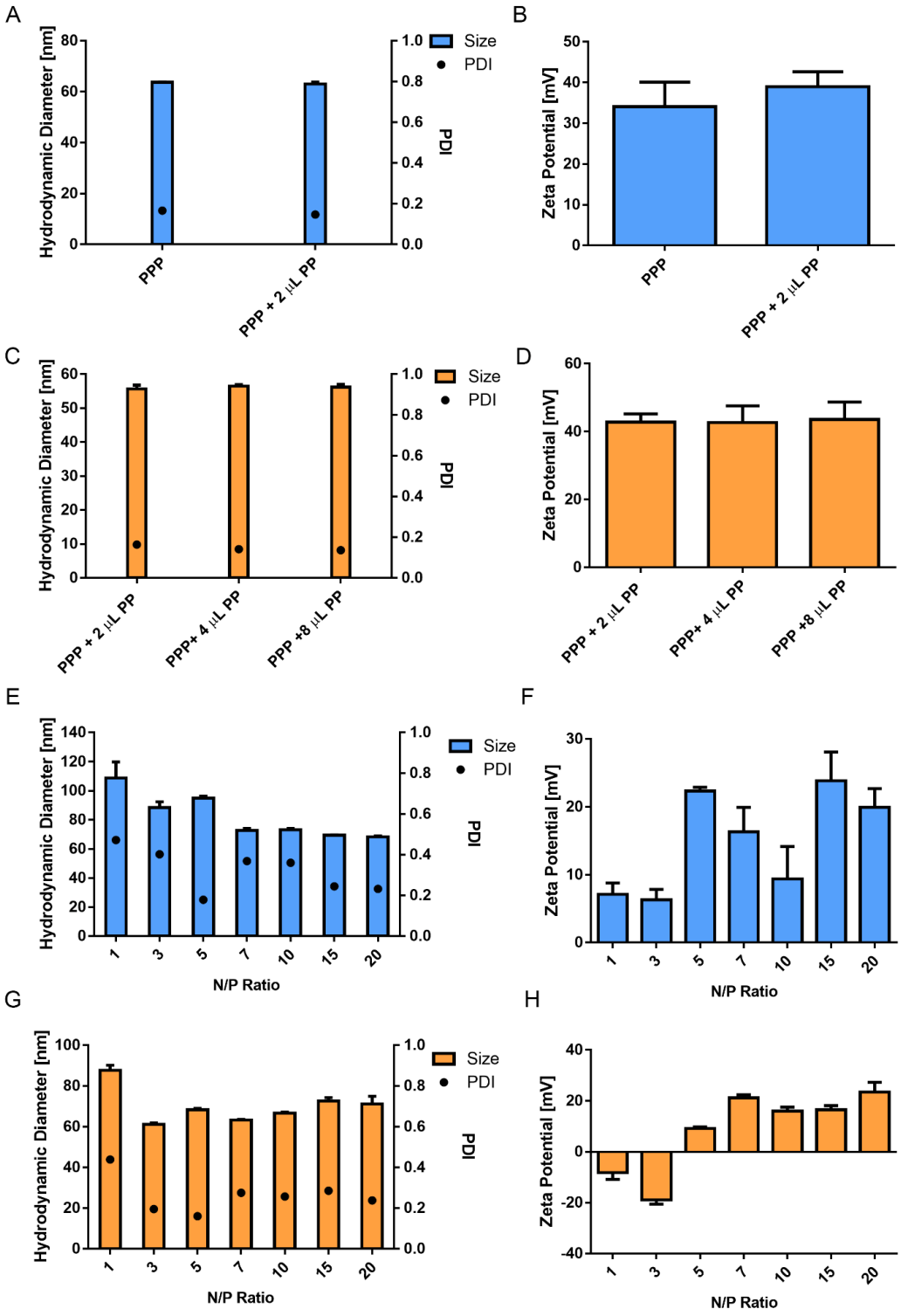

Figure 5. Size and zeta potential of PEI-PCL-PEI/PEG-PCL blank nanoparticles with different amounts of PEG-PCL (A, B, C, D). Size and zeta potential of PEI-PCL-PEI NPs-siRNA complexes (E, F). Size and zeta potential of PEI-PCL-PEI/PEG-PCL NPs-siRNA complexes (G, H, 2 µL PEG-PCL). PPP: PEI5K-PCL5K-PEI5K (5 mg/mL, 200 µL), PP: PEG-PCL (5 mg/mL).

2.7 siRNA encapsulation efficiency of the PEI-PCL-PEI/PEG-PCL nanoparticles

The siRNA encapsulation efficiency of the PEI-PCL-PEI nanoparticles with and without PEG-PCL was determined by SYBR gold assay. As shown in **Figure 6**, the NPs with 2 µL PEG-PCL have lower encapsulation efficiency at N/P 1 and 3, which could be due to steric hindrance of PEG-PCL. However, this hindrance effect was compensated for at higher N/P ratios. Both nanoparticle types (PEI-PCL-PEI NPs and PEI-PCL-PEI/PEG-PCL NPs) can quantitatively encapsulate siRNA from N/P 5 on. Compared with the nanoparticles prepared from PEI-PCL (800 Da-40 kDa) (**Figure 2**, method 1) which cannot quantitatively encapsulate siRNA even at N/P 15, the siRNA encapsulation efficiency of this PEI5K-PCL5K-PEI5K based NPs is highly efficient.

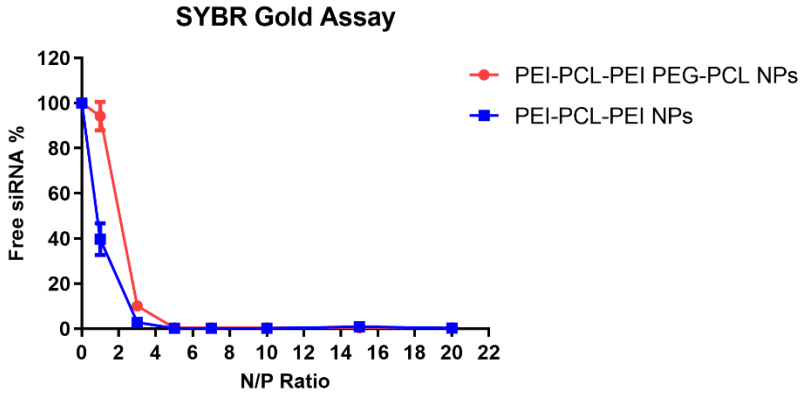

Figure 6. siRNA encapsulation efficiency of PEI-PCL-PEI NPs and PEI-PCL-PEI/PEG-PCL nanoparticles measured by SYBR gold assay at increasing N/P ratios. The fluorescence of free siRNA was set as 100%, Mean ± SD, *n* = 3.

2.8 Dye quenching assay

A dye quenching assay was also applied to investigate the binding behavior of nucleic acids by PEI-PCL-PEI nanoparticles with and without PEG-PCL. The Cy5-labeled siRNA is encapsulated in the polyplexes and when the spatial proximity of the Cy5-siRNA molecules are close enough, the fluorescence of Cy5 will be quenched by each other. [244] As shown in **Figure 7**, the relative fluorescence intensity was lowest at N/P 5, which means that the highest number of siRNA molecules was encapsulated per particle at this N/P ratio. This result corresponds

to the SYBR gold assay result where siRNA was quantitatively encapsulated from N/P of 5 or higher. It was described earlier that with an increase of the N/P ratio beyond this point the siRNA molecules are distributed to more nanoparticles. Thus the amount of siRNA in each particle is less leading to a decreased quenching effect and increased relative fluorescence intensity.[244]

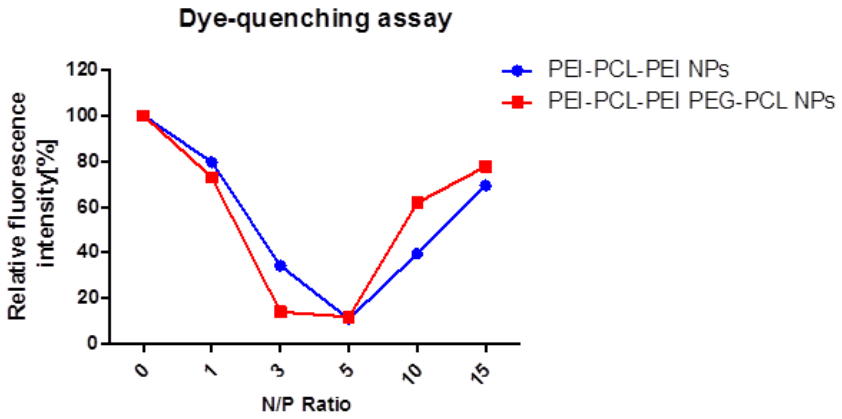

Figure 7. Dye quenching assay. The fluorescence of Cy5-labeled siRNA molecules is quenched by each other in a "multimolecular complex" due to close spatial proximity. Both curves have a minimum fluorescence at N/P = 5, after which the fluorescence increases again due to a decreased number of siRNA molecules per nanoparticle.

2.9 Cellular uptake of PEI-PCL-PEI/PEG-PCL nanoparticles

The cellular uptake of PEI-PCL-PEI/PEG-PCL nanoparticles loaded with AF488-siRNA was measured by flow cytometry. As shown in **Figure 8**, the cellular uptake of PEI-PCL-PEI (PPP) nanoparticles without any PEG-PCL showed relatively low cellular uptake. The formulation PEI-PCL-PEI (5 mg/mL, 200 µL) with PEG-PCL (5 mg/ml, 2 µL) showed the highest cellular uptake at N/P 7 which is even higher than the uptake mediated by hyperbranched PEI with a molecular of 25 kDa (hyPEI25K, N/P 7). Interestingly, the NPs-siRNA complexes with 4 µL PEG-PCL and 8 µL also showed a lower cellular uptake than the formulations with 2 µL PEG-PCL. For the nanoparticles with various amounts of PEG-PCL, the cellular uptake at N/P 10 is a bit lower, which could be due to possible cytotoxicity. The nanoparticles with PEG-PCL showed higher cellular uptake which was hypothesized to be a result of PEG mediating serum stability in a serum-

containing cell culture medium.[103] However, too much PEG is known to shield the positive charge of PEI, which in principle could improve cellular bioavailability but also weakens the interaction of the nanoparticles with the cell membrane, thus leading to a decreased cellular uptake.[26] We also found that PEI-PCL-PEI should be freshly synthesized, and the solubility of PEI-PCL-PEI in acetone decreased after storage at -20 °C, which could be due to PCL aggregation or partial degradation of PCL as well as PEI gelling.

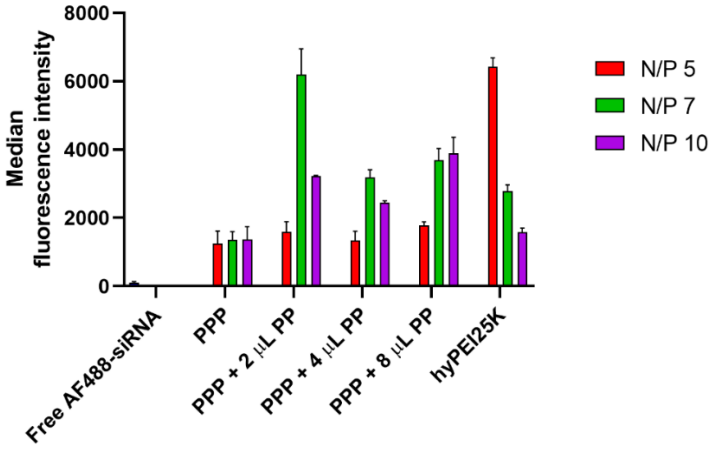

Figure 8. Cellular uptake of PEI-PCL-PEI/PEG-PCL NPs loaded with AF488-siRNA in H1299 cells quantified by flow cytometry and corrected by the autofluorescence of untreated cells. PPP: PEI-PCL-PEI, 5 mg/mL, 200 µL. PP: PEG-PCL, 5 mg/mL.

2.10 GFP knockdown of PEI-PCL-PEI/PEG-PCL nanoparticles

To evaluate the gene silencing efficiency of the nanoparticles on the protein level, we evaluated knockdown of enhanced green fluorescent protein knockdown (eGFP) in stably expressing cells after transfection with PEI-PCL-PEI nanoparticles containing different amounts of PEG-PCL nanoparticles at N/P 7. Only N/P 7 was chosen based on the cellular uptake results. As shown in **Figure 9**, the knockdown efficiency of PEI-PCL-PEI nanoparticles with 2 µL, 4 µL and 8 µL PEG-PCL was 38.29%, 40.28% and 42.34% respectively. Regardless of the formulations' different behavior in the cellular uptake experiment, their knockdown efficiency was comparable, which could be due to the limited endosomal escape

ability of the nanoparticles. Endosomal escape is the biggest obstacle to intracellular siRNA delivery. Once internalized, the nanoparticles can be entrapped in endosome/lysosomes, thus leading to the degradation of siRNA.[7] It was hypothesized that only a small part of the internalized nanoparticles escaped successfully from the endosomes, thus resulting in similar GFP knockdown efficiency. Compared to working with the triblock copolymer PEI-PCL-PEG,[99] the amount of PEG-PCL in a blend system can be adjusted very easily. It should be noted that PEG on the one hand can improve biocompatibility, and on the hand may decrease the transfection efficiency of nanoparticles due to the shielding effect of positive charges.[26] Hence, flexible adjustment may allow for facile tuning of the formulation. Besides, when PEG is modified with targeting ligands, the amount of targeting ligands usually needs to be optimized to achieve high cellular uptake and accumulation in the targeted issue or organs.[245] Therefore, the blended PEG-PCL strategy allows more flexibility and ease of fine-tuning the formulation.

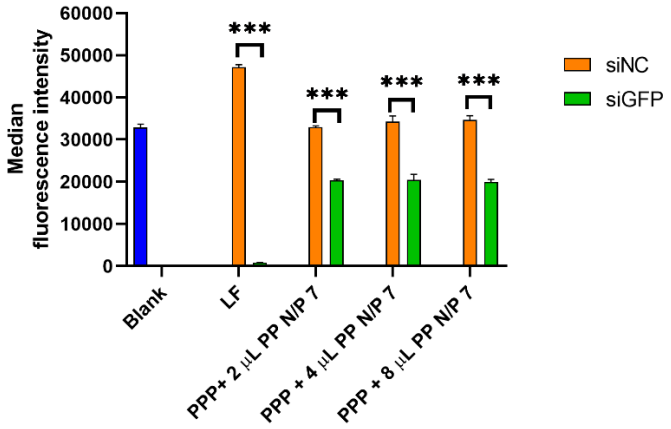

Figure 9. Green fluorescent protein (GFP) knockdown within a H1299 cell line stably expressing eGFP (H1299/eGFP cells). LF: Lipofectamine™ 2000, PPP: PEI5K-PCL5K-PEI5K, PP: PEG-PCL, siNC: negative control siRNA, siGFP: siRNA against eGFP. (Mean ± SD, n = 3, one-way ANOVA, $^{***}p < 0.001$)

3. Conclusion

In this project, we first utilized the commercially available PEI-PCL (800 Da-40 kDa) and PEG-PCL (5 kDa-4 kDa) to prepare nanoparticles. Based on the nano-precipitation method, we developed three preparation methods and evaluated the siRNA encapsulation efficiency, size and zeta potential, and cellular uptake of the nanoparticles and found that the formulation technique had a strong impact on siRNA encapsulation and cellular siRNA uptake. However, we also found that the cellular uptake of PEI-PCL (800 Da-40 kDa) based nanoparticles was too low due to the low binding capacity and low stability of PEI-PCL in the presence of poly-anions such as the proteins in serum. Increasing the molecular weight of PEI to 5 kDa significantly improved the siRNA encapsulation efficiency and cellular uptake. The final formulation PEI-PCL-PEI/PEG-PCL showed high cellular uptake comparable with hyperbranched PEI (25 kDa) and also achieved a significant gene silencing. These results suggested that the PEI-PCL-PEI/PEG-PCL nanoparticle system could be a promising vehicle for siRNA delivery.

4. Experimental Section/Methods

Materials

Polyethylenimine (branched PEI, M_n = 5 kDa, Lupasol® G100 and Lupasol@ WF, M_n = 25 kDa, BASF, Germany), polyethylenimine-*g*-polycaprolactone (PEI-PCL, 800 Da-40 kDa), polyethylene glycol-*b*-polycaprolactone (PEG-PCL, 5 kDa-4 kDa) and polycaprolactone-diacrylate (PCL-diacrylate, Mn = 5 kDa) were purchased from PolySciTech® (Akina, Inc., USA). N, N-Dimethylformamide (DMF), Chloroform-D (Eurisotop, Germany), siRNA targeting green fluorescent protein (siGFP) and scrambled non-specific control (siNC) were purchased from IDT (Integrated DNA Technologies, Inc., Leuven, Belgium) and the sequences are shown in **Table 1**. Further, polyethylenimine (branched PEI, M_n = 10 kDa), 2,4,6-trinitrobenzesulfonic acid (TNBS), RPMI-1640 medium, fetal bovine serum (FBS), Penicillin-Streptomycin (P/S), G418 disulfate salt solution, Dulbecco's phosphate buffered saline (PBS), 0.05% trypsin-EDTA solution, heparin sodium salt, HEPES (4-(2-hydroxyethyl)-1-piperazineethanesulfonic acid) and sodium acetate were purchased from Sigma-Aldrich (Taufkirchen, Germany). AlexaFluor 488 (AF488),

AlexaFluor 647 (AF647) and SYBR gold dye were obtained from Life Technologies (Darmstadt, Germany).

Table 1. Sequences of siRNAs used in this study

Name	Sense strand (5'-3')	Antisense strand (3'-5')
siNC	pCGUUAAUCGCGUAUAAUACGCGUat	CAGCAAUUAGCGCAUAUUAUGCGCAUAp
siGFP	pACCCUGAAGUUCAUCUGCACCACcg	ACUGGGACUUCAAGUAGACGGGUGGC

"p" represents a phosphate residue, lower case letters denote 2'-deoxyribonucleotides, capital letters express ribonucleotides, and underlined capital letters are 2'-O-methylribonucleotides.

Methods

Preparation and characterization of PEI-PCL/PEG-PCL based nanoparticles: The PEI-PCL/PEG-PCL nanoparticles were prepared by nanoprecipitation (solvent displacement method) and three methods were developed based on nanoprecipitation (**Scheme 1**).

Method 1: PEI-PCL (800 Da-40 kDa) and PEG-PCL (5 kDa-4 kDa) were dissolved in 400 µL tetrahydrofuran (THF) with concentrations of 2 mg/mL and 0.05 mg/mL. The polymer solution in THF was then added to 800 µL 10 mM HEPES buffer dropwise while stirring and was kept stirring at 350 rpm under a fume hood for 3 h to evaporate the THF. When the blank nanoparticles were prepared, nanoparticles were post-loaded with siRNA via simply incubation with the blank nanoparticles.

Method 2: A specific amount of siRNA calculated according to the desired N/P ratio was added to 800 µL 10 mM HEPES buffer. In parallel, 400 µL PEI-PCL/PEG-PCL THF solution was prepared as in method I and was added to the siRNA solution dropwise which was stirred at 350 rpm under a fume hood for 3 h.

Method 3: A specific amount of siRNA calculated according to the desired N/P ratio was mixed with 200 µL THF, and the PEI-PCL/PEG-PCL THF solution as prepared in method 1 in 200 µL THF was mixed with the siRNA THF solution and incubated at room temperature for 30 min. The siRNA/PEI-PCL/PEG-PCL was

then added dropwise to 800 µL 10 mM HEPES buffer and stirred at 350 rpm under a fume hood for 3 h.

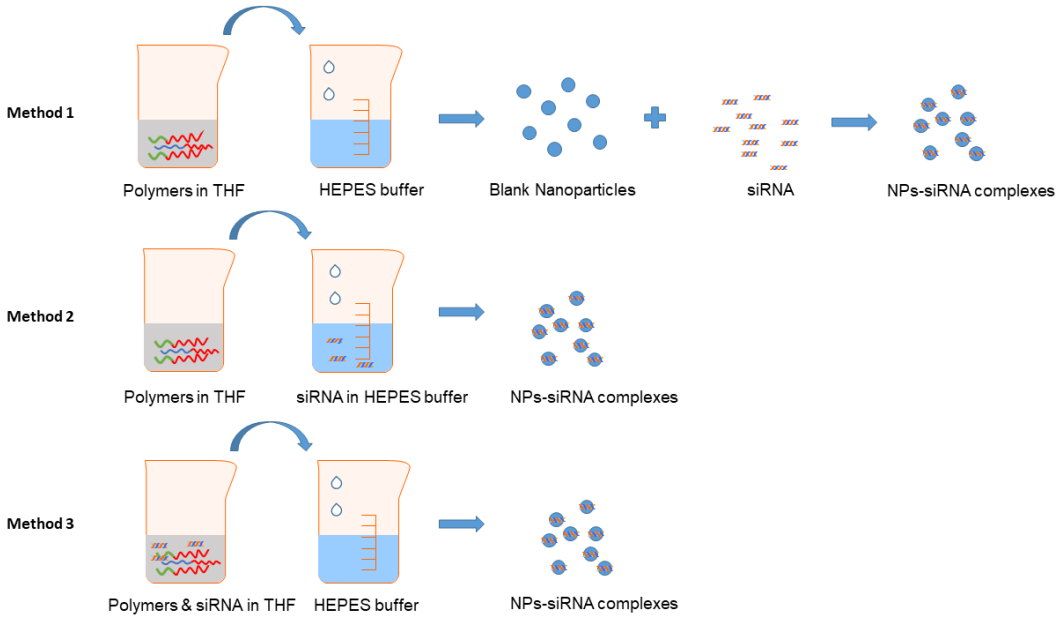

Scheme 1. Schematic illustration of NPs-siRNA complexes preparation methods 1-3.

For the preparation of NPs-siRNA complexes, the amounts of PEI-PCL polymers were calculated according to the following equation:

$$m(\text{PEI-PCL})\ (\text{in pg}) = 50\ \text{pmol} \times 52 \times \text{N/P} \times 43.1\ \text{g/mol} / 3.08\%$$

where 52 is the number of nucleotides of the 25/27mer siRNA; N/P ratio is the molar ratio of the polymer's protonable amine groups (N) and the siRNA phosphate groups (P); 43.1 g/mol is the protonable unit of PEI; 3.08% is the PEI amount in PEI-PCL determined by TNBS assay as described in the following section.

The size and zeta potential of the blank nanoparticles (NPs) and siRNA-loaded nanoparticle complexes (NPs-siRNA) dispersed in 10 mM HEPES buffer were determined using the Nano ZS (Malvern Instruments Inc., Malvern, UK), for each measurement, measurements were taken in triplicate with 15 runs each and the mean value was reported.

SYBR gold assay of PEI-PCL/PEG-PCL based nanoparticles: SYBR gold assays were performed to determine the siRNA encapsulation efficiency of the NPs prepared as described above. In brief, the NPs-siRNA complexes were prepared at various N/P ratios via methods 1, 2, and 3. The NPs-siRNA was then added to black 96-well plates with 100 µL for each well in triplicates. Subsequently, 30 µL SYBR gold (4X) solution was added to each well and incubated in the dark at room temperature for 10 min. Free siRNA was used as a control for the 100% fluorescence value. The fluorescence was finally determined in a microplate reader (TECAN, Switzerland, excitation: 485/20 nm emission: 520/20 nm).

Cellular uptake of PEI-PCL/PEG-PCL based nanoparticles: To determine the cellular uptake of NPs-siRNA, Alexa Fluor 647 labeled siRNA (AF647-siRNA) was used to prepare the NPs-siRNA. H1299 cells were seeded in 24-well plates (50,000 cells/well) and grown in the CO_2 incubator 24 h before use. Afterwards, NPs-siRNA complexes (50 pmol AF647-siRNA/ well) diluted in RPMI-1640 complete medium were added and incubated with the cells in the incubator for 24 h. Subsequently, the NPs-siRNA solution was discarded, and the cells were rinsed with PBS and detached with 0.05% Trypsin-EDTA. The detached cells were then washed with PBS another 2 times and analyzed via flow cytometry (Attune NxT Acoustic Focusing Cytometer, Thermo Fisher, Darmstadt, Germany) excited with a 638 nm laser and detected with a RL1 filter (670/14 nm).

Heparin competition of PEI-PCL/PEG-PCL based nanoparticles: To estimate the different behaviors of the NPs-siRNA obtained by different preparation methods in cellular uptake and evaluate their stability in the presence of competing polyanions, heparin competition assays were performed. In brief, the NPs-siRNA (N/P 10) were prepared by methods 2 and 3 in HEPES buffer (pH 7.4) or sodium acetate buffer (pH 4.5), and free siRNA was used as negative control and set as 100% fluorescence value. The NPs-siRNA complexes and free siRNA were added to a 96 well plate (60 µL/well), and heparin solution with various concentrations from 0.1 to 1 USP/well was added (10 µL/well) and incubated at room temperature for 30 min. Subsequently, 4 X SYBR gold solution was added (30 µL/well) and incubated in the dark for 10 min. Intercalation-caused fluorescence

was determined with a microplate reader (TECAN, Switzerland, excitation: 485/20 nm emission: 520/20 nm).

Synthesis of PEI5K-PCL5K-PEI5K: PEI5K-PCL5K-PEI5K was synthesized as illustrated in **Scheme 2.** In brief, 100 mg PEI5K (branched PEI, Mn = 5 kDa) was dissolved in 5 mL N,N'-dimethylformamide (DMF) and stirred at 40 ℃ for about 10 min, then 50 mg polycaprolactone-diacrylate (PCL-diacrylate, Mn = 5 kDa) in 5 mL DMF was added dropwise to the PEI solution. After stirring at 40 ℃ for 48 h, the solution was transferred to a dialysis kit (MWCO 6 kDa, Sigma) and the reaction mixture was dialyzed against distilled water for 2 days. Finally, the aqueous product solution was lyophilized and the desired product was isolated as a colorless solid. The chemical structure of the product was characterized via ^{1}H NMR spectroscopy. Yield: 31%-54%

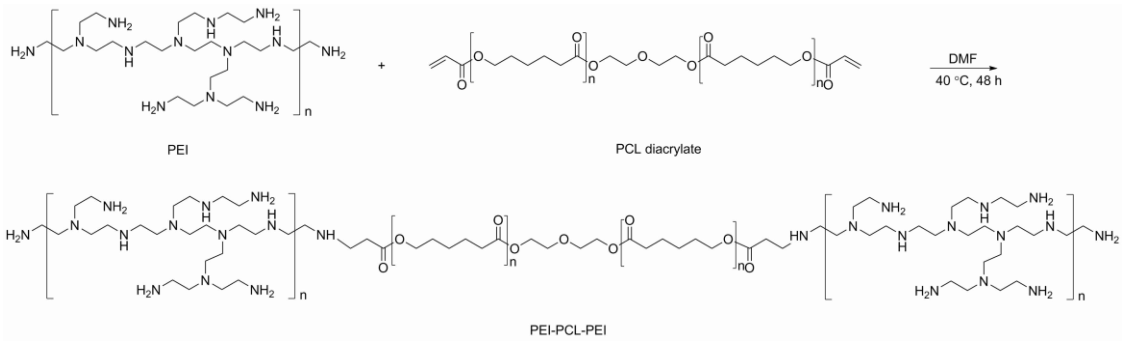

Scheme 2. Synthesis route of PEI5K-PCL5K-PEI5K

TNBS assay of PEI5K-PCL5K-PEI5K: To determine the PEI content in the copolymer PEI5K-PCL5K-PEI5K, a TNBS assay was carried out. TNBS (2,4,6-Trinitrobenzene Sulfonic Acid) is a rapid and sensitive assay reagent for the determination of free amino groups.[246] Primary amines, upon reaction with TNBS, form a highly chromogenic derivative, which has specific absorbance and can be used for quantitative measurements of amines.[247] A series of PEI5K high-purity water solutions were prepared as the standard solutions. An aliquot of 100 µL sample and the standard solution was mixed with 30 µL of a 1.76% TNBS solution (w/v in 0.1 M Borax) in a transparent microwell plate. After incubation at room temperature for 1 h, sample absorbance was assessed at 405 nm in a microplate reader (TECAN, Switzerland). Results were compared with the standard dilution series.

Preparation and characterization of PEI-PCL-PEI/PEG-PCL based nanoparticles: The nanoparticles were prepared via solvent displacement method (nanoprecipitation) similar to method 1 described above. In brief, 200 µL PEI-PCL-PEI (5 kDa-5 kDa-5 kDa, 5 mg/mL) and 2 µL, 4 µL or 8 µL of PEG-PCL (5 kDa-4 kDa, 5 mg/mL) in acetone was mixed and then injected into 1 mL distilled water while stirring (350 rpm). After stirring and evaporating the acetone in a fume hood for 3 h, the NPs in distilled water were characterized using a NanoZS zeta sizer (Malvern Instruments Inc., Malvern, UK).

For the preparation of siRNA-loaded nanoparticle-siRNA complexes (micelleplexes), the amounts of blank nanoparticles were calculated according to the following equation:

$$m(\text{PEI-PCL-PEI}) \text{ (in pg)} = 50 \text{ pmol} \times 52 \times N/P \times 43.1 \text{ g/mol} / 64.75\%$$

where 52 is the number of nucleotides of the 25/27mer siRNA; N/P ratio is the molar ratio of the polymer's protonale amine groups (N) and the siRNA phosphate groups (P); 43.1 g/mol is the protonable unit of PEI; 64.75% is the PEI amount in PEI-PCL-PEI determined by TNBS assay. The nanoparticle suspension was mixed with the siRNA solution and incubated at room temperature for 2 h to form micelleplexes ready to be used in subsequent experiments.

SYBR Gold assay of PEI-PCL-PEI/PEG-PCL based nanoparticles: To determine the siRNA encapsulation efficiency of the nanoparticles, SYBR Gold assays were performed. In brief, the micelleplexes at N/P 1, 3, 5, 7, 10, 15 and 20 were prepared. To this extent, 100 µL of the micelleplexes were added to a 96-well plate in triplicate. Free siRNA solution with the same amount of siRNA (N/P = 0) was used as negative control, and the fluorescence value was set as 100%. Subsequently, 30 µL of SYBR gold solution (4x) was added to the plate and incubated in the dark at room temperature for 10 min. Finally, the fluorescence was determined using a microplate reader (TECAN, Switzerland, excitation: 485/20 nm emission: 520/20 nm.).

Dye quenching assay: Dye quenching of covalently modified molecules is another method to investigate the binding behavior of nucleic acids by polycations.[244] PEI-PCL-PEI NPs and PEI-PCL-PEI/PEG-PCL NPs were prepared as described above. Here, 30 pmol Cy5-siRNA was complexed with nanoparticles at different N/P ratios. The remaining fluorescence of the micelleplex suspensions (100 µL) was determined using a microplate reader (TECAN, Switzerland, excitation: 621/20 nm, emission: 666/20 nm). Free Cy5-siRNA in 10 mM HEPES buffer represents 100% fluorescence.

Cellular uptake of PEI-PCL-PEI/PEG-PCL based nanoparticles: The nanoparticles were prepared as described above. Alexa Fluor 488 labeled siRNA (AF488-siRNA) was then incubated with the blank nanoparticles at room temperature for 2 h to form micelleplexes, and the cellular uptake was assessed by flow cytometry with a 488 nm laser for excitation and BL1 filter (530/30 nm) for detection.

GFP knockdown of PEI-PCL-PEI/PEG-PCL based nanoparticles: The nanoparticles were prepared as described above. For nanoparticle loading, scrambled siRNA (siNC) or siRNA against GFP (siGFP) was incubated with the blank nanoparticles at room temperature for 2 h. H1299/eGFP cells were seeded in 24-well plate (25000 cells in 500 µL medium/well), after growth in CO_2 incubator (37 ℃, 5% CO_2) for 24 h, the cells were transfected with micelleplexes (NPs-siRNA complexes) composed of siNC (50 pmol/well) or siGFP (50 pmol/well). Lipofectamine™ 2000 formulated with siNC and siGFP were controlled groups. After 48 h in the incubator, the transfected cells were detached and washed with PBS for flow cytometry measurements (Attune Cytometer, Thermo Fisher Scientific, Darmstadt, Germany), with a 488 nm laser for excitation and BL1 filter (530/30 nm) for detection.

Supporting Information

Supporting Information is available from the Wiley Online Library or from the author.

Acknowledgements

Yao Jin appreciate the financial support from China Scholarship Council (CSC201906010329). This project is funded by ERC -2014-StG – 637830 to Olivia Merkel.

Conflict of interest

The authors declare no conflicts of interest.

Table of content

*Yao Jin, Friederike Adams, Judith Möller, Lorenz Isert, Christoph M. Zimmermann, David Keul, Olivia M. Merkel**

Synthesis and application of low molecular weight PEI-based copolymers for siRNA delivery with smart polymer blends

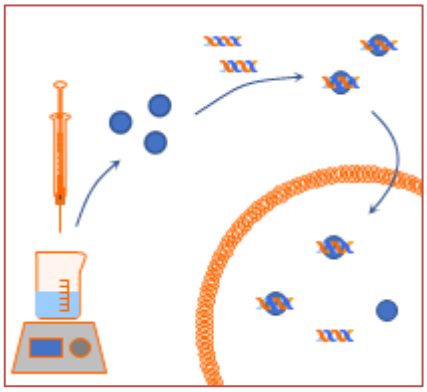

To efficiently deliver siRNA and decrease the cytotoxicity caused by high molecular weight PEI, relatively low molecular weight PEI based-polymers PEI-PCL and PEI-PCL-PEI were used to prepare nanoparticles with or without PEG-PCL by solvent displacement polymer blending. After screening and *in vitro* characterization, the PEI-PCL-PEI/PEG-PCL based nanoparticles proved promising for siRNA delivery.

Supporting Information

Synthesis and application of low molecular weight PEI-based copolymers for siRNA delivery with smart polymer blends

*Yao Jin, Friederike Adams, Judith Möller, Lorenz Isert, Christoph M. Zimmermann, David Keul, Olivia M. Merkel**

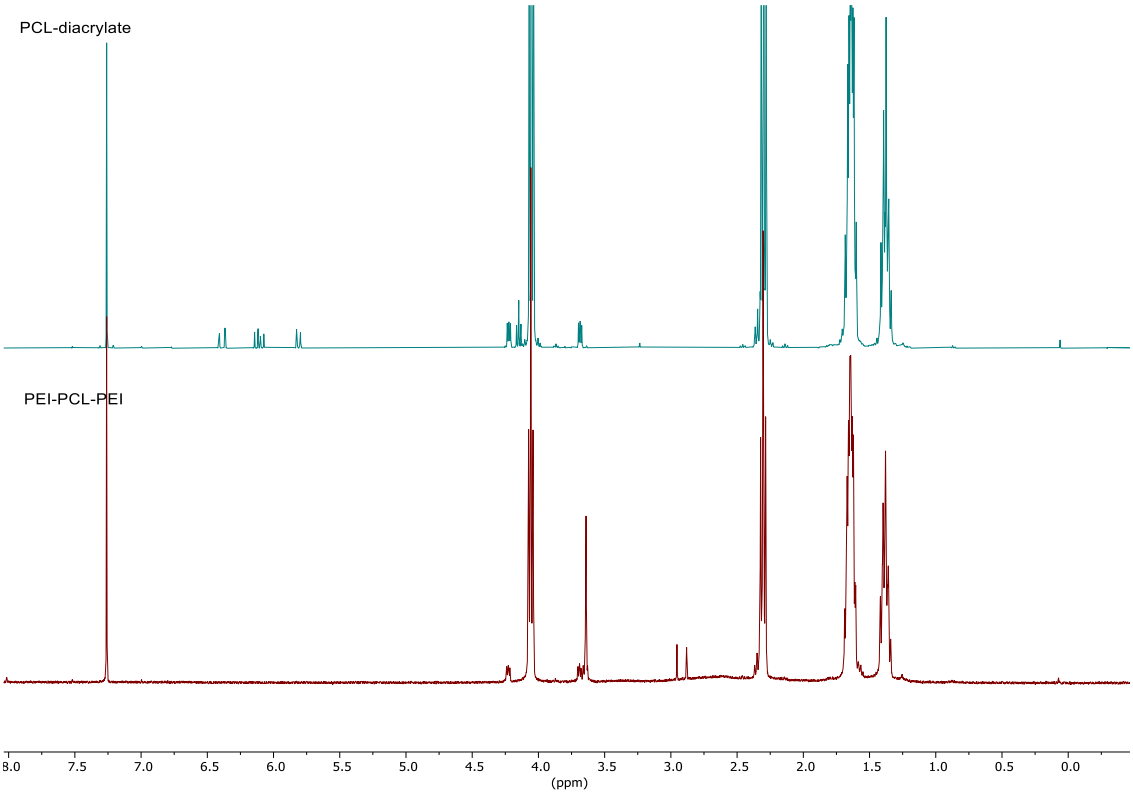

Figure S1. ^{1}H NMR of PCL-diacrylate and PEI-PCL-PEI in $CDCl_3$

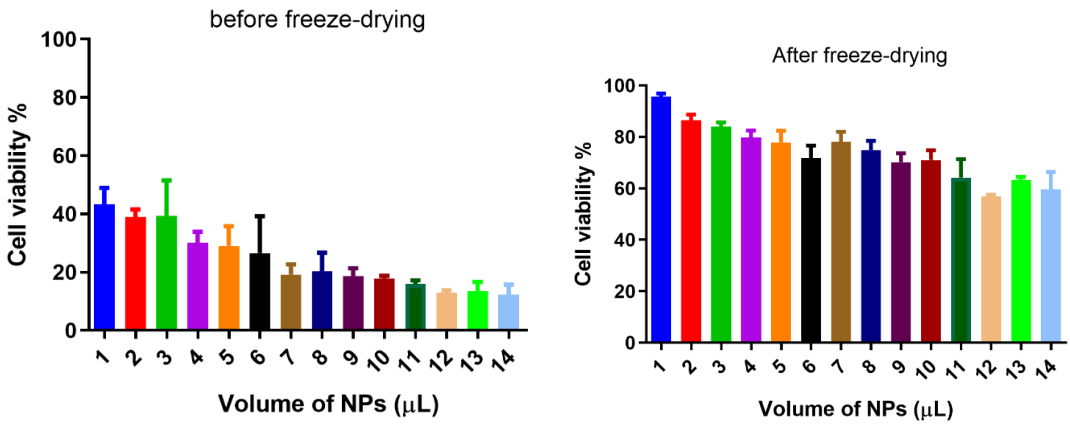

Figure S2. MTT assay of PEI-PCL/PEG-PCL nanoparticles (method 1) evaporating under fume hood for 3 hours (before freeze-drying) and after freeze-drying, the x axis indicates the volume of NPs per 100 µL medium for each well in a 96-well plate, the concentration of the NP stock suspension added is 1.37 mg/mL. The amount of NPs for other *in vitro* evaluation experiments is less than 10 µL NPs per 100 µL medium.

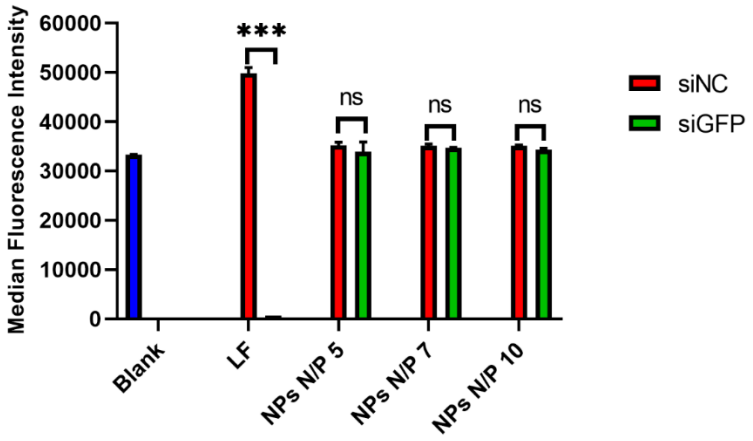

Figure S3. Enhanced green fluorescence protein knockdown of PEI-PCL/PEG-PCL NPs prepared by method 3. (Mean ± SD, $n = 2$, two-way ANOVA with multiple comparisons, $^{***}p < 0.001$, $^{ns}p > 0.05$)

Summary and outlook

The main aim of the studies in this dissertation was to synthesize novel polymers for siRNA delivery. Poly(β-amino ester)s and low molecular weight PEI-based copolymers were synthesized and evaluated in these projects.

Chapter 1 is the starting point of the spermine-based Poly(β-amino ester)s. In this chapter, spermine was first protected with ethyl trifluoroacetate and Boc anhydride. After removing the protecting group from ethyl trifluoroacetate and purification by column chromatography, the monomer tri-boc-spermine was obtained and characterized by ^{1}H NMR and ESI-MS. Tri-boc-spermine was polymerized with 1,4-butanediol diacrylate to obtain the polymer named as P(BSpBAE). The polymer was finally deprotected to yield another polymer P(SpBAE). The polymers' chemical structures were characterized by ^{1}H NMR, and the molecular weight of P(BSpBAE) was determined by GPC (Mn = 3565 Da, PDI 1.73). P(SpBAE) was first evaluated for siRNA delivery. Unfortunately, although this polymer can encapsulate siRNA efficiently according to the SYBR gold assays, the cellular uptake of P(SpBAE) polyplexes was low and the polyplexes can hardly knock down GFP expression in cell culture. According to the properties of P(SpBAE) and the current literature, we assumed that hydrophobic modification could improve its gene silencing efficacy. Considering that N-Boc groups are hydrophobic, we innovatively tried the N-Boc protected polymer for siRNA encapsulation and delivery. Interestingly, the polymer P(BSpBAE) achieved higher uptake than Lipofectamine^{TM} 2000, and this polymer also achieved around 60% GFP knockdown. We further investigated the endosomal entrapment and cellular uptake of the two types of polyplexes and found that hydrophobic modification altered the cellular uptake mechanism and that P(BSpBAE) polyplexes had lower endosomal entrapment. To achieve therapeutically relevant gene silencing, we silenced mutated KRAS in lung cancer cells and performed a migration assay. Interestingly, both of the polyplexes inhibited the migration of lung cancer cells (A549) as confirmed by KRAS silencing on the protein level by western blot analysis.

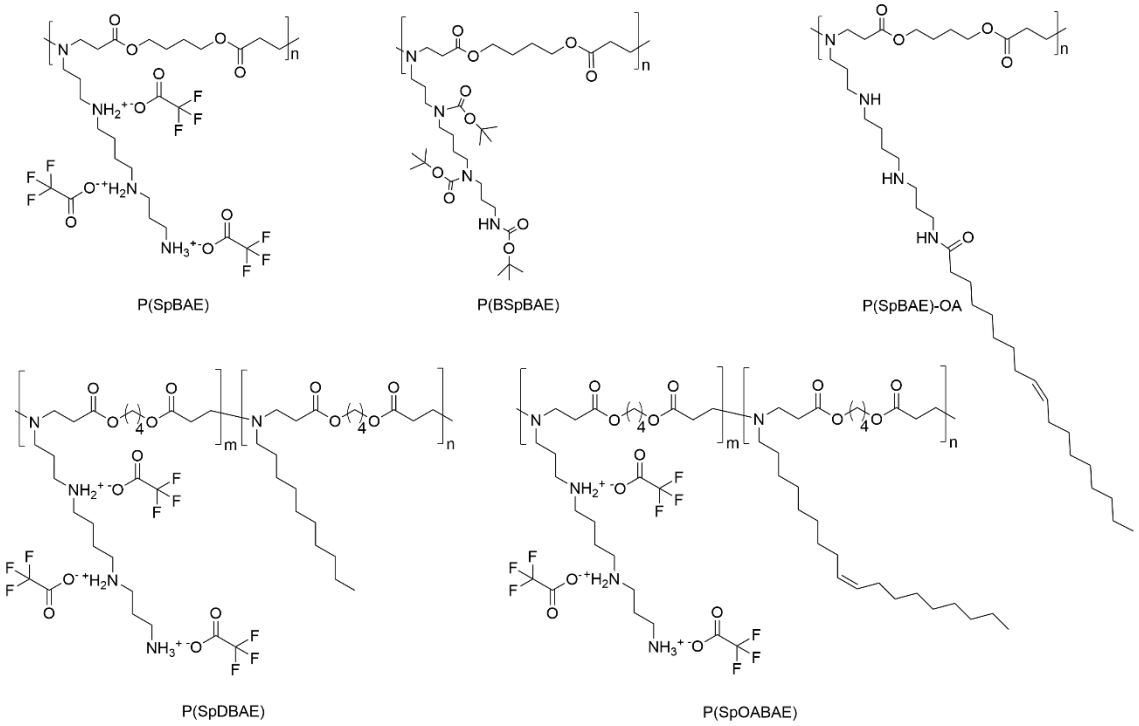

Figure 1. The chemical structures of spermine-based poly(β-amino ester)s.

Chapter 2 further investigates hydrophobic modifications of P(SpBAE)s. Decylamine was used to co-polymerize with tri-boc-spermine and 1,4-butanediol diacrylate, and the resulting polymer P(BSpDBAE) was characterized by ^{1}H NMR and GPC (M_n = 5987 Da, PDI 1.83). After deprotection, the polymer was named P(SpDBAE). P(SpDBAE) was able to fully encapsulate siRNA from N/P 5 on, the sizes of the polyplexes were around 50 nm except for polyplex formulations at N/P 1 and 3 (~140 nm). The polyplexes also showed significantly higher cellular uptake than hyperbranched PEI (25 kDa) and the GFP knockdown efficiency was around 90%. This chapter confirmed the benefits of hydrophobic modification and indicated that this amphiphilic spermine, decylamine-based poly(β-amino ester) is a very promising material for polymeric siRNA delivery.

Chapter 3 studies the role of the hydrophobic modification. Oleylamine which contains an unsaturated double bond was co-polymerized with tri-boc-spermine and 1,4-butanediol diacrylate. To compare the effect of the hydrophobic modification, we synthesized polymers P(SpOABAE) with 10%, 30%, and 50% of oleylamine units named Sp0.9/OA0.1; Sp0.7/OA0.3 and Sp0.5/OA0.5, respectively. The cellular uptake of the polyplexes and GFP knockdown efficiency of the polyplexes were determined by flow cytometry. Sp0.5/OA0.5 showed the highest cellular uptake and the best GFP knockdown performance of more than 90%. An

endosomal entrapment assay was also performed and found that the P(SpOA-BAE) with a higher ratio of oleylamine (Sp0.5/OA0.5) achieved better endosomal escape. This polymer was also spray dried and still showed excellent GFP knockdown after storage for 4 months. These results suggested that appropriate modification of PBAEs with hydrophobic segments could improve the endosomal escape of the polyplexes and enhance the gene silencing efficiency.

Chapter 4 reports the siRNA delivery study with low molecular weight PEI-based copolymers. The commercially available PEI-PCL (800 Da-40 kDa) was first employed to prepare nanoparticles in a blending approach with PEG-PCL. Based on the solvent displace method, we developed three methods for siRNA encapsulation. The siRNA encapsulation efficiency, size, and zeta potential of the nanoparticles and cellular uptake of each method were all analyzed. To further improve the siRNA encapsulation efficiency, PEI5K-PCL5K-PEI5K was synthesized and evaluated in blends with PEG-PCK. PEI5K-PCL5K-PEI5K/PEG-PCL nanoparticles achieved higher cellular uptake and around 40% GFP knockdown efficiency.

With the synthesis of these polymers, one question we are wondering about is what properties a polymer should have for siRNA delivery. Based on the chemical structures and properties of our polymers including the PBAEs and PEI-based copolymers, this thesis addresses several points: (1) a structure/property relationship exists, and the architecture of the polymers can affect the siRNA delivery efficiency; (2) the brush-like PBAEs' side chains (spermine) can enhance the interaction of siRNA with the polymer; (3) amphiphilic polymers achieved better endosomal escape and gene silencing efficacy than hydrophilic polymers, with the best results when the hydrophobic segments were around 30% - 50% of the polymer molecular weight; (4) despite the hydrophobic monomers and hydrophilic monomers being located randomly in the PBAE polymer molecule, the hydrophobic interaction of the hydrophobic segments enhanced the stability of the polyplexes. However, these conclusions are just based on several polymers, and to draw a universal rule, a high-throughput synthesis may be needed to obtain more convincing principles. Therefore, in the future more computer simulations should be employed for predictions. Calculating the hydrophilic-lipophilic balance (HLB)

and partition coefficient (Log P) which are related to the amphiphilicity of the polymers and modeling the siRNA-polymer interactions and the interaction between polyplexes/micelleplexes and cells could be interesting research topics.

Lastly, the polymers synthesized here can also be modified with ligands, for example, transferrin, folate, and many more to achieve a targeted delivery of siRNA. And polymers that efficiently deliver siRNA could also be tested for mRNA delivery as well.

References

1. Fire, A.; Xu, S.; Montgomery, M. K.; Kostas, S. A.; Driver, S. E.; Mello, C. C., Potent and specific genetic interference by double-stranded RNA in Caenorhabditis elegans. *nature* **1998,** *391* (6669), 806-811.

2. Sajid, M. I.; Moazzam, M.; Kato, S.; Yeseom Cho, K.; Tiwari, R. K., Overcoming Barriers for siRNA Therapeutics: From Bench to Bedside. *Pharmaceuticals* **2020,** *13* (10), 294.

3. Caplen, N. J.; Parrish, S.; Imani, F.; Fire, A.; Morgan, R. A., Specific inhibition of gene expression by small double-stranded RNAs in invertebrate and vertebrate systems. *Proc Natl Acad Sci U S A* **2001,** *98* (17), 9742-7.

4. Elbashir, S. M.; Harborth, J.; Lendeckel, W.; Yalcin, A.; Weber, K.; Tuschl, T., Duplexes of 21-nucleotide RNAs mediate RNA interference in cultured mammalian cells. *Nature* **2001,** *411* (6836), 494-8.

5. Chendrimada, T. P.; Gregory, R. I.; Kumaraswamy, E.; Norman, J.; Cooch, N.; Nishikura, K.; Shiekhattar, R., TRBP recruits the Dicer complex to Ago2 for microRNA processing and gene silencing. *Nature* **2005,** *436* (7051), 740-744.

6. Gregory, R. I.; Chendrimada, T. P.; Cooch, N.; Shiekhattar, R., Human RISC couples microRNA biogenesis and posttranscriptional gene silencing. *Cell* **2005,** *123* (4), 631-640.

7. Dominska, M.; Dykxhoorn, D. M., Breaking down the barriers: siRNA delivery and endosome escape. *Journal of cell science* **2010,** *123* (8), 1183-1189.

8. Cavallaro, G.; Sardo, C.; Craparo, E. F.; Porsio, B.; Giammona, G., Polymeric nanoparticles for siRNA delivery: Production and applications. *Int J Pharm* **2017,** *525* (2), 313-333.

9. Tatiparti, K.; Sau, S.; Kashaw, S. K.; Iyer, A. K., siRNA Delivery Strategies: A Comprehensive Review of Recent Developments. *Nanomaterials (Basel)* **2017,** *7* (4).

10. Esau, C. C.; Monia, B. P., Therapeutic potential for microRNAs. *Advanced Drug Delivery Reviews* **2007,** *59* (2), 101-114.

11. McAnuff, M. A.; Rettig, G. R.; Rice, K. G., Potency of siRNA versus shRNA mediated knockdown in vivo. *J Pharm Sci* **2007,** *96* (11), 2922-30.

12. Wang, J.; Lu, Z.; Wientjes, M. G.; Au, J. L.-S., Delivery of siRNA therapeutics: barriers and carriers. *The AAPS journal* **2010,** *12* (4), 492-503.

13. Lorenzer, C.; Dirin, M.; Winkler, A.-M.; Baumann, V.; Winkler, J., Going beyond the liver: Progress and challenges of targeted delivery of siRNA therapeutics. *Journal of Controlled Release* **2015,** *203*, 1-15.

14. Van de Water, F. M.; Boerman, O. C.; Wouterse, A. C.; Peters, J. G.; Russel, F. G.; Masereeuw, R., Intravenously administered short interfering RNA accumulates in the kidney and selectively suppresses gene function in renal proximal tubules. *Drug metabolism and disposition* **2006,** *34* (8), 1393-1397.

15. Czauderna, F.; Fechtner, M.; Dames, S.; Aygün, H.; Klippel, A.; Pronk, G. J.; Giese, K.; Kaufmann, J., Structural variations and stabilising modifications of

synthetic siRNAs in mammalian cells. *Nucleic Acids Research* **2003,** *31* (11), 2705-2716.

16. Xia, J.; Noronha, A.; Toudjarska, I.; Li, F.; Akinc, A.; Braich, R.; Frank-Kamenetsky, M.; Rajeev, K. G.; Egli, M.; Manoharan, M., Gene silencing activity of siRNAs with a ribo-difluorotoluyl nucleotide. *ACS Chem Biol* **2006,** *1* (3), 176-83.

17. Dowler, T.; Bergeron, D.; Tedeschi, A.-L.; Paquet, L.; Ferrari, N.; Damha, M. J., Improvements in siRNA properties mediated by 2′-deoxy-2′-fluoro-β-d-arabinonucleic acid (FANA). *Nucleic Acids Research* **2006,** *34* (6), 1669-1675.

18. Gao, K.; Huang, L., Achieving efficient RNAi therapy: progress and challenges. *Acta Pharmaceutica Sinica B* **2013,** *3* (4), 213-225.

19. Hoshika, S.; Minakawa, N.; Shionoya, A.; Imada, K.; Ogawa, N.; Matsuda, A., Study of Modification Pattern–RNAi Activity Relationships by Using siRNAs Modified with 4′-Thioribonucleosides. *ChemBioChem* **2007,** *8* (17), 2133-2138.

20. Amarzguioui, M.; Holen, T.; Babaie, E.; Prydz, H., Tolerance for mutations and chemical modifications in a siRNA. *Nucleic Acids Research* **2003,** *31* (2), 589-595.

21. Peer, D.; Lieberman, J., Special delivery: targeted therapy with small RNAs. *Gene Ther* **2011,** *18* (12), 1127-33.

22. Whitehead, K. A.; Langer, R.; Anderson, D. G., Knocking down barriers: advances in siRNA delivery. *Nat Rev Drug Discov* **2009,** *8* (2), 129-38.

23. Ku, S. H.; Jo, S. D.; Lee, Y. K.; Kim, K.; Kim, S. H., Chemical and structural modifications of RNAi therapeutics. *Advanced drug delivery reviews* **2016,** *104*, 16-28.

24. Du, J.; Sun, Y.; Shi, Q. S.; Liu, P. F.; Zhu, M. J.; Wang, C. H.; Du, L. F.; Duan, Y. R., Biodegradable nanoparticles of mPEG-PLGA-PLL triblock copolymers as novel non-viral vectors for improving siRNA delivery and gene silencing. *Int J Mol Sci* **2012,** *13* (1), 516-33.

25. Luo, G.; Jin, C.; Long, J.; Fu, D.; Yang, F.; Xu, J.; Yu, X.; Chen, W.; Ni, Q., RNA interference of MBD1 in BxPC-3 human pancreatic cancer cells delivered by PLGA-poloxamer nanoparticles. *Cancer Biol Ther* **2009,** *8* (7), 594-8.

26. Santel, A.; Aleku, M.; Keil, O.; Endruschat, J.; Esche, V.; Fisch, G.; Dames, S.; Löffler, K.; Fechtner, M.; Arnold, W.; Giese, K.; Klippel, A.; Kaufmann, J., A novel siRNA-lipoplex technology for RNA interference in the mouse vascular endothelium. *Gene Ther* **2006,** *13* (16), 1222-34.

27. Ishida, T.; Harada, M.; Wang, X. Y.; Ichihara, M.; Irimura, K.; Kiwada, H., Accelerated blood clearance of PEGylated liposomes following preceding liposome injection: Effects of lipid dose and PEG surface-density and chain length of the first-dose liposomes. *Journal of Controlled Release* **2005,** *105* (3), 305-317.

28. Ishida, T.; Kiwada, H., Accelerated blood clearance (ABC) phenomenon upon repeated injection of PEGylated liposomes. *International Journal of Pharmaceutics* **2008,** *354* (1), 56-62.

29. Ju, Y.; Lee, W. S.; Pilkington, E. H.; Kelly, H. G.; Li, S.; Selva, K. J.; Wragg, K. M.; Subbarao, K.; Nguyen, T. H. O.; Rowntree, L. C.; Allen, L. F.; Bond, K.; Williamson, D. A.; Truong, N. P.; Plebanski, M.; Kedzierska, K.; Mahanty, S.; Chung, A. W.; Caruso, F.; Wheatley, A. K.; Juno, J. A.; Kent, S. J., Anti-PEG Antibodies Boosted in Humans by SARS-CoV-2 Lipid Nanoparticle mRNA Vaccine. *ACS Nano* **2022**.

30. Boussif, O.; Lezoualc'h, F.; Zanta, M. A.; Mergny, M. D.; Scherman, D.; Demeneix, B.; Behr, J.-P., A versatile vector for gene and oligonucleotide transfer into cells in culture and in vivo: polyethylenimine. *Proceedings of the National Academy of Sciences* **1995,** *92* (16), 7297-7301.

31. DiCiccio, J. E.; Steinberg, B. E., Lysosomal pH and analysis of the counter ion pathways that support acidification. *Journal of General Physiology* **2011,** *137* (4), 385-390.

32. Hu, Y.-B.; Dammer, E. B.; Ren, R.-J.; Wang, G., The endosomal-lysosomal system: from acidification and cargo sorting to neurodegeneration. *Translational neurodegeneration* **2015,** *4* (1), 1-10.

33. Behr, J.-P., The proton sponge: a trick to enter cells the viruses did not exploit. *CHIMIA International Journal for Chemistry* **1997,** *51* (1-2), 34-36.

34. Nguyen, J.; Szoka, F. C., Nucleic acid delivery: the missing pieces of the puzzle? *Accounts of chemical research* **2012,** *45* (7), 1153-1162.

35. Bus, T.; Traeger, A.; Schubert, U. S., The great escape: how cationic polyplexes overcome the endosomal barrier. *Journal of Materials Chemistry B* **2018,** *6* (43), 6904-6918.

36. Dubruel, P.; Christiaens, B.; Vanloo, B.; Bracke, K.; Rosseneu, M.; Vandekerckhove, J.; Schacht, E., Physicochemical and biological evaluation of cationic polymethacrylates as vectors for gene delivery. *European journal of pharmaceutical sciences* **2003,** *18* (3-4), 211-220.

37. Tang, M.; Szoka, F., The influence of polymer structure on the interactions of cationic polymers with DNA and morphology of the resulting complexes. *Gene therapy* **1997,** *4* (8), 823-832.

38. Itaka, K.; Harada, A.; Yamasaki, Y.; Nakamura, K.; Kawaguchi, H.; Kataoka, K., In situ single cell observation by fluorescence resonance energy transfer reveals fast intra‐cytoplasmic delivery and easy release of plasmid DNA complexed with linear polyethylenimine. *The Journal of Gene Medicine: A cross‐disciplinary journal for research on the science of gene transfer and its clinical applications* **2004,** *6* (1), 76-84.

39. Butt, A. M.; Abdullah, N.; Rani, N. N. I. M.; Ahmad, N.; Amin, M. C. I. M., Endosomal Escape of Bioactives Deployed via Nanocarriers: Insights Into the Design of Polymeric Micelles. *Pharmaceutical Research* **2022,** *39* (6), 1047-1064.

40. Lee, E. S.; Kim, D.; Youn, Y. S.; Oh, K. T.; Bae, Y. H., A virus‐mimetic nanogel vehicle. *Angewandte Chemie International Edition* **2008,** *47* (13), 2418-2421.

41. Vaidyanathan, S.; Orr, B. G.; Banaszak Holl, M. M., Role of Cell Membrane–Vector Interactions in Successful Gene Delivery. *Accounts of Chemical Research* **2016,** *49* (8), 1486-1493.

42. Bieber, T.; Meissner, W.; Kostin, S.; Niemann, A.; Elsasser, H.-P., Intracellular route and transcriptional competence of polyethylenimine–DNA complexes. *Journal of Controlled Release* **2002,** *82* (2-3), 441-454.

43. Rehman, Z. U.; Hoekstra, D.; Zuhorn, I. S., Mechanism of polyplex-and lipoplex-mediated delivery of nucleic acids: real-time visualization of transient membrane destabilization without endosomal lysis. *ACS nano* **2013,** *7* (5), 3767-3777.

44. Yue, Y.; Jin, F.; Deng, R.; Cai, J.; Dai, Z.; Lin, M. C.; Kung, H.-F.; Mattebjerg, M. A.; Andresen, T. L.; Wu, C., Revisit complexation between DNA and polyethylenimine—Effect of length of free polycationic chains on gene transfection. *Journal of Controlled Release* **2011,** *152* (1), 143-151.

45. Grandinetti, G.; Smith, A. E.; Reineke, T. M., Membrane and nuclear permeabilization by polymeric pDNA vehicles: efficient method for gene delivery or mechanism of cytotoxicity? *Molecular pharmaceutics* **2012,** *9* (3), 523-538.

46. White, J. M.; Whittaker, G. R., Fusion of enveloped viruses in endosomes. *Traffic* **2016,** *17* (6), 593-614.

47. Lagache, T.; Sieben, C.; Meyer, T.; Herrmann, A.; Holcman, D., Stochastic model of acidification, activation of hemagglutinin and escape of influenza viruses from an endosome. *Frontiers in Physics* **2017,** *5*, 25.

48. Miyauchi, K.; Kim, Y.; Latinovic, O.; Morozov, V.; Melikyan, G. B., HIV enters cells via endocytosis and dynamin-dependent fusion with endosomes. *Cell* **2009,** *137* (3), 433-444.

49. Kwon, E. J.; Bergen, J. M.; Pun, S. H., Application of an HIV gp41-Derived Peptide for Enhanced Intracellular Trafficking of Synthetic Gene and siRNA Delivery Vehicles. *Bioconjugate Chemistry* **2008,** *19* (4), 920-927.

50. Oliveira, S.; van Rooy, I.; Kranenburg, O.; Storm, G.; Schiffelers, R. M., Fusogenic peptides enhance endosomal escape improving siRNA-induced silencing of oncogenes. *International Journal of Pharmaceutics* **2007,** *331* (2), 211-214.

51. Heyes, J.; Palmer, L.; Bremner, K.; MacLachlan, I., Cationic lipid saturation influences intracellular delivery of encapsulated nucleic acids. *Journal of controlled release* **2005,** *107* (2), 276-287.

52. Farhood, H.; Serbina, N.; Huang, L., The role of dioleoyl phosphatidylethanolamine in cationic liposome mediated gene transfer. *Biochimica et Biophysica Acta (BBA)-Biomembranes* **1995,** *1235* (2), 289-295.

53. Payne, C. K.; Jones, S. A.; Chen, C.; Zhuang, X., Internalization and trafficking of cell surface proteoglycans and proteoglycan‐binding ligands. *Traffic* **2007,** *8* (4), 389-401.

54. Yameen, B.; Choi, W. I.; Vilos, C.; Swami, A.; Shi, J.; Farokhzad, O. C., Insight into nanoparticle cellular uptake and intracellular targeting. *Journal of controlled release* **2014,** *190*, 485-499.

55. Rejman, J.; Oberle, V.; Zuhorn, I. S.; Hoekstra, D., Size-dependent internalization of particles via the pathways of clathrin-and caveolae-mediated endocytosis. *Biochemical journal* **2004,** *377* (1), 159-169.

56. Von Gersdorff, K.; Sanders, N. N.; Vandenbroucke, R.; De Smedt, S. C.; Wagner, E.; Ogris, M., The internalization route resulting in successful gene expression depends on both cell line and polyethylenimine polyplex type. *Molecular therapy* **2006,** *14* (5), 745-753.

57. Midoux, P.; Breuzard, G.; Gomez, J. P.; Pichon, C., Polymer-based gene delivery: a current review on the uptake and intracellular trafficking of polyplexes. *Current gene therapy* **2008,** *8* (5), 335-352.

58. ur Rehman, Z.; Hoekstra, D.; Zuhorn, I. S., Protein kinase A inhibition modulates the intracellular routing of gene delivery vehicles in HeLa cells, leading to productive transfection. *Journal of controlled release* **2011,** *156* (1), 76-84.

59. Rejman, J.; Bragonzi, A.; Conese, M., Role of clathrin-and caveolae-mediated endocytosis in gene transfer mediated by lipo-and polyplexes. *Molecular therapy* **2005,** *12* (3), 468-474.

60. Glick, D.; Barth, S.; Macleod, K. F., Autophagy: cellular and molecular mechanisms. *The Journal of pathology* **2010,** *221* (1), 3-12.

61. Man, N.; Chen, Y.; Zheng, F.; Zhou, W.; Wen, L.-P., Induction of genuine autophagy by cationic lipids in mammalian cells. *Autophagy* **2010,** *6* (4), 449-454.

62. Reilly, M. J.; Larsen, J. D.; Sullivan, M. O., Polyplexes traffic through caveolae to the Golgi and endoplasmic reticulum en route to the nucleus. *Molecular pharmaceutics* **2012,** *9* (5), 1280-1290.

63. Parton, R. G., Caveolae meet endosomes: a stable relationship? *Developmental cell* **2004,** *7* (4), 458-460.

64. Kerr, M. C.; Teasdale, R. D., Defining Macropinocytosis. *Traffic* **2009,** *10* (4), 364-371.

65. Lim, J. P.; Gleeson, P. A., Macropinocytosis: an endocytic pathway for internalising large gulps. *Immunol Cell Biol* **2011,** *89* (8), 836-43.

66. Desai, A. S.; Hunter, M. R.; Kapustin, A. N., Using macropinocytosis for intracellular delivery of therapeutic nucleic acids to tumour cells. *Philosophical Transactions of the Royal Society B* **2019,** *374* (1765), 20180156.

67. Barquinero, J.; Eixarch, H.; Perez-Melgosa, M., Retroviral vectors: new applications for an old tool. *Gene Ther* **2004,** *11 Suppl 1*, S3-9.

68. Judge, A. D.; Sood, V.; Shaw, J. R.; Fang, D.; McClintock, K.; MacLachlan, I., Sequence-dependent stimulation of the mammalian innate immune response by synthetic siRNA. *Nat Biotechnol* **2005,** *23* (4), 457-62.

69. Allen, T. M.; Cullis, P. R., Liposomal drug delivery systems: From concept to clinical applications. *Advanced Drug Delivery Reviews* **2013,** *65* (1), 36-48.

70. Schroeder, A.; Levins, C. G.; Cortez, C.; Langer, R.; Anderson, D. G., Lipid-based nanotherapeutics for siRNA delivery. *Journal of Internal Medicine* **2010,** *267* (1), 9-21.

71. Zimmermann, T. S.; Lee, A. C. H.; Akinc, A.; Bramlage, B.; Bumcrot, D.; Fedoruk, M. N.; Harborth, J.; Heyes, J. A.; Jeffs, L. B.; John, M.; Judge, A. D.; Lam, K.; McClintock, K.; Nechev, L. V.; Palmer, L. R.; Racie, T.; Röhl, I.; Seiffert, S.; Shanmugam, S.; Sood, V.; Soutschek, J.; Toudjarska, I.; Wheat, A. J.; Yaworski, E.; Zedalis, W.; Koteliansky, V.; Manoharan, M.; Vornlocher, H.-P.; MacLachlan, I., RNAi-mediated gene silencing in non-human primates. *Nature* **2006,** *441* (7089), 111-114.

72. Kon, E.; Elia, U.; Peer, D., Principles for designing an optimal mRNA lipid nanoparticle vaccine. *Curr Opin Biotechnol* **2022,** *73*, 329-336.

73. Yonezawa, S.; Koide, H.; Asai, T., Recent advances in siRNA delivery mediated by lipid-based nanoparticles. *Adv Drug Deliv Rev* **2020,** *154-155*, 64-78.

74. Lv, H.; Zhang, S.; Wang, B.; Cui, S.; Yan, J., Toxicity of cationic lipids and cationic polymers in gene delivery. *Journal of Controlled Release* **2006,** *114* (1), 100-109.

75. Mintzer, M. A.; Simanek, E. E., Nonviral Vectors for Gene Delivery. *Chemical Reviews* **2009,** *109* (2), 259-302.

76. Pack, D. W.; Hoffman, A. S.; Pun, S.; Stayton, P. S., Design and development of polymers for gene delivery. *Nat Rev Drug Discov* **2005,** *4* (7), 581-93.

77. Dong, Y.; Siegwart, D. J.; Anderson, D. G., Strategies, design, and chemistry in siRNA delivery systems. *Adv Drug Deliv Rev* **2019,** *144*, 133-147.

78. Leeuwenhoek, A. v., Observationes D. Anthonii Lewenhoeck, de natis'e semine genitali animalculis. *Philosophical Transactions of the Royal Society of London* **1978,** *12* (142), 1040-1046.

79. Elsayed, M.; Corrand, V.; Kolhatkar, V.; Xie, Y.; Kim, N. H.; Kolhatkar, R.; Merkel, O. M., Influence of oligospermines architecture on their suitability for siRNA delivery. *Biomacromolecules* **2014,** *15* (4), 1299-310.

80. Igarashi, K.; Kashiwagi, K., Polyamines: mysterious modulators of cellular functions. *Biochemical and biophysical research communications* **2000,** *271* (3), 559-564.

81. Szybalska, E. H.; Szybalski, W., GENETICS OF HUMAN CELL LINES, IV. DNA-MEDIATED HERITABLE TRANSFORMATION OF A BIOCHEMICAL TRAIT. *Proceedings of the National Academy of Sciences* **1962,** *48* (12), 2026-2034.

82. Shim, M. S.; Kwon, Y. J., Dual mode polyspermine with tunable degradability for plasmid DNA and siRNA delivery. *Biomaterials* **2011,** *32* (16), 4009-4020.

83. Hardy, J. G.; Kostiainen, M. A.; Smith, D. K.; Gabrielson, N. P.; Pack, D. W., Dendrons with spermine surface groups as potential building blocks for nonviral vectors in gene therapy. *Bioconjugate chemistry* **2006,** *17* (1), 172-178.

84. Kolhatkar, V.; Khambati, H.; Lote, A.; Shanine, P.; Insley, T.; Sen, S.; Munirathinam, G.; Král, P.; Kolhatkar, R., Star-Shaped Tetraspermine Enhances Cellular Uptake and Cytotoxicity of T-Oligo in Prostate Cancer Cells. *Pharmaceutical Research* **2015,** *32* (1), 196-210.

85. Lote, A. R.; Kolhatkar, V. R.; Insley, T.; Král, P.; Kolhatkar, R., Oligospermines and Nucleic Acid Interaction: A Structure Property Relationship Study. *ACS Macro Letters* **2014,** *3* (8), 829-833.

86. Jiang, H.; Kwon, J.; Kim, Y.; Kim, E.; Arote, R.; Jeong, H.; Nah, J.; Choi, Y.; Akaike, T.; Cho, M.-H., Galactosylated chitosan-graft-polyethylenimine as a gene carrier for hepatocyte targeting. *Gene Therapy* **2007,** *14* (19), 1389-1398.

87. Köping-Höggård, M.; Vårum, K.; Issa, M.; Danielsen, S.; Christensen, B.; Stokke, B.; Artursson, P., Improved chitosan-mediated gene delivery based on easily dissociated chitosan polyplexes of highly defined chitosan oligomers. *Gene therapy* **2004,** *11* (19), 1441-1452.

88. Jiang, H. L.; Lim, H. T.; Kim, Y. K.; Arote, R.; Shin, J. Y.; Kwon, J. T.; Kim, J. E.; Kim, J. H.; Kim, D.; Chae, C.; Nah, J. W.; Choi, Y. J.; Cho, C. S.; Cho, M. H., Chitosan-graft-spermine as a gene carrier in vitro and in vivo. *Eur J Pharm Biopharm* **2011,** *77* (1), 36-42.

89. Merdan, T.; Kopeček, J.; Kissel, T., Prospects for cationic polymers in gene and oligonucleotide therapy against cancer. *Advanced drug delivery reviews* **2002,** *54* (5), 715-758.

90. Brissault, B.; Kichler, A.; Guis, C.; Leborgne, C.; Danos, O.; Cheradame, H., Synthesis of linear polyethylenimine derivatives for DNA transfection. *Bioconjugate chemistry* **2003,** *14* (3), 581-587.

91. Tauhardt, L.; Kempe, K.; Knop, K.; Altuntaş, E.; Jäger, M.; Schubert, S.; Fischer, D.; Schubert, U. S., Linear polyethyleneimine: optimized synthesis and characterization–on the way to “pharmagrade” batches. *Macromolecular Chemistry and Physics* **2011,** *212* (17), 1918-1924.

92. Jones, G. D.; Langsjoen, A.; NEUMANN, S. M. M. C.; Zomlefer, J., The polymerization of ethylenimine. *The Journal of Organic Chemistry* **1944,** *9* (2), 125-147.

93. von Harpe, A.; Petersen, H.; Li, Y.; Kissel, T., Characterization of commercially available and synthesized polyethylenimines for gene delivery. *Journal of controlled release* **2000,** *69* (2), 309-322.

94. Ziebarth, J. D.; Wang, Y., Understanding the protonation behavior of linear polyethylenimine in solutions through Monte Carlo simulations. *Biomacromolecules* **2010,** *11* (1), 29-38.

95. Won, Y.-Y.; Sharma, R.; Konieczny, S. F., Missing pieces in understanding the intracellular trafficking of polycation/DNA complexes. *Journal of Controlled Release* **2009,** *139* (2), 88.

96. Benjaminsen, R. V.; Mattebjerg, M. A.; Henriksen, J. R.; Moghimi, S. M.; Andresen, T. L., The possible “proton sponge” effect of polyethylenimine (PEI) does not include change in lysosomal pH. *Molecular Therapy* **2013,** *21* (1), 149-157.

97. Gosselin, M. A.; Guo, W.; Lee, R. J., Efficient gene transfer using reversibly cross-linked low molecular weight polyethylenimine. *Bioconjugate chemistry* **2001,** *12* (6), 989-994.

98. Malek, A.; Merkel, O.; Fink, L.; Czubayko, F.; Kissel, T.; Aigner, A., In vivo pharmacokinetics, tissue distribution and underlying mechanisms of various PEI(-PEG)/siRNA complexes. *Toxicol Appl Pharmacol* **2009,** *236* (1), 97-108.

99. Liu, Y.; Samsonova, O.; Sproat, B.; Merkel, O.; Kissel, T., Biophysical characterization of hyper-branched polyethylenimine-graft-polycaprolactone-block-mono-methoxyl-poly(ethylene glycol) copolymers (hy-PEI-PCL-mPEG) for siRNA delivery. *J Control Release* **2011,** *153* (3), 262-8.

100. Dahlman, J. E.; Barnes, C.; Khan, O. F.; Thiriot, A.; Jhunjunwala, S.; Shaw, T. E.; Xing, Y.; Sager, H. B.; Sahay, G.; Speciner, L., In vivo endothelial siRNA delivery using polymeric nanoparticles with low molecular weight. *Nature nanotechnology* **2014,** *9* (8), 648-655.

101. Endres, T. K.; Beck-Broichsitter, M.; Samsonova, O.; Renette, T.; Kissel, T. H., Self-assembled biodegradable amphiphilic PEG-PCL-lPEI triblock copolymers at the borderline between micelles and nanoparticles designed for drug and gene delivery. *Biomaterials* **2011,** *32* (30), 7721-31.

102. Sun, T.-M.; Du, J.-Z.; Yao, Y.-D.; Mao, C.-Q.; Dou, S.; Huang, S.-Y.; Zhang, P.-Z.; Leong, K. W.; Song, E.-W.; Wang, J., Simultaneous delivery of siRNA and paclitaxel via a “two-in-one” micelleplex promotes synergistic tumor suppression. *ACS nano* **2011,** *5* (2), 1483-1494.

103. Mosqueira, V.; Legrand, P.; Gref, R.; Heurtault, B.; Appel, M.; Barratt, G., Interactions between a macrophage cell line (J774A1) and surface-modified poly (D, L-lactide) nanocapsules bearing poly (ethylene glycol). *Journal of drug targeting* **1999,** *7* (1), 65-78.

104. Liu, Y.; Steele, T.; Kissel, T., Degradation of Hyper‐Branched Poly (ethylenimine)‐graft‐poly (caprolactone)‐block‐monomethoxyl‐poly (ethylene glycol) as a Potential Gene Delivery Vector. *Macromolecular rapid communications* **2010,** *31* (17), 1509-1515.

105. Endres, T.; Zheng, M.; Kilic, A.; Turowska, A.; Beck-Broichsitter, M.; Renz, H.; Merkel, O. M.; Kissel, T., Amphiphilic biodegradable PEG-PCL-PEI triblock copolymers for FRET-capable in vitro and in vivo delivery of siRNA and quantum dots. *Molecular pharmaceutics* **2014,** *11* (4), 1273-81.

106. Xie, Y.; Kim, N. H.; Nadithe, V.; Schalk, D.; Thakur, A.; Kilic, A.; Lum, L. G.; Bassett, D. J. P.; Merkel, O. M., Targeted delivery of siRNA to activated T cells via transferrin-polyethylenimine (Tf-PEI) as a potential therapy of asthma. *J Control Release* **2016,** *229*, 120-129.

107. Kandil, R.; Xie, Y.; Heermann, R.; Isert, L.; Jung, K.; Mehta, A.; Merkel, O. M., Coming in and Finding Out: Blending Receptor-Targeted Delivery and Efficient Endosomal Escape in a Novel Bio-Responsive siRNA Delivery System for Gene Knockdown in Pulmonary T Cells. *Adv Ther (Weinh)* **2019,** *2* (7).

108. Liu, L.; Zheng, M.; Librizzi, D.; Renette, T.; Merkel, O. M.; Kissel, T., Efficient and Tumor Targeted siRNA Delivery by Polyethylenimine-graft-polycaprolactone-block-poly(ethylene glycol)-folate (PEI-PCL-PEG-Fol). *Molecular pharmaceutics* **2016,** *13* (1), 134-43.

109. Liu, Y.; Li, Y.; Keskin, D.; Shi, L., Poly(beta-Amino Esters): Synthesis, Formulations, and Their Biomedical Applications. *Adv Healthc Mater* **2019,** *8* (2), e1801359.

110. Galli, G.; Laus, M.; Angeloni, A. S.; Ferruti, P.; Chiellini, E., Thermotropic poly(β-aminoester)s containing azoxy groups. *Die Makromolekulare Chemie, Rapid Communications* **1983,** *4* (10), 681-686.

111. Danusso, F.; Ferruti, P., Synthesis of tertiary amine polymers. *Polymer* **1970,** *11* (2), 88-113.

112. Lynn, D. M.; Langer, R., Degradable poly (β-amino esters): synthesis, characterization, and self-assembly with plasmid DNA. *Journal of the American Chemical Society* **2000,** *122* (44), 10761-10768.

113. Cordeiro, R. A.; Serra, A.; Coelho, J. F. J.; Faneca, H., Poly(beta-amino ester)-based gene delivery systems: From discovery to therapeutic applications. *J Control Release* **2019,** *310*, 155-187.

114. Lynn, D. M.; Anderson, D. G.; Putnam, D.; Langer, R., Accelerated Discovery of Synthetic Transfection Vectors: Parallel Synthesis and Screening of a Degradable Polymer Library. *Journal of the American Chemical Society* **2001,** *123* (33), 8155-8156.

115. Akinc, A.; Anderson, D. G.; Lynn, D. M.; Langer, R., Synthesis of Poly(β-amino ester)s Optimized for Highly Effective Gene Delivery. *Bioconjugate Chemistry* **2003,** *14* (5), 979-988.

116. Cordeiro, R.; Santos, G.; Faneca, H.; Serra, A.; Coelho, J., Comparative biocompatibility evaluation of poly (β-amino ester) and poly [2-(dimethylamino) ethyl methacrylate]. *European Cells and Materials* **2013,** *26* (6), 67.

117. Bishop, C. J.; Ketola, T.-M.; Tzeng, S. Y.; Sunshine, J. C.; Urtti, A.; Lemmetyinen, H.; Vuorimaa-Laukkanen, E.; Yliperttula, M.; Green, J. J., The Effect and Role of Carbon Atoms in Poly(β-amino ester)s for DNA Binding and Gene Delivery. *Journal of the American Chemical Society* **2013,** *135* (18), 6951-6957.

118. Lynn, D. M.; Amiji, M. M.; Langer, R., pH‐responsive polymer microspheres: Rapid release of encapsulated material within the range of intracellular pH. *Angewandte Chemie International Edition* **2001,** *40* (9), 1707-1710.

119. Anderson, D. G.; Akinc, A.; Hossain, N.; Langer, R., Structure/property studies of polymeric gene delivery using a library of poly(β-amino esters). *Molecular Therapy* **2005,** *11* (3), 426-434.

120. Akinc, A.; Lynn, D. M.; Anderson, D. G.; Langer, R., Parallel Synthesis and Biophysical Characterization of a Degradable Polymer Library for Gene Delivery. *Journal of the American Chemical Society* **2003,** *125* (18), 5316-5323.

121. Jensen, S. A.; Day, E. S.; Ko, C. H.; Hurley, L. A.; Luciano, J. P.; Kouri, F. M.; Merkel, T. J.; Luthi, A. J.; Patel, P. C.; Cutler, J. I.; Daniel, W. L.; Scott, A. W.; Rotz, M. W.; Meade, T. J.; Giljohann, D. A.; Mirkin, C. A.; Stegh, A. H., Spherical Nucleic Acid Nanoparticle Conjugates as an RNAi-Based Therapy for Glioblastoma. *Science Translational Medicine* **2013,** *5* (209), 209ra152-209ra152.

122. Yu, Q.; Xiong, X.-q.; Zhao, L.; Xu, T.-t.; Bi, H.; Fu, R.; Wang, Q.-h., Biodistribution and toxicity assessment of superparamagnetic iron oxide

nanoparticles in vitro and in vivo. *Current Medical Science* **2018,** *38* (6), 1096-1102.

123. Heidari, R.; Khosravian, P.; Mirzaei, S. A.; Elahian, F., siRNA delivery using intelligent chitosan-capped mesoporous silica nanoparticles for overcoming multidrug resistance in malignant carcinoma cells. *Scientific reports* **2021,** *11* (1), 1-14.

124. Mitrach, F.; Schmid, M.; Toussaint, M.; Dukic-Stefanovic, S.; Deuther-Conrad, W.; Franke, H.; Ewe, A.; Aigner, A.; Wölk, C.; Brust, P., Amphiphilic Anionic Oligomer-Stabilized Calcium Phosphate Nanoparticles with Prospects in siRNA Delivery via Convection-Enhanced Delivery. *Pharmaceutics* **2022,** *14* (2), 326.

125. Li, D.; Ahmed, M.; Khan, A.; Xu, L.; Walters, A. A.; Ballesteros, B.; Al-Jamal, K. T., Tailoring the architecture of cationic polymer brush-modified carbon nanotubes for efficient sirna delivery in cancer immunotherapy. *ACS applied materials & interfaces* **2021,** *13* (26), 30284-30294.

126. Farokhzad, O. C.; Langer, R., Impact of Nanotechnology on Drug Delivery. *ACS Nano* **2009,** *3* (1), 16-20.

127. Rozema, D. B.; Lewis, D. L.; Wakefield, D. H.; Wong, S. C.; Klein, J. J.; Roesch, P. L.; Bertin, S. L.; Reppen, T. W.; Chu, Q.; Blokhin, A. V., Dynamic PolyConjugates for targeted in vivo delivery of siRNA to hepatocytes. *Proceedings of the National Academy of Sciences* **2007,** *104* (32), 12982-12987.

128. Biessen, E. A.; Beuting, D. M.; Roelen, H. C.; van de Marel, G. A.; Van Boom, J. H.; Van Berkel, T. J., Synthesis of cluster galactosides with high affinity for the hepatic asialoglycoprotein receptor. *Journal of medicinal chemistry* **1995,** *38* (9), 1538-1546.

129. Brown, C. R.; Gupta, S.; Qin, J.; Racie, T.; He, G.; Lentini, S.; Malone, R.; Yu, M.; Matsuda, S.; Shulga-Morskaya, S.; Nair, A. V.; Theile, C. S.; Schmidt, K.; Shahraz, A.; Goel, V.; Parmar, R. G.; Zlatev, I.; Schlegel, M. K.; Nair, J. K.; Jayaraman, M.; Manoharan, M.; Brown, D.; Maier, M. A.; Jadhav, V., Investigating the pharmacodynamic durability of GalNAc-siRNA conjugates. *Nucleic Acids Res* **2020,** *48* (21), 11827-11844.

130. Ho, W.; Zhang, X. Q.; Xu, X., Biomaterials in siRNA Delivery: A Comprehensive Review. *Adv Healthc Mater* **2016,** *5* (21), 2715-2731.

131. Zamore, P. D.; Tuschl, T.; Sharp, P. A.; Bartel, D. P., RNAi: double-stranded RNA directs the ATP-dependent cleavage of mRNA at 21 to 23 nucleotide intervals. *Cell* **2000,** *101* (1), 25-33.

132. McManus, M. T.; Sharp, P. A., Gene silencing in mammals by small interfering RNAs. *Nature reviews genetics* **2002,** *3* (10), 737-747.

133. Uludağ, H.; Parent, K.; Aliabadi, H. M.; Haddadi, A., Prospects for RNAi Therapy of COVID-19. *Frontiers in Bioengineering and Biotechnology* **2020,** *8* (916).

134. Lam, J. K.-W.; Liang, W.; Chan, H.-K., Pulmonary delivery of therapeutic siRNA. *Advanced drug delivery reviews* **2012,** *64* (1), 1-15.

135. Check, E., Harmful potential of viral vectors fuels doubts over gene therapy. *Nature* **2003,** *423* (6940), 573-575.

136. Lai, W.-F., In vivo nucleic acid delivery with PEI and its derivatives: current status and perspectives. *Expert review of medical devices* **2011,** *8* (2), 173-185.

137. Oh, Y.-K.; Park, T. G., siRNA delivery systems for cancer treatment. *Advanced drug delivery reviews* **2009,** *61* (10), 850-862.

138. Lynn, D. M.; Langer, R., Degradable Poly(β-amino esters): Synthesis, Characterization, and Self-Assembly with Plasmid DNA. *Journal of the American Chemical Society* **2000,** *122* (44), 10761-10768.

139. Green, J. J.; Langer, R.; Anderson, D. G., A Combinatorial Polymer Library Approach Yields Insight into Nonviral Gene Delivery. *Accounts of Chemical Research* **2008,** *41* (6), 749-759.

140. Eltoukhy, A. A.; Siegwart, D. J.; Alabi, C. A.; Rajan, J. S.; Langer, R.; Anderson, D. G., Effect of molecular weight of amine end-modified poly (β-amino ester) s on gene delivery efficiency and toxicity. *Biomaterials* **2012,** *33* (13), 3594-3603.

141. Gao, H.; Cheng, T.; Liu, J.; Liu, J.; Yang, C.; Chu, L.; Zhang, Y.; Ma, R.; Shi, L., Self-regulated multifunctional collaboration of targeted nanocarriers for enhanced tumor therapy. *Biomacromolecules* **2014,** *15* (10), 3634-3642.

142. Estévez-Torres, A.; Baigl, D., DNA compaction: fundamentals and applications. *Soft Matter* **2011,** *7* (15), 6746.

143. El Osta, B.; Behera, M.; Kim, S.; Berry, L. D.; Sica, G.; Pillai, R. N.; Owonikoko, T. K.; Kris, M. G.; Johnson, B. E.; Kwiatkowski, D. J., Characteristics and outcomes of patients with metastatic KRAS-mutant lung adenocarcinomas: the lung cancer mutation consortium experience. *Journal of Thoracic Oncology* **2019,** *14* (5), 876-889.

144. Lievre, A.; Bachet, J.-B.; Le Corre, D.; Boige, V.; Landi, B.; Emile, J.-F.; Côté, J.-F.; Tomasic, G.; Penna, C.; Ducreux, M., KRAS mutation status is predictive of response to cetuximab therapy in colorectal cancer. *Cancer research* **2006,** *66* (8), 3992-3995.

145. Mehta, A.; Dalle Vedove, E.; Isert, L.; Merkel, O. M., Targeting KRAS Mutant Lung Cancer Cells with siRNA-Loaded Bovine Serum Albumin Nanoparticles. *Pharm Res* **2019,** *36* (9), 133.

146. Sotillo, R.; Schvartzman, J.-M.; Socci, N. D.; Benezra, R., Mad2-induced chromosome instability leads to lung tumour relapse after oncogene withdrawal. *Nature* **2010,** *464* (7287), 436-440.

147. Blagbrough, I. S.; Geall, A. J., Practical synthesis of unsymmetrical polyamine amides. *Tetrahedron letters* **1998,** *39* (5-6), 439-442.

148. Nalluri, S. K. M.; Voskuhl, J.; Bultema, J. B.; Boekema, E. J.; Ravoo, B. J., Light‐responsive capture and release of DNA in a ternary supramolecular complex. *Angewandte Chemie International Edition* **2011,** *50* (41), 9747-9751.

149. Hartl, N.; Adams, F.; Costabile, G.; Isert, L.; Doblinger, M.; Xiao, X.; Liu, R.; Merkel, O. M., The Impact of Nylon-3 Copolymer Composition on the Efficiency of siRNA Delivery to Glioblastoma Cells. *Nanomaterials (Basel)* **2019,** *9* (7).

150. Tuma, R. S.; Beaudet, M. P.; Jin, X.; Jones, L. J.; Cheung, C.-Y.; Yue, S.; Singer, V. L., Characterization of SYBR Gold nucleic acid gel stain: a dye optimized for use with 300-nm ultraviolet transilluminators. *Analytical biochemistry* **1999,** *268* (2), 278-288.

151. Jin, Y.; Liu, Q.; Zhou, C.; Hu, X.; Wang, L.; Han, S.; Zhou, Y.; Liu, Y., Intestinal oligopeptide transporter PepT1-targeted polymeric micelles for further enhancing the oral absorption of water-insoluble agents. *Nanoscale* **2019**.

152. Zou, Y.; Zhou, Y.; Jin, Y.; He, C.; Deng, Y.; Han, S.; Zhou, C.; Li, X.; Zhou, Y.; Liu, Y., Synergistically Enhanced Antimetastasis Effects by Honokiol-Loaded pH-Sensitive Polymer-Doxorubicin Conjugate Micelles. *ACS Appl Mater Interfaces* **2018,** *10* (22), 18585-18600.

153. Stille, J. K., Step-growth polymerization. ACS Publications: 1981.

154. Jere, D.; Kim, T. H.; Arote, R. B.; Jiang, H. L.; Cho, M. H.; Nah, J. W.; Cho, C. S. In *A poly (β-amino ester) of spermine and poly (ethylene glycol) diacrylate as a gene carrier*, Key Engineering Materials, Trans Tech Publ: 2007; pp 425-428.

155. Chen, J.; Huang, S.-W.; Liu, M.; Zhuo, R.-X., Synthesis and degradation of poly(beta-aminoester) with pendant primary amine. *Polymer* **2007,** *48* (3), 675-681.

156. Lee, J.-S.; Green, J. J.; Love, K. T.; Sunshine, J.; Langer, R.; Anderson, D. G., Gold, poly (β-amino ester) nanoparticles for small interfering RNA delivery. *Nano letters* **2009,** *9* (6), 2402-2406.

157. Kim, J.; Kang, Y.; Tzeng, S. Y.; Green, J. J., Synthesis and application of poly(ethylene glycol)-co-poly(β -amino ester) copolymers for small cell lung cancer gene therapy. *Acta Biomaterialia* **2016,** *41*, 293-301.

158. Kozielski, K. L.; Tzeng, S. Y.; Green, J. J., A bioreducible linear poly(beta-amino ester) for siRNA delivery. *Chem Commun (Camb)* **2013,** *49* (46), 5319-21.

159. Baradaran Eftekhari, R.; Maghsoudnia, N.; Dorkoosh, F. A., Chloroquine: a brand-new scenario for an old drug. *Expert Opinion on Drug Delivery* **2020,** *17* (3), 275-277.

160. Maxfield, F. R., Weak bases and ionophores rapidly and reversibly raise the pH of endocytic vesicles in cultured mouse fibroblasts. *The Journal of cell biology* **1982,** *95* (2), 676-681.

161. Dowdy, S. F., Overcoming cellular barriers for RNA therapeutics. *Nat Biotechnol* **2017,** *35* (3), 222-229.

162. Smith, S. A.; Selby, L. I.; Johnston, A. P. R.; Such, G. K., The Endosomal Escape of Nanoparticles: Toward More Efficient Cellular Delivery. *Bioconjug Chem* **2019,** *30* (2), 263-272.

163. Karlsson, J.; Tzeng, S. Y.; Hemmati, S.; Luly, K. M.; Choi, O.; Rui, Y.; Wilson, D. R.; Kozielski, K. L.; Quiñones‐Hinojosa, A.; Green, J. J., Photocrosslinked Bioreducible Polymeric Nanoparticles for Enhanced Systemic siRNA Delivery as Cancer Therapy. *Advanced Functional Materials* **2021,** *31* (17), 2009768.

164. Agirre, M.; Zarate, J.; Ojeda, E.; Puras, G.; Desbrieres, J.; Pedraz, J., Low Molecular Weight Chitosan (LMWC)-based Polyplexes for pDNA Delivery: From Bench to Bedside. *Polymers* **2014,** *6* (6), 1727-1755.

165. Bonner, D. K.; Zhao, X.; Buss, H.; Langer, R.; Hammond, P. T., Crosslinked linear polyethylenimine enhances delivery of DNA to the cytoplasm. *Journal of Controlled Release* **2013,** *167* (1), 101-107.

166. Park, B. G.; Kim, Y. J.; Min, J. H.; Cheong, T.-C.; Nam, S. H.; Cho, N.-H.; Kim, Y. K.; Lee, K. B., Assessment of Cellular Uptake Efficiency According to Multiple Inhibitors of Fe3O4-Au Core-Shell Nanoparticles: Possibility to Control Specific Endocytosis in Colorectal Cancer Cells. *Nanoscale research letters* **2020,** *15* (1), 1-10.

167. Kou, L.; Sun, J.; Zhai, Y.; He, Z., The endocytosis and intracellular fate of nanomedicines: Implication for rational design. *Asian Journal of Pharmaceutical Sciences* **2013,** *8* (1), 1-10.

168. Sahay, G.; Alakhova, D. Y.; Kabanov, A. V., Endocytosis of nanomedicines. *Journal of Controlled Release* **2010,** *145* (3), 182-195.

169. Tsuchida, N.; Ryder, T.; Ohtsubo, E., Nucleotide sequence of the oncogene encoding the p21 transforming protein of Kirsten murine sarcoma virus. *Science* **1982,** *217* (4563), 937-9.

170. Kim, B.-K.; Hwang, G.-B.; Seu, Y.-B.; Choi, J.-S.; Jin, K. S.; Doh, K.-O., DOTAP/DOPE ratio and cell type determine transfection efficiency with DOTAP-liposomes. *Biochimica et Biophysica Acta (BBA) - Biomembranes* **2015,** *1848* (10, Part A), 1996-2001.

171. Fakhr, E.; Zare, F.; Teimoori-Toolabi, L., Precise and efficient siRNA design: a key point in competent gene silencing. *Cancer gene therapy* **2016,** *23* (4), 73-82.

172. Valencia-Serna, J.; Kucharski, C.; Chen, M.; Kc, R.; Jiang, X.; Brandwein, J.; Uludag, H., siRNA-mediated BCR-ABL silencing in primary chronic myeloid leukemia cells using lipopolymers. *J Control Release* **2019,** *310*, 141-154.

173. Wang, M. Z.; Niu, J.; Ma, H. J.; Dad, H. A.; Shao, H. T.; Yuan, T. J.; Peng, L. H., Transdermal siRNA delivery by pH-switchable micelles with targeting effect suppress skin melanoma progression. *J Control Release* **2020,** *322*, 95-107.

174. Uludağ, H.; Parent, K.; Aliabadi, H. M.; Haddadi, A., Prospects for RNAi therapy of COVID-19. *Frontiers in Bioengineering and Biotechnology* **2020**, 916.

175. Mehta, A.; Michler, T.; Merkel, O. M., siRNA Therapeutics against Respiratory Viral Infections-What Have We Learned for Potential COVID-19 Therapies? *Adv Healthc Mater* **2021,** *10* (7), e2001650.

176. O'Driscoll, C. M.; Bernkop-Schnürch, A.; Friedl, J. D.; Préat, V.; Jannin, V., Oral delivery of non-viral nucleic acid-based therapeutics-do we have the guts for this? *European Journal of Pharmaceutical Sciences* **2019,** *133*, 190-204.

177. Wang, X.; Liang, Q.; Mao, Y.; Zhang, R.; Deng, Q.; Chen, Y.; Zhu, R.; Duan, S.; Yin, L., Bioreducible, branched poly(beta-amino ester)s mediate

anti-inflammatory ICAM-1 siRNA delivery against myocardial ischemia reperfusion (IR) injury. *Biomater Sci* **2020,** *8* (14), 3856-3870.

178. Kozielski, K. L.; Tzeng, S. Y.; Hurtado De Mendoza, B. A.; Green, J. J., Bioreducible cationic polymer-based nanoparticles for efficient and environmentally triggered cytoplasmic siRNA delivery to primary human brain cancer cells. *ACS nano* **2014,** *8* (4), 3232-3241.

179. Liu, S.; Gao, Y.; A, S.; Zhou, D.; Greiser, U.; Guo, T.; Guo, R.; Wang, W., Biodegradable Highly Branched Poly(β-Amino Ester)s for Targeted Cancer Cell Gene Transfection. *ACS Biomaterials Science & Engineering* **2016,** *3* (7), 1283-1286.

180. Eliyahu, H.; Siani, S.; Azzam, T.; Domb, A. J.; Barenholz, Y., Relationships between chemical composition, physical properties and transfection efficiency of polysaccharide–spermine conjugates. *Biomaterials* **2006,** *27* (8), 1646-1655.

181. Duan, S.-Y.; Ge, X.-M.; Lu, N.; Wu, F.; Yuan, W.; Jin, T., Synthetic polyspermine imidazole-4, 5-amide as an efficient and cytotoxicity-free gene delivery system. *International journal of nanomedicine* **2012,** *7*, 3813.

182. Lebhardt, T.; Roesler, S.; Beck-Broichsitter, M.; Kissel, T., Polymeric nanocarriers for drug delivery to the lung. *Journal of Drug Delivery Science and Technology* **2010,** *20* (3), 171-180.

183. Jiang, H.-L.; Hong, S.-H.; Kim, Y.-K.; Islam, M. A.; Kim, H.-J.; Choi, Y.-J.; Nah, J.-W.; Lee, K.-H.; Han, K.-W.; Chae, C., Aerosol delivery of spermine-based poly (amino ester)/Akt1 shRNA complexes for lung cancer gene therapy. *International journal of pharmaceutics* **2011,** *420* (2), 256-265.

184. Mosmann, T., Rapid colorimetric assay for cellular growth and survival: Application to proliferation and cytotoxicity assays. *Journal of Immunological Methods* **1983,** *65* (1), 55-63.

185. Gwak, S. J.; Macks, C.; Jeong, D. U.; Kindy, M.; Lynn, M.; Webb, K.; Lee, J. S., RhoA knockdown by cationic amphiphilic copolymer/siRhoA polyplexes enhances axonal regeneration in rat spinal cord injury model. *Biomaterials* **2017,** *121*, 155-166.

186. Dosta, P.; Ramos, V.; Borrós, S., Stable and efficient generation of poly(β-amino ester)s for RNAi delivery. *Molecular Systems Design & Engineering* **2018,** *3* (4), 677-689.

187. Parhamifar, L.; Larsen, A. K.; Hunter, A. C.; Andresen, T. L.; Moghimi, S. M., Polycation cytotoxicity: a delicate matter for nucleic acid therapy—focus on polyethylenimine. *Soft Matter* **2010,** *6* (17).

188. Anderson, D. G.; Lynn, D. M.; Langer, R., Semi‐automated synthesis and screening of a large library of degradable cationic polymers for gene delivery. *Angewandte Chemie International Edition* **2003,** *42* (27), 3153-3158.

189. Choosakoonkriang, S.; Lobo, B. A.; Koe, G. S.; Koe, J. G.; Middaugh, C. R., Biophysical characterization of PEI/DNA complexes. *Journal of pharmaceutical sciences* **2003,** *92* (8), 1710-1722.

190. Ge, X.; Feng, J.; Chen, S.; Zhang, C.; Ouyang, Y.; Liu, Z.; Yuan, W., Biscarbamate cross-linked low molecular weight Polyethylenimine polycation as

an efficient intra-cellular delivery cargo for cancer therapy. *Journal of nanobiotechnology* **2014,** *12* (1), 1-8.

191. Wheeler, K. E.; Chetwynd, A. J.; Fahy, K. M.; Hong, B. S.; Tochihuitl, J. A.; Foster, L. A.; Lynch, I., Environmental dimensions of the protein corona. *Nat Nanotechnol* **2021,** *16* (6), 617-629.

192. Zhu, D.; Yan, H.; Zhou, Z.; Tang, J.; Liu, X.; Hartmann, R.; Parak, W. J.; Feliu, N.; Shen, Y., Detailed investigation on how the protein corona modulates the physicochemical properties and gene delivery of polyethylenimine (PEI) polyplexes. *Biomater Sci* **2018,** *6* (7), 1800-1817.

193. Tai, W., Current Aspects of siRNA Bioconjugate for In Vitro and In Vivo Delivery. *Molecules* **2019,** *24* (12).

194. Szybalska, E. H.; Szybalski, W., Genetics of human cell lines, IV. DNA-mediated heritable transformation of a biochemical trait. *Proceedings of the National Academy of Sciences of the United States of America* **1962,** *48* (12), 2026.

195. Dong, Y.; Skoultchi, A. I.; Pollard, J. W., Efficient DNA transfection of quiescent mammalian cells using poly-L-ornithine. *Nucleic acids research* **1993,** *21* (3), 771-772.

196. Emi, N.; Kidoaki, S.; Yoshikawa, K.; Saito, H., Gene transfer mediated by polyarginine requires a formation of big carrier-complex of DNA aggregate. *Biochemical and biophysical research communications* **1997,** *231* (2), 421-424.

197. Wu, G. Y.; Wu, C. H., Receptor-mediated in vitro gene transformation by a soluble DNA carrier system. *Journal of Biological Chemistry* **1987,** *262* (10), 4429-4432.

198. Benns, J. M.; Choi, J.-S.; Mahato, R. I.; Park, J.-S.; Kim, S. W., pH-Sensitive Cationic Polymer Gene Delivery Vehicle: N-Ac-poly(l-histidine)-graft-poly(l-lysine) Comb Shaped Polymer. *Bioconjugate Chemistry* **2000,** *11* (5), 637-645.

199. Gilleron, J.; Querbes, W.; Zeigerer, A.; Borodovsky, A.; Marsico, G.; Schubert, U.; Manygoats, K.; Seifert, S.; Andree, C.; Stöter, M., Image-based analysis of lipid nanoparticle–mediated siRNA delivery, intracellular trafficking and endosomal escape. *Nature biotechnology* **2013,** *31* (7), 638-646.

200. Endoh, T.; Ohtsuki, T., Cellular siRNA delivery using cell-penetrating peptides modified for endosomal escape. *Advanced drug delivery reviews* **2009,** *61* (9), 704-709.

201. Oliveira, S.; Fretz, M. M.; Høgset, A.; Storm, G.; Schiffelers, R. M., Photochemical internalization enhances silencing of epidermal growth factor receptor through improved endosomal escape of siRNA. *Biochimica et Biophysica Acta (BBA)-Biomembranes* **2007,** *1768* (5), 1211-1217.

202. Varkouhi, A. K.; Scholte, M.; Storm, G.; Haisma, H. J., Endosomal escape pathways for delivery of biologicals. *J Control Release* **2011,** *151* (3), 220-8.

203. Alshamsan, A.; Haddadi, A.; Incani, V.; Samuel, J.; Lavasanifar, A.; Uludağ, H., Formulation and Delivery of siRNA by Oleic Acid and Stearic Acid Modified Polyethylenimine. *Molecular pharmaceutics* **2009,** *6* (1), 121-133.

204. Thanou, M.; Florea, B. I.; Geldof, M.; Junginger, H. E.; Borchard, G., Quaternized chitosan oligomers as novel gene delivery vectors in epithelial cell lines. *Biomaterials* **2002,** *23* (1), 153-159.

205. Rata-Aguilar, A.; Segovia-Ramos, N.; Jódar-Reyes, A. B.; Ramos-Pérez, V.; Borrós, S.; Ortega-Vinuesa, J. L.; Martín-Rodríguez, A., The role of hydrophobic alkyl chains in the physicochemical properties of poly (β-amino ester)/DNA complexes. *Colloids and Surfaces B: Biointerfaces* **2015,** *126*, 374-380.

206. Incani, V.; Lavasanifar, A.; Uludağ, H., Lipid and hydrophobic modification of cationic carriers on route to superior gene vectors. *Soft Matter* **2010,** *6* (10).

207. Mastrobattista, E.; Hennink, W. E., Charged for success. *Nature materials* **2012,** *11* (1), 10-12.

208. Rybakovsky, E.; Valenzano, M. C.; DiGuilio, K. M.; Buleza, N. B.; Moskalenko, D. V.; Harty, R. N.; Mullin, J. M., Improving Transient Transfection Efficiency in a Differentiated, Polar Epithelial Cell Layer. *J Biomol Tech* **2019,** *30* (2), 19-24.

209. Callaghan, P. J.; Ferrick, B.; Rybakovsky, E.; Thomas, S.; Mullin, J. M., Epithelial barrier function properties of the 16HBE14o- human bronchial epithelial cell culture model. *Biosci Rep* **2020,** *40* (10), BSR20201532.

210. Tong, J.; Zhou, X.-d.; Perelman, Juliy M.; Kolosov, Victor P., Effect of epithelium ATP release on cyclic pressure-induced airway mucus secretion. *Biosci Rep* **2014,** *34* (1).

211. Castellani, S.; Di Gioia, S.; di Toma, L.; Conese, M., Human Cellular Models for the Investigation of Lung Inflammation and Mucus Production in Cystic Fibrosis. *Analytical Cellular Pathology* **2018,** *2018*, 3839803.

212. Izumisawa, T.; Hattori, Y.; Date, M.; Toma, K.; Maitani, Y., Cell line-dependent internalization pathways determine DNA transfection efficiency of decaarginine-PEG-lipid. *International Journal of Pharmaceutics* **2011,** *404* (1), 264-270.

213. Hu, Y. B.; Dammer, E. B.; Ren, R. J.; Wang, G., The endosomal-lysosomal system: from acidification and cargo sorting to neurodegeneration. *Transl Neurodegener* **2015,** *4*, 18.

214. Scott, L. J., Givosiran: First Approval. *Drugs* **2020,** *80* (3), 335-339.

215. Weng, Y.; Xiao, H.; Zhang, J.; Liang, X.-J.; Huang, Y., RNAi therapeutic and its innovative biotechnological evolution. *Biotechnology Advances* **2019,** *37* (5), 801-825.

216. Scott, L. J.; Keam, S. J., Lumasiran: first approval. *Drugs* **2021,** *81* (2), 277-282.

217. Godbey, W.; Wu, K. K.; Mikos, A. G., Size matters: molecular weight affects the efficiency of poly (ethylenimine) as a gene delivery vehicle. *Journal of Biomedical Materials Research: An Official Journal of The Society for Biomaterials, The Japanese Society for Biomaterials, and The Australian Society for Biomaterials* **1999,** *45* (3), 268-275.

218. Fischer, D.; Bieber, T.; Li, Y.; Elsässer, H.-P.; Kissel, T., A novel non-viral vector for DNA delivery based on low molecular weight, branched polyethylenimine: effect of molecular weight on transfection efficiency and cytotoxicity. *Pharmaceutical research* **1999,** *16* (8), 1273-1279.

219. Seymour, L. W.; Duncan, R.; Strohalm, J.; Kopeček, J., Effect of molecular weight (Mw) of N-(2-hydroxypropyl)methacrylamide copolymers on body distribution and rate of excretion after subcutaneous, intraperitoneal, and intravenous administration to rats. *Journal of Biomedical Materials Research* **1987,** *21* (11), 1341-1358.

220. Ge, X.; Feng, J.; Chen, S.; Zhang, C.; Ouyang, Y.; Liu, Z.; Yuan, W., Biscarbamate cross-linked low molecular weight Polyethylenimine polycation as an efficient intra-cellular delivery cargo for cancer therapy. *Journal of Nanobiotechnology* **2014,** *12* (1), 13.

221. Kichler, A., Gene transfer with modified polyethylenimines. *The Journal of Gene Medicine: A cross‐disciplinary journal for research on the science of gene transfer and its clinical applications* **2004,** *6* (S1), S3-S10.

222. Zheng, M.; Zhong, Y.; Meng, F.; Peng, R.; Zhong, Z., Lipoic acid modified low molecular weight polyethylenimine mediates nontoxic and highly potent in vitro gene transfection. *Molecular pharmaceutics* **2011,** *8* (6), 2434-2443.

223. Liu, Z.; Zhang, Z.; Zhou, C.; Jiao, Y., Hydrophobic modifications of cationic polymers for gene delivery. *Progress in Polymer Science* **2010,** *35* (9), 1144-1162.

224. Incani, V.; Lavasanifar, A.; Uludağ, H., Lipid and hydrophobic modification of cationic carriers on route to superior gene vectors. *Soft Matter* **2010,** *6* (10), 2124-2138.

225. Shuai, X.; Merdan, T.; Unger, F.; Wittmar, M.; Kissel, T., Novel Biodegradable Ternary Copolymers hy-PEI-g-PCL-b-PEG: Synthesis, Characterization, and Potential as Efficient Nonviral Gene Delivery Vectors. *Macromolecules* **2003,** *36* (15), 5751-5759.

226. Liu, Y.; Nguyen, J.; Steele, T.; Merkel, O.; Kissel, T., A new synthesis method and degradation of hyper-branched polyethylenimine grafted polycaprolactone block mono-methoxyl poly (ethylene glycol) copolymers (hy-PEI-g-PCL-b-mPEG) as potential DNA delivery vectors. *Polymer* **2009,** *50* (16), 3895-3904.

227. Mora-Huertas, C. E.; Fessi, H.; Elaissari, A., Influence of process and formulation parameters on the formation of submicron particles by solvent displacement and emulsification–diffusion methods: Critical comparison. *Advances in Colloid and Interface Science* **2011,** *163* (2), 90-122.

228. Vitale, S. A.; Katz, J. L., Liquid Droplet Dispersions Formed by Homogeneous Liquid−Liquid Nucleation: “The Ouzo Effect”. *Langmuir* **2003,** *19* (10), 4105-4110.

229. Ganachaud, F.; Katz, J. L., Nanoparticles and nanocapsules created using the Ouzo effect: spontaneous emulisification as an alternative to ultrasonic and high-shear devices. *Chemphyschem* **2005,** *6* (2), 209-16.

230. Chacón, M.; Berges, L.; Molpeceres, J.; Aberturas, M. R.; Guzman, M., Optimized preparation of poly d,l (lactic-glycolic) microspheres and nanoparticles for oral administration. *International Journal of Pharmaceutics* **1996,** *141* (1), 81-91.

231. Anarjan, N.; Jaberi, N.; Yeganeh-Zare, S.; Banafshehchin, E.; Rahimirad, A.; Jafarizadeh-Malmiri, H., Optimization of Mixing Parameters for α-Tocopherol Nanodispersions Prepared Using Solvent Displacement Method. *Journal of the American Oil Chemists' Society* **2014,** *91* (8), 1397-1405.

232. Saad, W. S.; Prud'homme, R. K., Principles of nanoparticle formation by flash nanoprecipitation. *Nano Today* **2016,** *11* (2), 212-227.

233. Guhagarkar, S. A.; Malshe, V. C.; Devarajan, P. V., Nanoparticles of polyethylene sebacate: a new biodegradable polymer. *Aaps Pharmscitech* **2009,** *10* (3), 935-942.

234. Ameller, T.; Marsaud, V.; Legrand, P.; Gref, R.; Renoir, J.-M., Pure antiestrogen RU 58668—loaded nanospheres: morphology, cell activity and toxicity studies. *European journal of pharmaceutical sciences* **2004,** *21* (2-3), 361-370.

235. Beck-Broichsitter, M.; Rytting, E.; Lebhardt, T.; Wang, X.; Kissel, T., Preparation of nanoparticles by solvent displacement for drug delivery: A shift in the "ouzo region" upon drug loading. *European Journal of Pharmaceutical Sciences* **2010,** *41* (2), 244-253.

236. Moghimi, S. M.; Hunter, A. C.; Murray, J. C., Long-circulating and target-specific nanoparticles: theory to practice. *Pharmacological reviews* **2001,** *53* (2), 283-318.

237. Kly, S.; Andrew, L. J.; Moloney, E. G.; Huang, Y.; Wulff, J. E.; Moffitt, M. G., Hierarchical Self-Assembly Route to "Polyplex-in-Hydrophobic-Core" Micelles for Gene Delivery. *Chemistry of Materials* **2021,** *33* (17), 6860-6875.

238. Izumrudov, V.; Bronich, T. K.; Novikova, M.; Zezin, A.; Kabanov, V., Substitution reactions in ternary systems of macromolecules. *Polymer science USSR* **1982,** *24* (2), 367-378.

239. Bolcato-Bellemin, A.-L.; Bonnet, M.-E.; Creusat, G.; Erbacher, P.; Behr, J.-P., Sticky overhangs enhance siRNA-mediated gene silencing. *Proceedings of the National Academy of Sciences* **2007,** *104* (41), 16050-16055.

240. Merkel, O. M.; Librizzi, D.; Pfestroff, A.; Schurrat, T.; Buyens, K.; Sanders, N. N.; De Smedt, S. C.; Béhé, M.; Kissel, T., Stability of siRNA polyplexes from poly (ethylenimine) and poly (ethylenimine)-g-poly (ethylene glycol) under in vivo conditions: effects on pharmacokinetics and biodistribution measured by Fluorescence Fluctuation Spectroscopy and Single Photon Emission Computed Tomography (SPECT) imaging. *Journal of Controlled Release* **2009,** *138* (2), 148-159.

241. Martens, T. F.; Remaut, K.; Demeester, J.; De Smedt, S. C.; Braeckmans, K., Intracellular delivery of nanomaterials: How to catch endosomal escape in the act. *Nano Today* **2014,** *9* (3), 344-364.

242. Dolai, J.; Mandal, K.; Jana, N. R., Nanoparticle Size Effects in Biomedical Applications. *ACS Applied Nano Materials* **2021,** *4* (7), 6471-6496.

243. Jamalzadeh, L.; Ghafoori, H.; Sariri, R.; Rabuti, H.; Nasirzade, J.; Hasani, H.; Aghamaali, M. R., Cytotoxic effects of some common organic solvents on MCF-7, RAW-264.7 and human umbilical vein endothelial cells. *Avicenna Journal of Medical Biochemistry* **2016,** *4* (1), 10-33453.

244. Zheng, M.; Pavan, G. M.; Neeb, M.; Schaper, A. K.; Danani, A.; Klebe, G.; Merkel, O. M.; Kissel, T., Targeting the Blind Spot of Polycationic Nanocarrier-Based siRNA Delivery. *ACS Nano* **2012,** *6* (11), 9447-9454.

245. Wiley, D. T.; Webster, P.; Gale, A.; Davis, M. E., Transcytosis and brain uptake of transferrin-containing nanoparticles by tuning avidity to transferrin receptor. *Proceedings of the National Academy of Sciences* **2013,** *110* (21), 8662-8667.

246. Habeeb, A. S. A., Determination of free amino groups in proteins by trinitrobenzenesulfonic acid. *Analytical biochemistry* **1966,** *14* (3), 328-336.

247. Hermanson, G. T., *Bioconjugate techniques*. Academic press: 2013.

List of publications and conference contributions

Publications:

• **Yao Jin**, Friederike Adams, Judith Möller, Lorenz Isert, Christoph Zimmermann, David Keul, and Olivia M. Merkel*. Synthesis and application of low molecular weight PEI-based copolymers for siRNA delivery with smart polymer blends. (Submitted)

• **Yao Jin**, Friederike Adams, and Olivia M. Merkel*. Synthesis and application of spermine-based amphiphilic poly(β-amino ester)s for siRNA delivery. (Submitted)

• **Yao Jin**, Friederike Adams, Lorenz Isert, Domizia Baldassi, and Olivia M. Merkel*. Synthesis and application of spermine-based poly(β-amino ester)s for siRNA delivery. (Manuscript in preparation)

• **Yao Jin,** Valentin Fell, Friederike Adams, and Olivia M. Merkel*. Synthesis of poly(β-amino ester)s and their applications for nucleic acid delivery. (Review, Manuscript in preparation)

Conference contributions:

• 13th international symposium on polymer therapeutics: from laboratory to clinical practice, Valencia, Spain, 2022. *Oral Presentation and Poster: Synthesis and application of spermine-based poly(β-amino ester)s for siRNA delivery.*

• Controlled release society (CRS) local chapter meeting, Aachen, Germany, 2022. *Poster Pitch: Synthesis and application of low molecular weight PEI-based copolymers for siRNA delivery.*

• Controlled release society (CRS) local chapter meeting, online, Germany, 2021. *Poster Pitch: Synthesis and application of spermine-based poly(β-amino ester)s for siRNA delivery.*

• International conference on nanomedicine and nanobiotechnology (ICONAN), Munich, Germany, 2019. *Listener*

Acknowledgments

My first and greatest thanks go to my Ph.D. supervisor, Prof. Merkel. Thank you for giving me the opportunity to do my doctorate in your working group and to work on the interesting projects! Thank you for your support and the many valuable tips and discussions. Your great enthusiasm for science, immense knowledge, as well as your warm and motivating manner, have always impressed me.

Special thanks go to my other examiners. Thank you, Prof. Wagner, for assessing my work as the second reviewer. I would also like to thank Prof. Frieß, Prof. Zahler, Prof. Bracher, and Prof. Winter. Thank you for taking the time to rate my work.

I would like to sincerely thank our former postdoc Friederike Adams. Rike is an expert in polymer chemistry. Thank you, Rike, for your supervision, excellent support and the many constructive discussions.

Thank the senior Ph.D. students Lorenz Isert, Domizia Baldassi, Christoph Zimmerman, Natascha Hartl, Bettina Gabold, Dr. Tobias Keil, Dr. Gemma Conte, and Dr. Weiwei Liu for sharing your knowledge and experience! Thank the master student Xiaoxuan Wang for her contribution to the project, and Thi My Hanh Ngo for her help. Thank Kate Kutsenok for being a very nice labmate. I would also like to thank all the other nice colleagues in these years: Dr. Benjamin Winkeljann, Dr. Simone Carneiro, Dr. Valentin Fell, Siyu Chen, David Keul, Gabriele Loiudice, Fabian Volk, Cynthia Zettl, Judith Möller, Joschka Müller, and Leonie Deßloch. Thank you for being very nice and friendly colleagues.

Thank our technician Gabriele Brandstäter for her support with ordering.

Thanks to all the colleagues from Professor Winter and Professor Frieß's group for the very nice working atmosphere.

Thank my friends Ling Zhuo, Yang Zou, and Xiaoyou Qu for answering my questions.

Thank my parents for supporting me spiritually throughout my Ph.D. study in Germany.

Last but not least, I would like to thank the China scholarship council for its financial support.